Study and optimization of new differential space-time modulation schemes based on the Weyl group for the second generation of MIMO systems

Hui Ji

Thèse

THESE INSA Rennes
sous le sceau de l'Université européenne de Bretagne
pour obtenir le titre de
DOCTEUR DE L'INSA DE RENNES
Spécialité : Electronique et Télécommunications

présentée par
Hui JI

ECOLE DOCTORALE : MATISSE
LABORATOIRE : IETR

Study and optimization of new differential space-time modulation schemes based on the Weyl group for the second generation of MIMO systems

Thèse soutenue le 09.11.2015
devant le jury composé de :

Marie-Laure BOUCHERET
Professeur à l'ENSEEIHT de Toulouse / *Présidente et rapporteur*

Jean-Pierre CANCES
Professeur à l'ENSIL de Limoges / *rapporteur*

Gheorghe ZAHARIA
Maître de Conférences à l'INSA de Rennes / Co-encadrant de thèse

Jean-François HELARD
Professeur à l'INSA de Rennes / Directeur de thèse

Study and optimization of new differential space-time modulation schemes based on the Weyl group for the second generation of MIMO systems

Hui JI

En partenariat avec

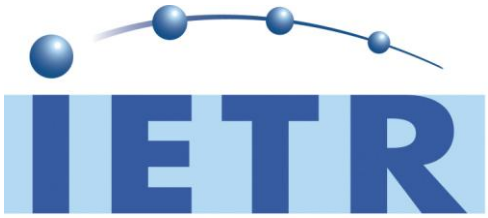

to my parents

Acknowledgement

My Ph.D. work could not have been completed without the support and encouragement from my family, friends and colleagues.

I would like to express my special appreciation and thanks to my advisors Prof. Jean-François Hélard and Maître de Conférences, Dr. Gheorghe Zaharia. At the difficult moments of my research, they provided me not only inspiring insights and ideas to overcome the technical problems, but also understanding and encouragement to help me stay strong towards the difficulty.

I would also like to thank my committee members, Prof. Marie-Laure Boucheret and Prof. Jean-Pierre Cancès for serving as my committee members even at hardship. I want to thank them for letting my defense be an enjoyable moment, and for their brilliant comments and suggestions.

I would like to thank my colleagues working at the IETR laboratory: Yaset Oliva, Mohamad Maaz, Bachir Habib, Mohamed El Mehdi Aichouch, Yvan Kokar and Roua Youssef for the friendly working environment, and for the nice discussions.

I thank my friends, Liu Ming, Peng Linning, Fu Hua, Xia Tian, Zhang Jinglin, Zhang Shunying, Zhao Yu, Wang Hongquan, Lian Caihua, Yi Xiaohui, Zou Wenbin, You Rong, Lu Weizhi, Li Weiyu, Bai Cong, Chu Xingrong, Zhang Xiaoli, Zhang Jiong, Sun Fan, Luo Yun, Bai Xiao, Wang Yu, R\'echo Jan, Driehaus Lena, Fan Xiao, Yao Dandan, Yuan Han, Wang Duo, Gu Qingyuan, Liu Wei, Liu Yi, Yang Yang, Wang Cheng, Tang Liang, Yao Zhigang, Fu Jia, Zhang Xu, Xu Jiali for their kind help and all the fun we have during the past years.

I would also like to thank Chinese Scholarship Council (CSC) for their funding support throughout my Ph.D. program.

At the end I would like express appreciation to my family, especially to my parents and my wife, for their unconditional love and endless support.

Contents

Résumé étendu en français **3**

1 Introduction **29**

1.1 Brief history of the wireless and mobile communications 29

1.2 Objectives and motivations 32

1.3 Overview of the thesis 34

1.4 The structure and outline 35

1.5 List of published papers 36

2 MIMO systems **37**

2.1 General model of a wireless communication system 37

2.1.1 Baseband representation of bandpass signals 39

2.1.2 Vector space representations 42

2.1.3 Channel model 43

2.2 Brief presentation of the history of MIMO systems 53

2.3 MIMO system model 58

2.4 Fundamentals of information theory 60

2.5 Capacity of MIMO communication channels 62

2.5.1 H is known to the receiver 63

2.5.2 H is unknown to the receiver 63

2.6 Error performance of MIMO systems 67

2.6.1 H is known to the receiver 67
2.6.2 H is unknown to the receiver 71
2.7 Conclusion 75

3 Non-coherent space-time coding **77**
3.1 Unitary space-time modulation 77
3.1.1 Transmission scheme 77
3.1.2 Detection scheme and design criteria of USTM constellations . 78
3.2 Differential unitary space-time modulation 80
3.2.1 Classical differential phase-shift keying 81
3.2.2 Multiple-antenna differential modulation 82
3.3 Differential space-time block code 88
3.3.1 Alamouti's STBC scheme 88
3.3.2 Differential transmission of Alamouti's STBC scheme 89
3.4 Matrix coded modulation 93
3.4.1 The transmission group of MCM 94
3.4.2 MCM with Hamming block coding 95
3.5 Conclusion 97

4 New differential space-time modulation with 2 transmit antennas **99**
4.1 General Model of Differential Space-Time Mo-dulation System . . . 99
4.2 The constellation for MIMO systems with 2 transmit antennas 101
4.3 Spectral efficiency $R = 2$ bps/Hz 104
4.3.1 Gray mapping 108
4.3.2 Justification of the design criterion 110
4.4 Spectral efficiency $R = 1$ and 3 bps/Hz 113
4.4.1 $R = 1$ bps/Hz 113
4.4.2 $R = 3$ bps/Hz 114
4.5 Conclusion 115

5 New DSTM with 4 and 8 transmit antennas **117**
5.1 Differential MIMO systems with 4 transmit antennas 117

5.1.1 Spectral efficiency $R = 1$ bps/Hz 120
5.1.2 DSTM for 4 transmit antennas with new mapping rule 124
5.1.3 DSTM for 4 transmit antennas with higher spectral efficiencies (R=2 and R=3) 126
5.2 Differential MIMO systems with 8 transmit antennas 128
5.3 Conclusion 130

6 New time-selective channel model 133
6.1 Usual channel model for differential MIMO systems 133
6.2 New and improved channel model 134
6.2.1 Time selective channel model 136
6.2.2 Block-constant MIMO channel model 137
6.2.3 Continuously changing MIMO channel model 142
6.3 Conclusion 146

Conclusion and prospect 147

A Gaussian random variables, vectors and matrices 153
A.1 Gaussian random variables 153
A.2 Gaussian random vectors 154
A.3 Gaussian random matrices 154

Résumé étendu en français

Chapitre 1 Introduction

Dans ce chapitre introductif on présente les motivations et les principales contributions des activités de recherche menées pendant cette thèse.

Dans un premier paragraphe on présence brièvement l'évolution des télécommunications sans fil à partir du 19e siècle.

Le deuxième paragraphe présente les objectifs et les motivations de l'étude. On indique d'abord les avantages des techniques MIMO: augmentation de la capacité du canal de transmission et de la robustesse des liaisons radio, grâce à la diversité d'espace. On introduit ensuite les deux types des systèmes MIMO, selon la connaissance (ou non) de l'état du canal de propagation (angl. CSI = Channel State Information). Si l'état du canal de propagation doit être connu (cas des systèmes MIMO dits «cohérents»), des signaux connus doivent être envoyés périodiquement pour l'estimation de la matrice de canal. Néanmoins, si le nombre des antennes augmente ou si le canal de propagation varie rapidement, l'estimation de la matrice de canal d'est plus très efficace. En plus, comme ce sondage périodique de canal nécessite un certain temps, la durée de la transmission des données utile plus au moins réduite et le débit utile des systèmes MIMO cohérent est diminué. Par conséquent, certains chercheurs (Marzetta, ensuite Hochwald et Sweldens) ont étudié des systèmes MIMO différentiels qui ne nécessitent pas la connaissance du canal de propagation. Pour ces systèmes, les colonnes des matrices transmises doivent être

unitaires. Ainsi, ils ont introduit les schémas DUSTM (Differential Unitary Space-Time Modulation). Il est également possible de combiner un code temps-espace avec un code correcteur d'erreurs pour des systèmes MIMO cohérents ou différentiel. C'est le cas des systèmes MIMO analysés par El Arab qui utilisent les matrices unitaires du groupe de Weyl de taille 2×2 et la technique MCM (Matrix Coded Modulation).

Dans le troisième paragraphe on décrit brièvement les principales contributions de la thèse:

1. En utilisant les matrices de taille 2×2 du groupe de Weyl on propose des systèmes MIMO différentiels avec 2, 4 et 8 antennes d'émission. Pour les systèmes MIMO avec 4 et 8 antennes d'émission, les groups de matrices unitaires sont obtenus en effectuant des produits de Kronecker des matrices du groupe de Weyl.

2. L'amélioration des performances des systèmes proposés est effectuée par la sélection des ensembles de matrices de transmission séparées par les plus grandes distances. Plus précisément, le critère de sélection des matrices est la distance minimale entre les matrices qui doit être maximisée.

3. Un autre critère utilisé pour l'amélioration des performances est la correspondance optimale entre les vecteurs binaires d'information et les matrices transmises. En effet, la hiérarchie entre les vecteurs binaires d'information établie selon la distance de Hamming doit correspondre à la hiérarchie entre les matrices de transmission.

4. Pour une évaluation réaliste des performances des systèmes proposés on considère une version améliorée du modèle de canal de propagation utilisé pour la simulation. D'habitude, les coefficients du canal de propagation suivent une loi de Rayleigh mais ils restent constants pendant un certain temps qui dépend du temps de cohérence du canal, donc de la vitesse de variation des conditions de propagation. Par contre, cette hypothèse ne correspond pas à la réalité. En plus, le passage d'une matrice de canal à la matrice de canal suivante impose une réinitialisation du système différentiel, situation qui ne

correspond non plus à la réalité. Afin d'éviter ces inconvénients et obtenir des estimations réalistes des performances, on accepte la variation des coefficients de la matrice de canal. Les valeurs intermédiaires des coefficients de canal entre 2 tirages aléatoires selon la loi de Rayleigh sont obtenues en utilisant le théorème d'échantillonnage. Les simulations effectuées montrent une certaine dégradation des performances des systèmes analysées par rapport aux performances obtenues en utilisant le modèle simple de canal considérant des valeurs constantes pendant un certain intervalle de temps. Cette dégradation est plus importante pour les canaux variant rapidement dans le temps (faible valeur du temps de cohérence normalisé par la durée d'un symbole émis).

Le quatrième paragraphe décrit le contenu de chaque chapitre de la thèse, tandis que le dernier paragraphe indique la liste des publications.

Chapitre 2 Systèmes MIMO

Dans ce chapitre on présente le schéma général d'un système de communications MIMO. Après une brève description des activités de recherche dédiées à l'étude des systèmes MIMO on rappelle les formules de calcul de capacité pour les systèmes MIMO cohérent et non-cohérent. Finalement, les performances des codes temps-espace sont analysées est quelques critères de qualité sont rappelés.

Le premier sous-chapitre rappelle la représentation en bande de base des signaux à bande limitée, ainsi que la relation entre le signal émis et le signal reçu dans le cas d'un canal de propagation variant dans le temps. La représentation des signaux à bande limitée dans un espace vectoriel N-dimensionnel est aussi rappelée. Quelques paramètres importants d'un canal de propagation sont aussi présentés: réponse impulsionnelle, trajets multiples, écart-type des retards (angl. RMS delay spread), évanouissements plats ou sélectifs en fréquence, décalage Doppler, temps de cohérence ou encore temps de cohérence par rapport à la durée d'un symbole émis. Dans le cas d'un canal de propagation avec un grand nombre de trajets, on démontre que la fonction d'autocorrélation statistique du signal reçu peut s'exprimer en fonction de la fonction de Bessel du premier ordre et du premier type et que

l'enveloppe du signal reçu suit une loi de Rayleigh en absence du trajet direct et une loi de Rice si ce trajet direct est présent. Le premier sous-chapitre se termine avec la représentation du bruit Gaussien pour les systèmes à bande limitée. Dans l'espace des signaux à bande limitée, en utilisant une base orthonormée d'ordre N, le bruit est représenté comme une variable aléatoire Gaussienne vectorielle de longueur N.

Le deuxième sous-chapitre présente une courte évolution des systèmes MIMO à partir des travaux de C. E. Shannon (1948). Au début, les systèmes MIMO étaient utilisés pour des applications sonar, radar ou sismiques. Leur utilisation pour les télécommunications à débuter dans les années 1970. Au niveau d'une station de base, les réseaux d'antennes assurent une diversité spatiale qui permet de lutter contre les effets de la propagation multi-trajet. On rappelle les contributions ce certains chercheurs à l'étude des systèmes MIMO: Winters (1987) qui a analysé la capacité du canal MIMO et a obtenu certains résultats intéressants, Teletar et Foschini (1995-1996) qui ont étudié la capacité du canal MIMO si le canal de propagation est connu par le récepteur, la technique BLAST (1996), Tarock (1998) qui a obtenu les critères de performance pour les codes temps-espace, Jafarkhani (2001) qui a introduit les codes les codes temps-espace en bloc super-orthogonaux (QO-STBC), etc. Les systèmes MIMO coopératifs et la nouvelle technique «massive MIMO »sont également rappelés et leurs avantages mentionnés. En même temps, l'utilisation des systèmes MIMO avec un grand nombre d'antennes diminue le débit utile et rend la connaissance en temps réel du canal plus difficile, surtout si le canal varie rapidement dans le temps. Par conséquent, des techniques MIMO qui ne nécessitent pas la connaissance du canal de propagation peuvent s'avérer intéressantes. On discute le modèle de canal ZMSW (zero mean spatially white) analysé par Zheng et Tse (2002) qui montrent que la capacité de canal peut être obtenue avec un nombre limité d'antennes. Les contributions de Lapidoth et Moser (2003) sont évoquées, ainsi que celles de Jafar et Goldsmith (2005).

Basés sur l'analyse de la capacité des systèmes MIMO avec le modèle ZMSW, Hochwald et Marzetta ont introduit en 2000 les schémas USTM (unitary space-time modulation) qui n'ont pas besoin de la connaissance du canal de propagation. Par contre, le problème à résoudre est la détermination des constellations de grande

taille qui assurent une faible probabilité d'erreur et une complexité de démodulation raisonnable. Il est possible de mentionner les contributions de Hochwald (2000), Tarokh (2002), Leus (2004) et Kim (2010) pour la génération des constellations plus simples à décoder tout en garantissant une faible probabilité d'erreur.

Enfin, pour les schémas MIMO différentiels on rappelle les schémas DUSTM proposés par Hochwald et Sweldens en (2000), les schémas DSTBC de Tarokh et Jafarkhani (2000-2001) qui généralisent le schéma d'Alamouti (1998) ou les schémas DSTM de Hughes (2000) utilisant des signaux PSK.

Enfin, on mentionne la modulation matricielle codée proposée par El Arab et Carlach (2011) utilisant des matrices unitaires du groupe de Weyl pour les systèmes MIMO de taille 2×2.

Le paragraphe suivant présente le modèle général d'un système MIMO, précise le modèle de canal de propagation utilisé et obtient la description matricielle relient le vecteur des signaux reçus du vecteur des symboles émis en présence du bruit blanc, additif, Gaussien. L'expression du rapport signal à bruit est aussi obtenue.

Le paragraphe 2.4 rappelle les notions d'information mutuelle moyenne et capacité pour un canal de transmission bruité. On donne la formule de calcul de la capacité pour un canal Gaussien.

Le paragraphe suivant donne les formule de calcul de capacité d'abord pour les systèmes MIMO cohérents, ensuite non-cohérents. Pour les systèmes MIMO cohérents on en déduit les critères du rang et du déterminant pour améliorer leur performance (diminuer la probabilité d'erreur). Pour les systèmes MIMO non-cohérents on indique le critère utilisé en réception pour minimiser la probabilité d'erreur (PEP = pair-wise error probability).

Chapitre 3 Codage temps-espace non-cohérent

Le codage temps-espace non-cohérent concerne les systèmes MIMO sans connaissance de la matrice de canal au niveau du récepteur. Parmi ces systèmes MIMO on peut citer ceux utilisant la modulation temps-espace unitaire (USTM), la modulation différentielle temps-espace unitaire (DUSTM), le codage différentiel temps-espace en

bloc (DSTBC), la modulation différentielle temps-espace (DSTM) et la modulation matricielle codée (MCM). L'idée utilisée par DUSTM et DSTM est la même.

Modulation unitaire espace-temps

Lors de l'analyse de la capacité des systèmes MIMO sans connaissance de la matrice de canal au niveau du récepteur Marzetta et Hochwald ont trouvé [25] que les matrices transmises doivent avoir une structure particulière: elles doivent être unitaires, d'où le terme de modulation unitaire espace-temps (USTM = Unitary Space-Time Modulation).

Schéma d'émission

Marzetta et Hochwald ont montré [25] que les matrices émises doivent avoir la structure $X = A\Theta$, où A est une matrice diagonale de taille $M \times M$ et Θ une matrice de taille $M \times T$. Les colonnes de la matrice Θ doivent être orthogonales entre elles : $\Theta\Theta^H = I_M$. Quand le temps de cohérence normalisé du canal est largement supérieur au nombre des antennes d'émission ou si $T > M$, avec un choix approprié des valeurs $a_k (k = 1, 2, ..., M)$ il est possible d'atteindre la capacité du canal.

Schéma de détection de détermination des constellations USTM

A partir du vecteur Y reçu, le récepteur détermine la matrice Θ_k qui maximise la probabilité $p(Y|\Theta_k)$:

$$\begin{aligned} \Theta_{ml} &= \arg \max_{\Theta_k \in \{\Theta_1, ..., \Theta_K\}} p(Y|\Theta_k) \\ &= \arg \max_{\Theta_k \in \{\Theta_1, ..., \Theta_K\}} \mathrm{Tr}[Y\Theta_k^H \Theta_k Y^H]. \end{aligned} \tag{3.1}$$

La probabilité d'erreur (PEP = pairwise error probability) est :

$$\begin{aligned} P_e =& \frac{1}{2} P\left(\mathrm{Tr}[Y\Theta_{k'}^H \Theta_{k'} Y^H] > \mathrm{Tr}[Y\Theta_k^H \Theta_k Y^H] | \Theta_k\right) \\ &+ \frac{1}{2} P\left(\mathrm{Tr}[Y\Theta_k^H \Theta_k Y^H] > \mathrm{Tr}[Y\Theta_{k'}^H \Theta_{k'} Y^H] | \Theta_{k'}\right), \end{aligned} \tag{3.2}$$

A partir de la borne supérieure de cette probabilité d'erreur (Chernoff upper bound), il est possible d'identifier deux critères pour la détermination des constellations USTM. Le premier critère doit minimiser:

$$\delta = \max_{1\leq k<k'\leq K} \frac{1}{\sqrt{M}} \|\Theta_k \Theta_{k'}^H\| = \max_{1\leq k<k'\leq K} \sqrt{\frac{1}{M}\sum_{m=1}^{M} d_{kk',m}^2}, \tag{3.4}$$

où $d_{kk',1}, \ldots, d_{kk',M}$ sont les valeurs singulières du produit $\Theta_k \Theta_{k'}^H$.

Un deuxième critère repose sur la maximisation du produit de diversité :

$$\zeta_{kk'}^2 = 1 - \frac{1}{M}\sum_{m=1}^{M} d_{kk',m}^2 + O(d_{kk',m}^4) = 1 - \frac{1}{M}\|\Theta_k \Theta_{k'}^H\|^2 + O(d_{kk',m}^4). \tag{3.5}$$

Modulation DUST

A partir de la modulation DPSK et des schémas USTM, Hochwald et Sweldens ont proposé [27] la modulation USTM différentielle, nommée DUSTM.

On explique d'abord la modulation PSK différentielle, ensuite, par analogie, on présente la modulation UST différentielle. Dans les deux cas, la condition principale est de pouvoir considérer le canal pratiquement invariant lors de la transmission de deux symboles successifs.

Pour la modulation DPSK, la relation utilisée en réception lors du décodage est:

$$\hat{\varphi}_{t+1} = \arg \min_{k=1,\ldots,K} |y_{t+1} - \varphi_k y_t|. \tag{3.13}$$

Pour la modulation DUSTM, la relation utilisée en réception lors du décodage est:

$$\begin{aligned}
\hat{V}_t &= \arg \min_{V_k \in \{V_1,\ldots,V_k\}} \|Y_t - Y_{t-1}V_k\| \\
&= \arg \min_{V_k \in \{V_1,\ldots,V_k\}} \mathrm{Tr}\{(Y_t - Y_{t-1}V_k)(Y_t - Y_{t-1}V_k)^H\} \\
&= \arg \max_{V_k \in \{V_1,\ldots,V_k\}} \Re\{\mathrm{Tr}[Y_{t-1}V_k Y_t^H]\} \\
&= \arg \max_{V_k \in \{V_1,\ldots,V_k\}} \Re\{\mathrm{Tr}[Y_t^H Y_{t-1}V_k]\}.
\end{aligned} \tag{3.17}$$

où Y_t et Y_{t-1} sont les matrices reçues aux instants t, respectivement $t-1$ et V_t l'une des matrices d'information. La matrice recherchée est donc la matrice qui minimise la norme de la matrice de la relation (3.17).

On démontre par la suite les deux critères qu'on peut utiliser pour identifier de bons ensembles de matrices d'information. Le premier critère impose la maximisation de la distance minimale entre deux matrices quelconques mais distinctes choisies dans l'ensemble des matrices d'information. Le deuxième critère impose la minimalisation du produit de diversité:

$$\zeta = \frac{1}{2} \min_{1 \leq k < k' \leq K} \zeta_{kk'} = \frac{1}{2} \min_{1 \leq k < k' \leq K} |\det(V_k - V_{k'})|^{\frac{1}{M}} . \tag{3.25}$$

Dans leurs travaux [27], Hochwald et Sweldens ont proposé un groupe cyclique de matrices où la matrice génératrice V est la racine d'ordre K de la matrice unité I_M : $V^K = I_M$. Les matrices d'information utilisées sont donc $V_k = V_1^k$, avec $k = 0, ..., K-1$. Pour $M = 1, 2, ..., 5$ et pour $R = 1, 2$, Hochwald et Sweldens ont déterminé par recherche exhaustive les meilleures matrices à utiliser pour obtenir les performances optimales. Les résultats sont donnés dans le Tableau 3.1. Les performances obtenues avec ces ensembles de matrices sont indiquées dans la Figure 3.1 (pour $R = 1$) et dans la Figure 3.2 (pour $R = 2$).

Code temps espace en bloc différentiel

En se basant sur le schéma d'Alamouti [18], Tarkh et Jafarkhani [28, 29] ont proposé un schéma différentiel pour les codes temps-espace en bloc (STBC = Space Time Block Codes).

Transmission différentielle avec le schéma STBC d'Alamouti

Après avoir présenté le schéma classique d'Alamouti, on décrit le fonctionnement du schéma différentiel basé sur le schéma d'Alamouti. En utilisant les modulations MDP2 (BPSK) et MDP4 (4PSK), on simule les performances des systèmes d'Alamouti et différentiels pour M = 2 et M = 4. Les résultats sont indiqués à la Figure 3.3. Pour les schémas différentiels on met en évidence (comme attendu) une

dégradation des performances de 3 dB.

Modulation Codée Matricielle

La modulation codée matricielle, proposée par A. El Arab, J-C Carlach et M. Hélard [30, 31] combine le codage de canal, la modulation et le codage temps-espace dans une unique fonction appliquée principalement aux systèmes MIMO non-cohérents. Le codage de canal est appliqué au plus des données binaires à transmettre. Si, par exemple, on utilise un code de Hamming H(8, 4, 4), on divise d'abord le flux binaire en vecteurs d'information de 4 bits qui sont codés. Après codage, pour chaque vecteur de 4 bits d'information on obtient un vecteur de 4 bits de contrôle. Ces 2 flux de données (d'information et de contrôle) sont appliqués à des entre-laceurs π_p et π_q et codés par la suite dans des paires de matrices inversibles (V_α, V_β) de taille 2×2. Ces deux matrices sont ensuite transmise par $M = 2$ antennes d'émission: $X_t = V_\alpha$ et $X_{t+1} = V_\beta$. Les matrices V_α et V_β appartiennent à des cosets C_p et C_q différents du groupe de matrices de Weyl. Le choix des couples (π_p, π_q) et (C_p, C_q) n'est pas indifférent. En effet, pour chaque couple (V_α, V_β) du produit cartésien $C_p \times C_q$, le couple (V_a, V_b) du même produit cartésien vérifiant la relation

$$V_\alpha V_a^{-1} - V_\beta V_b^{-1} = 0$$

doit être unique. A la réception, en utilisant les matrices reçues on vérifie cette relation pour la détection des matrices transmises.

Cette modulation a été utilisée seulement pour les systèmes MIMO de taille 2×2 à cause de la taille des matrices du groupe de Weyl. La structure de ce groupe unitaire de matrices est expliquée en précisant le mode de construction du sous-groupe C_0 et des autres cosets. Pour $N = 2$ antennes de réception on décrit la construction des mots de code pour le code correcteur d'une erreur et détecteur d'erreurs doubles H(8,4,4). On indique aussi la paire des permutations (π_p, π_q) utilisées pour l'entrelacement et le choix du couple de cosets (C_p, C_q) à utiliser pour vérifier la relation matricielle ci-dessus. La formule permettant le décodage est aussi obtenue.

L'analyse du groupe de matrices de Weyl nous a suggéré leur utilisation pour les

modulations temps-espace unitaires différentielles. Ces modulations différentielles seront présentées pour différentes valeurs de l'efficacité spectrale. Dans cette thèse les performances des systèmes MIMO différentiels seront analysées pour $M = 2, 4$ et 8 antennes d'émission sans l'utilisation des codes correcteurs d'erreurs. Pourtant le rajout d'un code correcteur d'erreur reste possible. Il pourrait s'appliquer directement au flux de données binaires avant le codage temps-espace différentiel. Au niveau du récepteur, le décodage correcteur d'erreurs devrait se faire après le décodage temps-espace différentiel. Pour $M = 4$ et 8 (et, en général, pour $M = 2k$ antennes d'émission, où $k \geq 2$ est un nombre entier), il suffit d'effectuer des produits de Kronecker des matrices du groupe de Weyl, comme il sera expliqué dans les chapitres suivants.

Chapitre 4 Nouvelle modulation temps-espace différentielle avec 2 antennes d'émission

Dans ce chapitre on propose la nouvelle modulation temps-espace différentielle pour les systèmes MIMO avec 2 antennes d'émission. Les matrices d'information associées aux vecteurs binaires sont des éléments du groupe de Weyl. Afin de réduire le taux d'erreur binaire (TEB), on utilise one correspondance (*angl.* mapping) de type Gray entre les vecteurs binaires et les matrices d'information. Le TEB peut être encore amélioré en utilisant, selon l'efficacité spectrale souhaitée, des ensembles de matrices d'information ayant le meilleur spectre de distances (des matrices séparées par les plus grandes distances). Un deuxième critère pour déterminer les meilleurs ensembles de matrices est le produit de diversité (*angl.* diversity product). Une comparaison avec les performances d'autres systèmes DSTBC et DUSTM montre les avantages des schémas proposés.

Modèle général d'un système à modulation temps-espace différentielle

Ce modèle est basé sur l'équation différentielle (2.59) du chapitre 2 :

$$Y = HX + W$$

Dans le cas général, la matrice X transmise est de taille $M \times M$, M étant le nombre d'antennes d'émission. Le flux des données binaires à transmettre est «coupé »en vecteurs binaires d'une certaine longueur et à chaque vecteur binaire on met en correspondance bijective une matrice d'information V sélectionnée dans un ensemble P. Au début, l'émetteur transmet une matrice de référence $X_0 = V_0$ à l'instant τ_0. Au premier vecteur binaire d'information on associe une matrice d'information V_{τ_1}, au second vecteur binaire d'information une matrice d'information V_{τ_2}, etc. La relation fondamentale de la transmission différentielle est:

$$X_{\tau+1} = X_\tau V_{i_{\tau+1}}, \quad \tau = 0, 1, \ldots \tag{4.1}$$

Les N antennes du récepteur reçoivent le flux de matrices $Y_0, \ldots, Y_\tau, Y_{\tau+1}, \ldots$ Selon la relation (2.59) on peut écrire:

$$Y_\tau = H_\tau X_\tau + W_\tau \tag{4.2}$$

et

$$Y_{\tau+1} = H_{\tau+1} X_{\tau+1} + W_{\tau+1} \tag{4.3}$$

Dans l'hypothèse que le canal de propagation peut être considéré invariant pendant l'émission de 2 matrices successives (donc, pendant l'émission de $2M$ symboles

de la constellation), on en déduit:

$$\begin{aligned} Y_{\tau+1} &= HX_{\tau+1} + W_{\tau+1} = HX_\tau V_{i_{\tau+1}} + W_{\tau+1} \\ &= (Y_\tau - W_\tau)V_{i_{\tau+1}} + W_{\tau+1} = Y_\tau V_{i_{\tau+1}} + W_{\tau+1} - W_\tau V_{i_{\tau+1}} \\ &= Y_\tau V_{i_{\tau+1}} + W'_{\tau+1}, \end{aligned} \tag{4.4}$$

où $W'_{\tau+1} = W_{\tau+1} - W_\tau V_{i_{\tau+1}}$. Cette relation conduit à la relation utilisée par le récepteur pour la prise de décision:

$$\begin{aligned} \hat{V}_{i_{\tau+1}} &= \arg\min_{V\in P} \|Y_{\tau+1} - Y_\tau V\| \\ &= \arg\min_{V\in P} \mathrm{Tr}\{(Y_{\tau+1} - Y_\tau V)^H (Y_{\tau+1} - Y_\tau V)\} \\ &= \arg\max_{V\in P} \mathrm{Tr}\{\mathrm{Re}(Y_{\tau+1}^H Y_\tau V)\}. \end{aligned} \tag{4.5}$$

La constellation pour les systèmes MIMO avec 2 antennes d'émission

Pour les systèmes MIMO avec 2 antennes d'émission, les matrices utilisées sont des éléments du groupe de Weyl. Il s'agit d'un groupe de 192 matrices unitaires complexes. Le maximum de l'efficacité spectrale est $R = 3,5$ bit/s/Hz. Ce groupe contient un sous-groupe C_0 de 16 matrices. Ce sous-groupe permet d'effectuer une partition du groupe de Weyl (noté par la suite G_w) en 12 cosets, le premier coset étant C_0. On peut vérifier que toute matrice V de C_0 est à une distance de 2 de 14 autres matrices de C_0 et à une distance de $2\sqrt{2} = 2.8284$ de $-V$. Afin d'identifier les meilleurs sous-ensembles de matrices à utiliser pour différentes valeurs de l'efficacité spectrale, le spectre des distances a été calculé pour les matrices du G_w. On a pu vérifier que chaque matrice de G_w a le même spectre des distances par rapport aux autres matrices de G_w. Ce spectre des distances est indiqué dans le tableau 4.1.

Efficacité spectrale R = 2 bit/s/Hz

Dans ce cas, les vecteurs binaires d'informations contiennent 4 bits. On peut avoir $2^4 = 16$ vecteurs d'information, donc il est nécessaire d'utiliser 16 matrices. Il a été

vérifié que C_0 est le sous-ensemble de G_w qui a le meilleur spectre de distances (la plus grande distance minimale entre 2 matrices distinctes de C_0). Par conséquent, les matrices de C_0 sont utilisées. Pour ces matrices, la constellation utilisée est 4PSK $\cup$ $\{0\}$. Ceci revient à dire que pendant la durée T_s de l'émission d'un symbole, seulement une antenne émet un signal de la constellation 4PSK avec la puissance normalisée égale à 1.

Le Tableau 4.2. indique la correspondance utilisée initialement entre les vecteurs binaires d'information et les matrices du sous-groupe C_0. Les distances entre les matrices du sous-groupe C_0 sont données dans la Tableau 4.3.

Le résultat de simulation pour ce schéma différentiel est indiqué à la figure 4.3.

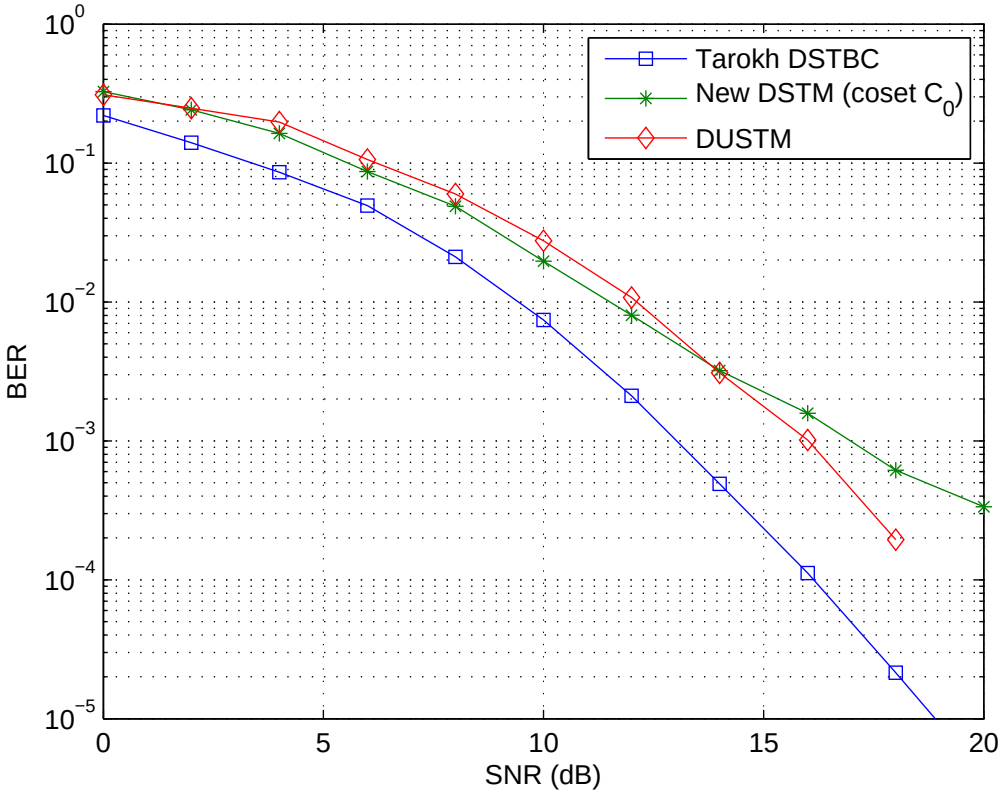

Figure 4.3.

Pour comparaison, on indique également la variation du TEB en fonction du SNR (dB) pour les schémas DSTBC [28] et DUSTM [27]. Par rapport au schéma DSTBC proposé par Tarokh, le résultat du schéma proposé est moins bon car aucune méthode de prétraitement n'est utilisée. Par contre, pour SNR inférieur à 14 dB,

le schéma proposé a des performances légèrement meilleures par rapport au schéma DUSTM. En effet, ce schéma DUSTM a été proposé pour des valeurs SNR élevées, selon le deuxième critère.

Codage de Gray

La correspondance entre les vecteurs binaires et les matrices du sous-groupe C_0 peut être améliorée en utilisant la même idée utilisée lors du codage de Gray. Plus précisément, on calcule la distance de Hamming entre les vecteurs binaires et on tient compte des distances entre les matrices de C_0 données dans le Tableau 4.3. Aux vecteurs séparés par une faible distance de Hamming on utilise des matrices de C_0 séparées par une faible distance, pour des vecteurs binaires séparés par une grande distance de Hamming on utilise des matrices de C_0 séparées par une grande distance. La nouvelle correspondance est donnée dans le Tableau 4.4, tandis que le résultat de la simulation avec cette nouvelle correspondance est donné à la Fig. 4.5. Par rapport au premier cas on observe une légère amélioration.

Le critère basé sur la distance

Dans ce paragraphe on décrit une étude qui permet de comparer les performances des 2 systèmes MIMO avec $R = 2$ bit/s/Hz. Le premier système utilise le sous-groupe C_0. Dans ce sous-groupe, chaque matrice est séparée par la matrice opposée par une distance $2\sqrt{2} = 2.8284$, tandis que par rapport aux autres matrices de C_0, elle a une distance de 2. Pour l'ensemble S considéré comme possible contra-candidat de C_0, la distance maximale entre une matrice et sa matrice opposée est toujours 2, par contre, par rapport aux autres matrices on a des distances de $\sqrt{2} = 1.4142 < 2$ et des distances de $\sqrt{6} = 2.4495 > 2$. Le résultat de simulation est donné à la figure 4.6 pour les deux ensembles utilisés C_0 et S. On constate que l'utilisation de l'ensemble S donne un résultat légèrement moins bon, ce qui prouve que la distance minimale $\sqrt{2} = 1.4142$ compte plus que la distance maximale $\sqrt{6} = 2.4495$. On retrouve le fait que le critère à utiliser est de maximiser la plus faible distance entre 2 matrices de l'ensemble considéré.

Le critère basé sur le produit de diversité

Suivant ce critère on construit un sous-ensemble de matrices S_d qui a un produit de diversité plus grand, de 0.5, valeur plus grande que la valeur 0.3826 utilisée pour le schéma DUSTM [27]. On compare dans la Fig. 4.7 les courbes BER en fonction du SNR pour le nouveau schéma utilisant les sous-ensembles de matrices S_d et C_0, ainsi que le schéma DUSTM. Le meilleur résultat est obtenu avec le sous-ensemble Sd. En effet, pour BER = 10^{-3}, le SNR du nouveau schéma réalisé avec le sous-ensemble de matrices Sd est 2 dB plus faible par rapport au schéma USTM et 3 dB plus faible par rapport au schéma DSTM utilisant le sous-ensemble C_0.

Efficacité spectrale $R = 1$ et 3 bit/s/Hz

$R = 1$ **bit/s/Hz**

Dans ce cas, les vecteurs binaires ont seulement 2 bits et 4 matrices sont utilisées. Selon le critère de distance, on utilise la matrice unitaire M_0 et la matrice opposée $M_4 = -M_0$ et on cherche on couple de matrices $(M_l, -M_l)$ qui, avec le couple $(M_0, -M_0)$ va donner les plus grandes distances. On constate que si la distance $D(M_0, M_l) > 2$, alors $D(M_4, M_l) < 2$. Par conséquent, on doit choisir la matrice M_l tel que $D(M_0, M_l) = 2$ et $D(M_4, M_l) = 2$. Selon la Tableau 4.1 on dispose de 102 matrices M_l (51 couples) pour lesquelles on a $D(M_0, M_l) = D(M_4, M_l) = 2$. Avec le deuxième critère, il est possible de sélectionner parmi ces 51 couples de matrices ceux qui maximisent le produit de diversité. On trouve 10 couples qui donnent avec (M_0, M_4) le produit de diversité maximum $\sqrt{2}/2$. Une solution possible est l'ensemble $\{M_0, M_4, M_8, M_{12}\}$. Dans le Tableau 4.6 on indique la correspondance «générale »ou «naturelle »entre les vecteurs binaires et les 4 matrices retenues mais aussi la correspondance de type Gray. Les résultats de simulation donnés à la Fig. 4.8 montrent que la correspondance de type Gray permet d'obtenir un meilleur résultat.

$R = 3$ **bit/s/Hz**

Pour $R = 3$ bit/s/Hz, les vecteurs d'information ont 6 bits et on utilise $2^6 = 64$ matrices. En utilisant les premières 64 matrices du groupe de Weyl, la simulation

effectuée permet l'évaluation des performances de ce système.

Chapitre 5 Nouvelle DSTM avec 4 et 8 antennes d'émission

Dans ce chapitre on étend les schémas obtenus dans le chapitre précédent aux systèmes MIMO avec 4 et 8 antennes d'émission. L'idée est des générer des groupes de matrices de taille 4×4 et 8×8 en effectuant des produits de Kronecker des matrices de taille 2×2 du groupe de Weyl. Une fois ces groupes de matrices déterminés, la démarche est similaire à celle utilisée dans le chapitre 4.

Systèmes MIMO différentiels avec 4 antennes d'émission

Dans un premier temps on définit le produit de Kronecker de deux matrices complexes de taille quelconque et on rappelle ses principales propriétés. On énonce et on démontre 2 théorèmes reliant la distance entre les matrices et le produit de Kronecker. Le deuxième théorème est d'une grande utilité. En effet, si dans le groupe de Weyl on a identifié un sous-ensemble S_n de n matrices ayant le meilleur spectre de distances, comme $\|M\| = \sqrt{2}$ pour toute matrice du groupe de Weyl, on en déduit aisément que le produit de Kronecker entre une matrice M quelconque de G_w et les matrices de S_n va générer un ensemble Σ_n de matrices de G_{w4} ayant aussi le meilleur spectre des distances. De même, le produit de Kronecker entre une matrice M quelconque de G_w et les matrices de Σ_n va générer un ensemble de matrices de G_{w8} ayant aussi le meilleur spectre des distances. Ainsi, l'identification des sous-ensembles de matrices ayant le meilleur spectre des distances devient très simple, le travail effectué pour les meilleurs sous-ensembles de G_w pouvant être utilisé par la suite.

Le produit de Kronecker entre les 192 matrices de G_w devrait donner 192^2 matrices de taille 4×4. En réalité, seulement $K = 4608$ matrices sont distinctes. On en déduit que pour $M = 4$ antennes d'émission on a une efficacité spectrale de maximum 3 bit/s/Hz.

Efficacité spectrale $R = 1$ bit/s/Hz

Dans ce cas on doit disposer de $2^{RM} = 16$ matrices distinctes. Comme dans Gw nous avons identifié C_0 comme étant le sous-ensemble avec le meilleur spectre de distances, le produit de Kronecker entre M_0 (matrice unité) et C_0 permet d'obtenir facilement un sous-ensemble C_{00} de G_{w4} ayant aussi le meilleur spectre de distances. Grâce au premier théorème, le spectre des distances des matrices de C_{00} s'obtient facilement en multipliant par $\|M\| = \sqrt{2}$ les distances entre les matrices de C_0 données au Tableau 4.3. Les résultats sont donnés au Tableau 5.1. Il est aussi intéressant de remarquer que le produit de Kronecker conserve pour chaque antenne d'émission la constellation utilisée par les systèmes MIMO avec 2 antennes d'émission : 4PSK $\cup \{0\}$. Comme pour les systèmes à 2 antennes d'émission, en utilisant les matrices du sous-ensemble C_{00}, à chaque instant, seulement une antenne Tx va émettre. Dans le tableau 5.2 on indique une correspondance «naturelle» entre les 16 vecteurs d'information de 4 bits et les 16 matrices du groupe G_{w4}. Avec cette correspondance, le résultat de la simulation pour une antenne de réception donné à la figure 5.1 montre que les performances du système sont moins bonnes que celles des systèmes DUSTM et DSTBC avec modulation BPSK. On étudie ensuite la possibilité de déterminer le sous-ensemble de matrices de G_{w4} en utilisant le critère du produit de diversité. On arrive à l'ensemble S_{div} indiqué par la relation:

$$\begin{aligned} S_{div} =& M_0 \otimes \{M_0, M_4, M_3, M_7, M_9, M_{13}, M_{10}, M_{14}\} \\ & \cup M_1 \otimes \{M_{33}, M_{37}, M_{34}, M_{38}, M_{40}, M_{44}, M_{43}, M_{47}\}. \end{aligned} \tag{5.11}$$

Le produit de diversité pour cet ensemble est $\zeta = \frac{1}{2} \min_{0 \leq k < k' \leq 16} |\det(V_k - V_{k'})|^{\frac{1}{M}} = 0.5946$, $V_k \in S_{div}$. Le résultat de la simulation est indiqué dans la figure 5.2.

On constate que cette fois le schéma DSTM proposé permet d'obtenir de meilleures performances par rapport aux schémas DSTBC [29] et DUSTM [27]. En effet, pour, le schéma propose assure un BER $= 10^{-3}$.

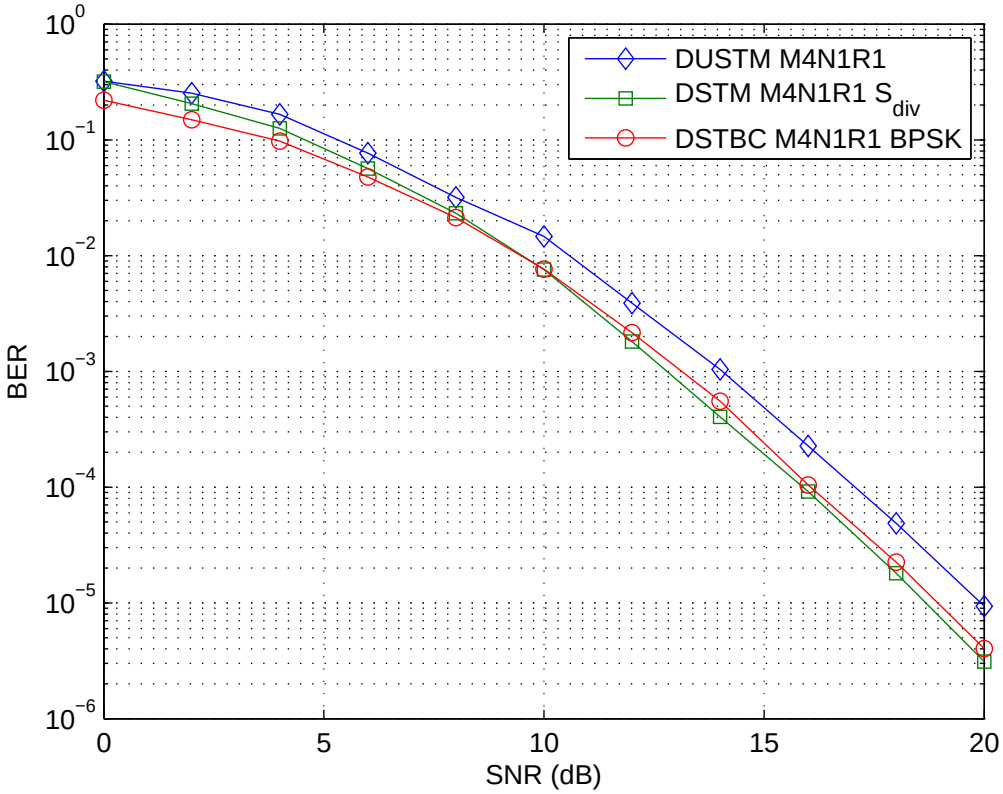

Figure 5.2 Comparison of DSTBC [29], DUSTM [27] and new DSTM scheme with set S_{div} (M=4, N=1, R=1)

DSTM pour 4 antennes d'émission avec nouvelle correspondance

Comme pour les systèmes à 2 antennes d'émission, il est possible d'optimiser la correspondance entre les 16 vecteurs de 4 bits et les matrices d'information de taille 4×4 de C_{00}. L'idée est la même : aux vecteurs binaires séparés par la plus grande distance de Hamming on met en correspondance les matrices séparées par la plus grande distance Euclidienne, c'est-à-dire 4. Pour les vecteurs binaires séparés par une distance de Hamming plus faible on met en correspondance les matrices séparées par une plus faible distance Euclidienne, c'est-à-dire, c'est-à-dire $2\sqrt{2}$. Le résultat de simulation donné à la figure 5.3 indique une légère amélioration des performances, car seulement 2 distances Euclidiennes sont possibles pour les 16 matrices de C_{00}.

DSTM pour 4 antennes d'émission et efficacité spectrale plus grande ($R = 2$ et $R = 3$)

Pour $R = 2$ bit/s/Hz, les vecteurs d'information ont 8 bits, donc $2^8 = 256$ matrices doivent être utilisées. Le choix simple serait de sélectionner les premières 256 matrices de G_{w4}.

Pour $R = 3$ bit/s/Hz, les vecteurs d'information ont 12 bits, donc $2^{12} = 4096$ matrices doivent être utilisées. Le choix simple serait de sélectionner dans ce cas les premières 4096 matrices de G_{w4}.

Les performances des systèmes MIMO ainsi obtenus sont données dans la Figure 5.4.

Afin d'améliorer les performances des systèmes conçus pour $R = 2$ bit/s/Hz, on utilise les deux critères: distance Euclidienne et produit de diversité. Pour le premier critère, on vérifie d'abord que la distance minimale qui sépare deux matrices de G_{w4} est de 1.5307. On identifie ainsi l'ensemble S_2 qui a 256 matrices et $d_{min} = 2$. La Figure 5.5 permet de remarquer l'amélioration des performances par rapport au cas précédent qui utilisait l'ensemble S_1 de matrices. Par rapport au schéma DUSTM [27], le schéma proposé a aussi des performances meilleures.

Concernant le critère du produit de diversité, pour tous les ensembles de 256 matrices on obtient ce produit nul, donc il n'est pas possible d'utiliser ce critère.

Pour $R = 3$ bit/s/Hz, dans la référence [27] on ne peut pas trouver un schéma, donc on n'a pas la possibilité de comparer les performances du système proposé.

Systèmes MIMO différentiels avec 8 antennes d'émission

Pour ces systèmes à 8 antennes d'émission il faut d'abord créer le groupe de matrices unitaires en effectuant le produit de Kronecker entre G_w et G_{w4}. On obtient 884736 matrices de taille 8×8 mais seulement 110592 matrices sont distinctes. On obtient une efficacité spectrale maximale $R_{max} = 2$ bit/s/Hz.

Pour $R = 0.5$ bit/s/Hz on utilise 16 vecteurs de 4 bits, donc 16 matrices de taille 8×8. Ces matrices sont des éléments de l'ensemble $S_{000} = M_0 \times (M_0 \times C_0)$ séparées par la plus grande distance minimale: $d_{min} = 4$. Selon le critère de la

distance Euclidienne, l'ensemble S_{000} est optimal. Par contre, cet ensemble a le produit de diversité nul. Pour améliorer encore les performances du système on utilise $S_{div2} = M_0 \times S_{div}$ comme un nouveau ensemble de matrices qui a le produit de diversité de 0.1487. Les résultats de simulation des systèmes utilisant ces ensembles de matrices sont donnés à la Figure 5.6. On constate l'amélioration des performances du système lors de l'utilisation de l'ensemble S_{div2}.

Pour $R = 1$ bit/s/Hz on utilise des vecteurs de 8 bits, donc 256 matrices. Dans un premier temps on utilise le sous-ensemble $S_{m8r1a} = M_0 \times S_1$. Ensuite, afin d'augmenter la plus faible valeur des distances séparant 2 matrices on utilise le sous-ensemble $S_{m8r1b} = M_0 \times S_2$. Ces sous-ensembles ont $d_min = 2.1648$, respectivement 2.8284. Finalement, on identifie le sous-ensemble Sm8r1c de 256 matrices avec $d_{min} = 4$.

Les résultats de simulation pour ces 3 cas sont représentés à la Figure 5.7.

Pour $R = 1.5$ bit/s/Hz on utilise les premières 4096 matrices de C_{000}, tandis que pour $R = 2$ bit/s/Hz on utilise les premières 65536 matrices de G_{w8}. Les résultats de simulation pour ces deux cas sont donnés à la Figure 5.8.

Chapitre 6 Nouveau modèle de canal pour modulation temps-espace différentielle

Dans ce chapitre on propose un nouveau modèle de canal pour la simulation des systèmes MIMO proposés pour 2, 4 et 8 antennes d'émission.

En effet, dans la littérature, la simulation des systèmes MIMO se fait souvent [28, 106, 107] en utilisant des canaux de propagation supposés invariants dans le temps pendant l'émission d'un certain nombre L de symboles qui dépend du temps de cohérence du canal, donc de sa vitesse de variation. Ceci revient à dire que lors de l'émission de L symboles successives on utilise la même matrice de canal. Pour les L symboles successifs suivant on utilise une autre matrice de canal obtenue par tirage aléatoire indépendant des tirages précédents. Bien que cette façon de procéder soit simple, elle ne correspond pas à la réalité, car le canal varie dans le

temps en permanence. En plus, pour les systèmes différentiels, ce changement brutal de la matrice de canal impose une réinitialisation du système, donc l'émission d'une matrice de référence (la matrice identité de taille $M \times M$). Cette réinitialisation ne correspond non plus à la réalité.

Dans [26, 27] pour la simulation des performances des systèmes MIMO considérés on utilise le modèle de Jakes. Ce modèle considère les coefficients de la matrice de canal indépendants spatialement mais corrélés dans le temps avec la fonction d'auto-corrélation $J_0(2\pi f_d t)$, où $J_0(x)$ est la fonction de Bessel d'ordre zéro du premier type et f_d la fréquence Doppler maximale. Le modèle de Jakes considère la réponse impulsionnelle d'un canal SISO comme une somme de sinusoïdes. C'est une version simplifiée du modèle de Clarke [108] utilisé pour la simulation d'un canal de Rayleigh.

Nouveau modèle de canal amélioré

Comme le modèle de canal de Rayleigh constant pendant un intervalle de temps déterminé par le temps de cohérence est trop simple pour être réaliste, on préfère s'approcher du cas réel en considérant que la matrice de canal peut être différente pour chaque matrice de transmission. Dans un premier temps on accepte que cette matrice de canal reste constante pendant l'émission d'une matrice de transmission mais elle peut être différente lors de l'émission de la matrice de transmission suivante. Plus précisément, on utilise des matrices de canal R_k donc les coefficients sont des variables de Rayleigh indépendantes. Sur l'axe du temps, l'écart entre deux matrices successives R_K et R_{K+1} est déterminé par le temps de cohérence du canal, donc par sa vitesse de variation. Ces matrices peuvent être considérées comme des échantillons de la matrice du canal MIMO qui varie dans le temps. En respectant le théorème de l'échantillonnage, des valeurs intermédiaires de la matrice de canal peuvent être déterminées. Le nombre N_m des matrices de transmission de taille $M \times M$ émises entre R_K et R_{K+1} doit vérifier l'inégalité

$$N_m M T_s \leq T_0$$

où M = nombre des antennes d'émission, T_s = durée d'un symbole émis et $T_0 = 1/f_0$, f_0 étant la fréquence d'échantillonnage qui doit vérifier la condition $f_0 > 2f_d$. La première matrice de transmission sera affectée par la matrice de canal R_K, les autres $N_m - 1$ matrices de transmission seront affectées par les matrices intermédiaires $H(i)$, avec $1 \leq i \leq N_{max} - 1$. Les matrices RK doivent se retrouver sur l'axe du temps aussi bien avant et après les matrices de canal $H(i)$ intermédiaires, placées entre R_K et R_{K+1}, comme indiqué dans la Figure 6.4:

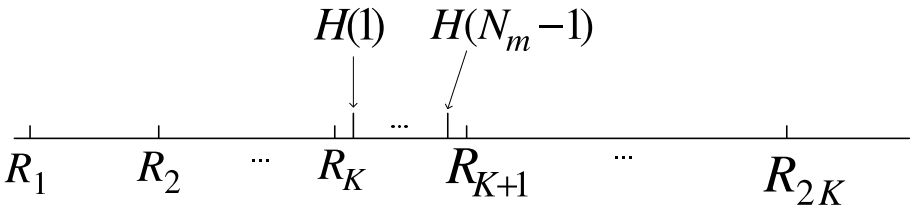

Figure 6.4 : Illustration de l'interpolation des matrices de canal $H(i)$, $1 \leq i \leq N_{max} - 1$.

Selon le théorème d'échantillonnage, le nombre des matrices R_K à utiliser pour le calcul des matrices de canal intermédiaires devrait être infini. On doit donc déterminer un nombre maximum Kmax et utiliser pour l'interpolation K_{max} matrices R_K placées avant les matrices $H(i)$ intermédiaires et K_{max} matrices R_K placées après les matrices $H(i)$. Le nombre K_{max} est déterminé pour avoir une erreur relative acceptable. Pour une erreur relative maximale inférieure à 10%, on démontre qu'il suffit de prendre $K_{max} = 30$.

En effectuant la simulation des systèmes MIMO différentiels avec 2, 4 et 8 antennes d'émission pour une efficacité spectrale $R = 2$ bit/s/Hz, il est possible de remarquer à la Figure 6.9 une dégradation supplémentaire des performances en utilisant ce nouveau modèle de canal.

Il est aussi intéressant de remarquer que cette dégradation des performances est accentuée pour les canaux de propagation variant rapidement dans le temps, donc caractérisés par un temps de cohérence réduit. La Figure 6.10 permet de mettre en évidence cette dégradation des performances pour différentes valeurs du temps de cohérence normalisé.

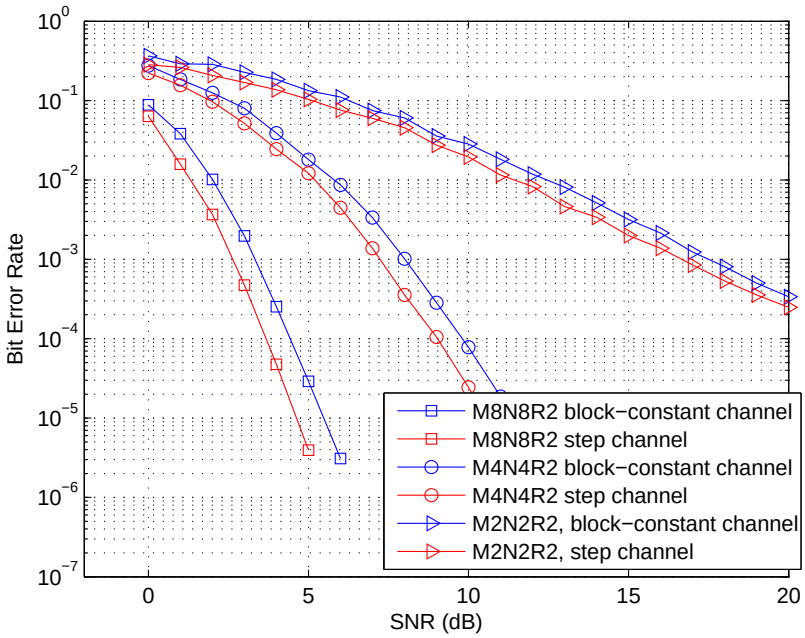

Figure 6.9: Performances des systèmes temps-espaces différentiels pour $R = 2$ bit/s/Hz.

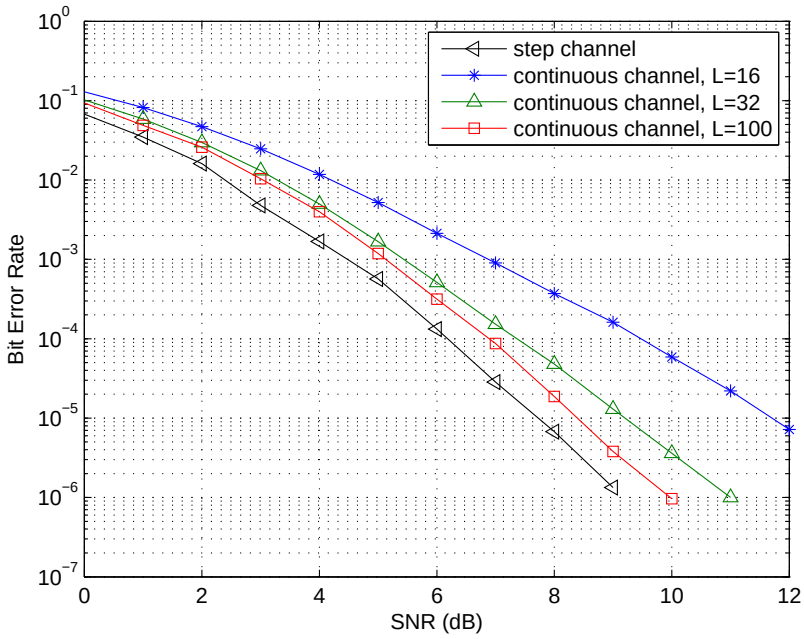

Figure 6.10 : Performances des systèmes DSTM M4N4R1 pour différents L.

Modèle de canal MIMO à variation continue

Il est possible de s'approcher plus du cas réel si on considère des matrices de canal différentes pour chaque colonne d'une matrice de transmission. Le principe d'interpolation reste le même, sauf qu'il faut calculer séparément les colonnes de la matrice reçue et ensuite appliquer la même méthode de détection. Dans ce cas, deux matrices successives de canal sont séparées seulement par T_s et pas par MT_s comme c'était le cas avec le modèle constant par bloc. Elles sont donc plus proches. Les simulations effectuées avec ce nouveau modèle de canal à variation continue sont donnés dans la Figure 6.12 pour $R = 1$ bit/s/Hz et dans la Figure 6.13 pour $R = 2$ bit/s/Hz. On peut constater que les performances déterminées avec ce nouveau modèle de canal sont presque aussi bonnes que celles obtenues avec le modèle simple de canal constant par trame mais bien meilleurs par rapports aux performances des mêmes systèmes déterminées avec le modèle de canal constant pas bloc.

1 Introduction

In this chapter, we present the motivations and main contributions of our research. Wireless communication has experienced remarkable evolution since its appearance at the end of the 19th century. Especially from the 1970s when the cellular systems were proposed and deployed, wireless and mobile communications underwent explosive growth for the services of voice, data access to Internet, video and so on. The ultimate goal of wireless communications is to communicate with anybody from anywhere at anytime. Huge amounts of work need to do to reach this objective.

1.1 Brief history of the wireless and mobile communications

Telecommunication is communication at a distance by technological means, particularly through electrical signals or electromagnetic waves.

In the 18th and 19th centuries, more and more properties of electricity (especially the relations between magnetism and electricity) were discovered. People begun to consider transmitting information taking advantage of this new technique. Electrical telegraphs were studied and applied at the beginning of the 19th century. In the second half of the 19th century, telephone was invented and improved by several researchers. With the theory of electromagnetic radiation formulated by James Clerk Maxwell in 1865 [1], communicate through free space with electromagnetic waves became possible. Heinrich Hertz verified and demonstrated the wireless propagation

in 1880 and 1887 respectively. Guglielmo Marconi built the first complete, commercially successful wireless telegraphy system based on radio transmission in 1894 [2] and patented a complete wireless system in 1897. During the following one hundred years, wireless communication systems have experienced impressive developments.

The invention of the diode by John Ambrose Fleming in 1904 and the triode by Lee de Forest in 1906 made possible rapid development of radio telephony. The invention of the transistor in 1947 by Bardeen, Braittain and Shockley, which later led to the development of integrated circuits, paved the way for miniaturisation of electronic systems.

After years of research and experimental developments, the first analog cellular system (which is called the 'first generation' of mobile communication systems) was deployed by NTT (Nippon Telegraph and Telephone) in Tokyo in 1979. The other well known cellular systems in this period are the Advanced Mobile Phone System (AMPS) in North America and Nodic Mobile Telephone (NMT) in the Nodic countries. These systems supplied mainly voice service and the quality was often inconsistent with "cross-talk" between users being a common problem. The number of subscribers of these systems was limited due to the technique and the cost.

During the 1980s, digital communication was widely researched and this new technique resulted the 'second generation' (2G) mobile communication systems in the 1990s. There were mainly two mobile communication systems in the global market: Europe developed GSM (originally Groupe Spécial Mobile and later Global System for Mobile Communications) standard and U.S.A. developed CDMA (Code-Division Multiple Access) standard. The GSM standard was based on Time-Division Multiple Access (TDMA). These systems differed from the previous generation by using digital instead of analog transmission. The second generation introduced a new variant of communication called SMS (Short Message Service) or text messaging. The 2G systems also supplied circuit-switched data service such as email and other data applications, initially at a modest peak data rate of 9.6 kbps. During the second half of the 1990s, packet data over cellular systems became a reality with General Packet Radio Services (GPRS) introduced in GSM. Although the data rate was fairly low (56 - 114 kbps), there was a great potential for applications over

packet data in mobile systems.

To meet the growing demand for data (such as email and access to browse the internet), the industry began to work on the next generation of technology known as 3G (the third generation), which supplies broadband services. Work on the third-generation communication system started in ITU (International Telecommunication Union) under the label IMT-2000 [3] and now the main IMT-2000 recommendation is ITU-R M.1457 [4]. In 1998, the Third Generation Partnership Project (3GPP) was formed by standards-developing organizations from all regions of the world to avoid parallel development. From then on, 3GPP has been playing a main role in the standardization of the 3G cellular communication systems and the wireless networks have experienced rapid evolution in terms of data rates. Meanwhile, the number of mobile subscribers increased tremendously from 2000 to 2010 with the first billion landmark in 2002 and the fifth billion in the middle of 2010. This growth has been fueled by low-cost mobile phones and efficient network coverage and capacity.

By 2009, there was a trend that 3G networks would be overwhelmed by the growth of bandwidth-intensive applications like streaming media. ITU proposed the concept IMT-Advanced for mobile systems with capacity beyond IMT-2000 in 2008 [5]. The system aims to supply 100 Mbps for high and 1 Gbps for low mobility. Two candidate proposals (LTE-Advanced from 3GPP and 802.16m from IEEE) were submitted to ITU in 2009. The mainly used techniques are orthogonal frequency division multiplex access (OFDMA) to improve the spectrum efficiency and multiple-input multiple-output (MIMO) to enlarge the channel capacity. Here, the term multiple-input multiple-output refers to the use of an array of antennas for both the transmitter end and receiver end. The peak data rate of LTE-Advanced are 1 Gbps and 500 Mbps for down-link (base station to user end) and up-link (user end to base station) respectively.

Recently, researchers have been trying to study new technologies to fulfil the demands of future wireless communications. For example, device-to-device communications [6], millimeter wave (mmWave) [7, 8], massive MIMO [9, 10], etc.

The concept massive MIMO is originally developed by Marzetta [11]. The base station end can be equipped with hundreds of antennas while the remote end which

is limited in size and cost can be with only a single antenna. This scheme have some extraordinary advantages compared with point-to-point MIMO systems. Under line-of-sight propagation conditions (i.e., Rician channel), the multiplexing effect will reduce dramatically in point-to-point MIMO systems while retained in the multiuser MIMO systems [12]. As the number of antennas at the base station grows to infinity, the effects of uncorrelated noise and small-scale fading can be ignored, the number of users per cell are independent of the size of the cell, and the required transmitted energy per bit vanishes. Furthermore, simple linear signal processing approaches can be used in massive MIMO systems to achieve these advantages [10]. However, the acquisition of channel state information and the phenomenon of pilot contamination impose fundamental limitations on massive MIMO systems.

1.2 Objectives and motivations

The way to the ultimate goal of wireless communication is still long to run. The bottlenecks are the data rate and robustness of wireless communication systems. Multiple-antenna technique which can supply space diversity and multiplexing is believed to be a necessity for the future wireless communication systems from its appearance. On one hand, the theoretical capacity of MIMO system is attractive [13–17]. However the methods/schemes to get this capacity are still under research, due to the difficulties of application. On the other hand, diversity effect can be obtained by multiple transmit antennas [18] and/or multiple receive antennas. Our research focuses on the MIMO systems.

The channel capacity gain of multiple antennas techniques is due to the *multiplexing effect* while the *space diversity* can improve the robustness of communication systems significantly. Basically, if the path gains between each transmit-receive antenna pairs fade independently, the channel matrix will have full rank with high probability, in which case multiple parallel spatial channels are created. By transmitting independent information streams in parallel through the spatial channels, the data rate can be increased. This effect is called spatial multiplexing [19]. In another way, with high non-correlation between the paths of each transmit-receive

pairs, the probability of all paths suffering deep fading simultaneously will be extremely low. The error performance of the system can be improved with all the transmit antennas sending the same signal and each receive antenna receive multiple copies of the signal simultaneously. This technique is called space diversity. There is a tradeoff between multiplexing and diversity [20].

Generally, MIMO systems can be divided into two types according to whether the receiver needs the precise channel state information (CSI). The first one is represented by the coherent MIMO systems which need to estimate the CSI at the receive side. References [13], [14] analyzed the capacity and the error performance of such systems with Gaussian noise. Several coding schemes have been proposed based on this assumption such as space-time block codes (STBC) [18, 21], space-time trellis codes (STTC) [22], Bell Labs layered space-time codes (BLAST) [23], etc.

Actually, the CSI is often obtained by training. Known signals are periodically transmitted to the receiver in order to estimate the channel coefficients. However, when many antennas are used or when the propagation channel changes rapidly, the training based scheme doesn't work effectively. For MIMO systems, the number of channel coefficients to be estimated is equal to the product of the number of transmit antennas by the number of receive antennas. In addition, given the number of transmit antennas, the number of receive antennas and the coherence time, the minimum length of the training symbols that guarantees meaningful estimates of the channel matrix is increasing with the number of transmit antennas [24], which results in the reduction of the overall system throughput. Therefore, MIMO systems that do not require to estimate the channel coefficients are very attractive in such cases, especially when the number of transmit and receive antennas is very large.

In [25], Marzetta and Hochwald analyzed the capacity of the MIMO systems without CSI. They found that the rows of transmission matrices (the symbol vectors of each transmit antenna) should be orthogonal to each other to achieve capacity. They called the code scheme with such particular structure unitary space-time modulation (USTM) [26]. In succession, Hochwald and Sweldens proposed the differential unitary space-time modulation (DUSTM) scheme [27]. There are no general systematic design criteria for these two schemes, i.e., their schemes are not opti-

mal. Meanwhile, based on Alamouti's transmit diversity scheme [18], Tarokh and Jafarkhani proposed a differential space-time block coding (DSTBC) scheme [28] for MIMO systems with 2 transmit antennas and expanded this scheme to systems with 4 transmit antennas in [29]. The demodulation of this scheme has a linear structure which leads the complexity quite low. However, the spectral efficiency of this scheme for 4 transmit antennas is limited to 1 bps/Hz and it is difficult to expand to MIMO systems with more transmit antennas while maintaining the low complexity of demodulation.

In [30, 31], El Arab *et al.* proposed a new space-time scheme for 2×2 MIMO systems in which channel error-correcting code and space-time code are combined and can be used in coherent and non-coherent MIMO systems. This technique is called "Matrix Coded Modulation" (MCM). The information bits are coded by error-correcting code which generates a stream of codewords. Each codeword of this scheme maps to a pair of transmitted matrices selected from the Weyl group. The pair of matrices have a specific relation which can avoid the computing of the channel matrix. Furthermore, if convolutional codes are used, the channel matrix can be estimated by iteration. However, this technique was considered only for MIMO systems with 2 transmit antennas.

In addition, in our research group of IETR in INSA-Rennes, we have studied the Space-Time Trellis Codes (STTC) schemes used for MIMO systems with CSI [32–43]. Based on this discussion, we focus on researching MIMO systems with large number of transmit antennas without the channel state information and differential schemes are the main considerations.

1.3 Overview of the thesis

This thesis focuses on the design of differential space-time modulation schemes for MIMO systems. The main contributions of this thesis can be summarized as follows:

1. Based on the Weyl group, we design a new differential space-time modulation scheme which could be expanded to MIMO systems with 2^n transmit anten-

nas. We consider MIMO systems with 2, 4 and 8 transmit antennas in our documents. For MIMO systems with 4 and 8 transmit antennas, the groups of unitary matrices are obtained by the Kronecker product of matrices of the Weyl group.

2. The performance of this new scheme can be improved by selecting the transmission set of matrices separated by the greatest distances. In fact, maximizing the minimum distance of the matrices can be seen as a design criterion.
3. Optional mapping between the sets of transmitted matrices and the information vectors is also a design criterion.
4. A new channel model which is suitable for differential space-time modulation scheme is also proposed. Conventionally, the channel coefficients are supposed to be constant during a fixed time interval. However, this situation does not correspond to the real world where Doppler effect makes the channel change continuously. Therefore, a channel model based on the Nyquist sampling theory is proposed and evaluated. Simulation results show the reasonableness of this new model.

1.4 The structure and outline

The contents of the thesis are structured as 6 parts:

- Chapter 1 here is the introduction of our document, which gives the motivation and main contributions of our research.
- Chapter 2 gives the general wireless communication model, followed by the research backgrounds of MIMO systems and fundamental MIMO theories including capacity and error performance of space-time codes.
- Some existing non-coherent space-time coding schemes, i.e., unitary space-time modulation (USTM), differential unitary space-time modulation (DUSTM), differential space-time block codes (DSTBC) and matrix-coded modulation (MCM) are presented in Chapter 3.
- In Chapter 4, we propose our new differential space-time modulation scheme which can be used for MIMO systems with 2 transmit antennas.

- We expand our designed DSTM scheme to MIMO systems with 4 and 8 transmit antennas in Chapter 5.
- In order to better simulate our proposed scheme, we design a new time selective channel model in Chapter 6. We evaluate the performance and the robustness of DSTM schemes with 2, 4 and 8 transmit antennas over this time selective channel.
- Finally, Chapter 7 concludes this document.

1.5 List of published papers

We published 5 international conference papers during our research.

- Hui Ji, Gheorghe Zaharia and Jean-François Hélard, "A New Differential Space-Time Modulation Scheme for MIMO Systems with Four Transmit Antennas", the 20th International Conference on Telecommunications (ICT 2013), Casablanca, Maroc, 6-8 May 2013.
- Hui Ji, Gheorghe Zaharia and Jean-François Hélard, "A New Differential Space-Time Modulation Scheme based on Weyl Group", the 11-th International Symposium on Signals, Circuits and Systems (ISSCS 2013), Iasi, Romania, 11-12 July 2013.
- Hui Ji, Gheorghe Zaharia and Jean-François Hélard, "A new DSTM scheme based on Weyl group for MIMO systems with 2, 4 and 8 transmit antennas", VTC 2014 Spring, Seoul, South Korea, 18-21 May 2014.
- Hui Ji, Gheorghe Zaharia and Jean-François Hélard, "Performance of DSTM MIMO Systems Based on Weyl Group in Time Selective Channel", European Wireless 2014, Barcelona, Spain 14-16, May, 2014.
- Hui Ji, Gheorghe Zaharia and Jean-François Hélard, "Performance of DSTM MIMO Systems in Continuously Changing Rayleigh Channel", the 12-th International Symposium on Signals, Circuits and Systems (ISSCS 2015), Iasi, Romania, 8-10 July 2015.

2 MIMO systems

In this chapter, we present the background of MIMO communication systems. First, the general wireless communication model and MIMO system model are presented. Second, we briefly present the research history of modern MIMO systems. Third, the channel capacities of coherent and noncoherent MIMO systems are examined respectively. The capacity of coherent MIMO systems has been studied maturely while it is difficult to get the capacity of noncoherent MIMO systems. Finally, the error performance of space-time codes are studied for coherent and noncoherent MIMO systems and some design criteria are represented.

2.1 General model of a wireless communication system

Typically, a simplified point-to-point digital communication system can be represented as shown in Fig. 2.1. The sequence of source bits b_i are grouped into sequential vectors of m bits, and each binary vector is mapped onto one of 2^m baseband signals $u_i(t)$ $(i = 0, 1, ..., 2^m - 1)$ according to some modulation scheme (e.g. QPSK). The waveform of $u(t)$ can be a *rectangular* pulse shape or a *raised cosine* pulse [44]. $u(t)$ is then converted to passband signal $x(t)$ which has a bandpass spectrum that is concentrated at $\pm f_c$ where f_c is selected so that $x(t)$ will propagate across the communication channel.

The transmitted and received signals of digital communication system with one

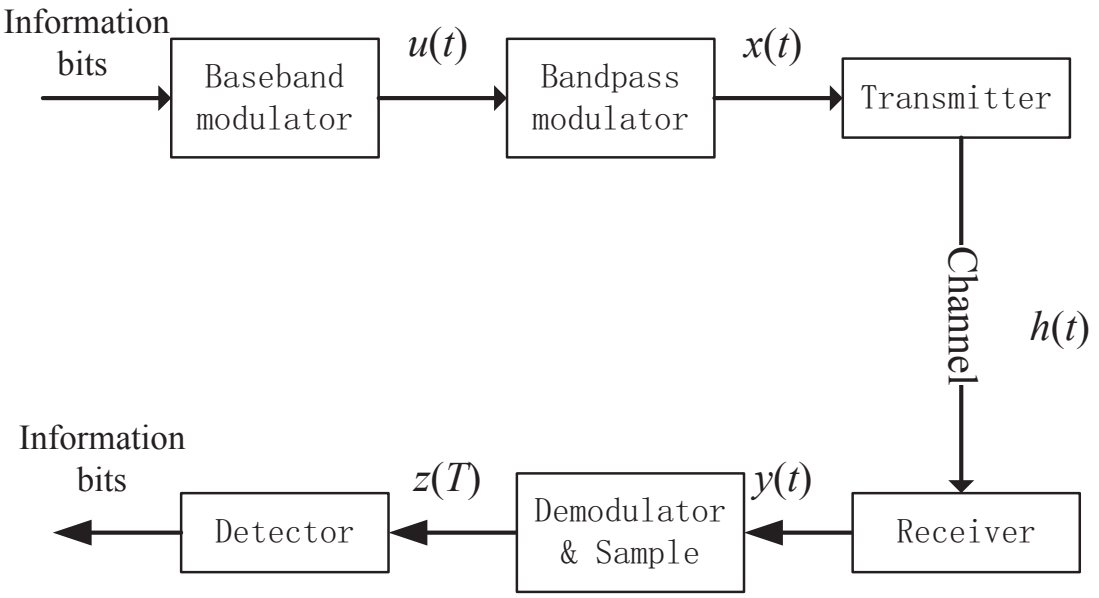

Figure 2.1: A general point-to-point communication system model.

transmit antenna and one receive antenna have the relation as follows:

$$\begin{aligned} y(t) &= g(t,\tau) * x(t) + w(t) \\ &= \int_0^\infty g(t,\tau)x(t-\tau)d\tau + w(t) \\ &= r(t) + w(t). \end{aligned} \tag{2.1}$$

where $x(t)$ is the transmitted signal, $g(t,\tau)$ is the channel impulse response, $*$ denotes convolution, $w(t)$ is the additive white Gaussian noise and $y(t)$ is the signal detected by the receiver. $y(t)$ is then demodulated to baseband signal $\tilde{u}(t)$ and sampled to get $z(T)$. The detector converts $z(T)$ to a constellation point and then maps the point onto the corresponding binary vector.

The instantaneous power of an electrical signal with voltage $v(t)$ or current $i(t)$ across a resistor R is define by

$$p(t) = \frac{v^2(t)}{R} = i^2(t)R. \tag{2.2}$$

In communication systems, power is often normalized by assuming R to be 1 Ω. Regardless of whether the signal $x(t)$ is a voltage or current waveform, we express

the instantaneous power as:

$$p(t) = x^2(t). \tag{2.3}$$

The energy dissipated by the signal $x(t)$ during the infinite time interval $(-\infty, \infty)$ is:

$$E_x = \lim_{T\to\infty} \int_{-T}^{T} |x(t)|^2 dt = \int_{-\infty}^{\infty} |x(t)|^2 dt, \tag{2.4}$$

and the average power is:

$$P_x = \lim_{T\to\infty} \frac{1}{2T} \int_{-T}^{T} |x(t)|^2 dt. \tag{2.5}$$

For a communication system, people mainly concern its *capacity* or *data rate* and *robustness* (the probability of making an error). Capacity is an intrinsic property of a channel and the robustness is determined by the coding scheme of a system. The aim of the development of modern communication systems is to make the data rate approach the capacity with less error probability and less transmit power.

2.1.1 Baseband representation of bandpass signals

In fact, the transmitted signal $x(t)$ is a real-valued continuous-time function. It is known that the Fourier transform $X(f)$ of a real-valued signal $x(t)$ has conjugate symmetry, i.e. $X(-f) = X^*(f)$. The transmitted bandpass signal $x(t)$ can be written as:

$$\begin{aligned} x(t) &= A(t)\cos(2\pi f_c t + \phi(t)) \\ &= A(t)\cos\phi(t)\cos(2\pi f_c t) - A(t)\sin\phi(t)\sin(2\pi f_c t) \\ &= x_I(t)\cos(2\pi f_c t) - x_Q(t)\sin(2\pi f_c t), \end{aligned} \tag{2.6}$$

where $A(t)$ is the amplitude, f_c is the carrier frequency and $\phi(t)$ is the phase. $x_I(t) = A(t)\cos\phi(t)$ is called the in-phase part of the transmitted signal and $x_Q(t) = A(t)\sin\phi(t)$ is called the quadrature-phase part of $x(t)$. In fact, the useful information is contained in $A(t)$ or $\phi(t)$. Therefore, for simplicity, we model the bandpass signal $x(t)$ into a complex baseband representation $u(t)$. Normally, the bandwidth B of $x(t)$ is much smaller than the carrier frequency f_c. This assumption is reason-

able while the carrier frequency of modern communication systems is of the order of magnitude GHz and the signal bandwidth is up to hundreds of MHz.

The baseband representation $u(t)$ only contains the useful part $A(t)$ and $\phi(t)$, and it is written as a complex function called the complex envelope of $x(t)$:

$$u(t) = A(t)(\cos\phi(t) + j\sin\phi(t)) = x_I(t) + jx_Q(t) = A(t)e^{j\phi(t)}, \tag{2.7}$$

where $j = \sqrt{-1}$.

In another way, the complex envelope can be expressed as below:

$$u(t) = [x(t) + j\hat{x}(t)]e^{-j2\pi f_c t}, \tag{2.8}$$

where $\hat{x}(t) = \frac{1}{\pi t} * x(t)$ is the Hilbert transform of the signal $x(t)$. When $A(t)$ has no frequency content above the carrier frequency f_c, by Bedrosian's theorem [45] the Hilbert transform of $x(t)$ can be written as:

$$\hat{x}(t) = A(t)\sin(2\pi f_c t + \phi(t)) = x_I(t)\sin(2\pi f_c t) + x_Q(t)\cos(2\pi f_c t). \tag{2.9}$$

Introducing this relation to (2.8), we can get the same result as (2.7). In this way, the transmitted signal has the form:

$$x(t) = \Re\left\{u(t)e^{j2\pi f_c t}\right\}. \tag{2.10}$$

Using properties of the Fourier transform we can show that

$$X(f) = \frac{1}{2}\left\{U(f - f_c) + U^*(-f - f_c)\right\}. \tag{2.11}$$

The spectrum of an arbitrary bandpass signal and the spectrum of its baseband representation are shown in Fig. 2.2.

It is easy to show that the average power of the transmitted signal $x(t)$ is $P_x = P_u/2$. Thus, to keep the power of $u(t)$ the same as that of $x(t)$, the factor $1/\sqrt{2}$ is

added to $u(t)$ which results:

$$u(t) = \frac{1}{\sqrt{2}} A(t) \left[\cos \phi(t) + j \sin \phi(t)\right] = \frac{1}{\sqrt{2}} [x_I(t) + j x_Q(t)], \tag{2.12}$$

and (2.8) becomes:

$$u(t) = \frac{1}{\sqrt{2}} [x(t) + j\hat{x}(t)] e^{-j2\pi f_c t}. \tag{2.13}$$

In digital computer simulations of bandpass signals, the sampling rate used in the simulation can be minimized by working with the complex envelope, $u(t)$, instead of with the bandpass signal, $x(t)$, because $u(t)$ is the baseband equivalent of the bandpass signal.

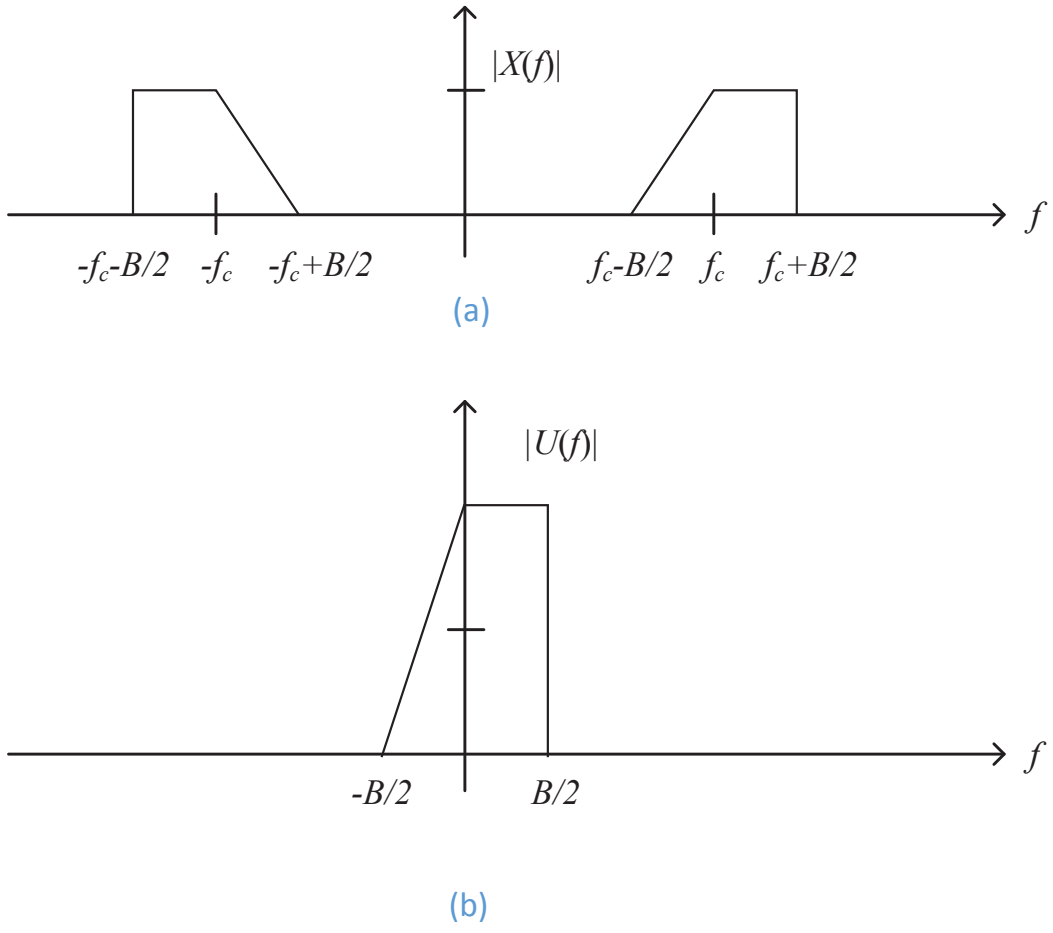

Figure 2.2: Spectrum of (a) bandpass and (b) complex baseband representation of the same signal.

2.1.2 Vector space representations

As mentioned before, $u(t)$ is a complex-enveloped baseband waveform selected from a finite set of $M = 2^m$ finite energy waveforms $\{u_0(t), ..., u_{M-1}(t)\}$. We now examine vector space in order to represent and analyse signals.

An N-dimensional complex vector space is defined by the set of complex orthonormal basis functions $\{\phi_0(t), \phi_1(t), ..., \phi_{N-1}(t)\}$, where

$$\int_{-\infty}^{\infty} \phi_i(t)\phi_i^*(t)dt = \delta_{ij} \tag{2.14}$$

and

$$\delta_{ij} = \begin{cases} 1, & i = j \\ 0, & otherwise. \end{cases} \tag{2.15}$$

All of the vectors in the N-dimensional vector space can be written as a linear combination of the basis functions. For example, the baseband waveforms $u_i(t)$ can be written as:

$$u_i(t) = \sum_{n=0}^{N-1} s_{i_n}\phi_n(t), \quad i = 0, ..., M-1, \tag{2.16}$$

where

$$s_{i_n} = \int_{-\infty}^{\infty} u_i(t)\phi_n^*(t)dt. \tag{2.17}$$

Therefor, the baseband signal $u_i(t)$ can be represented by a complex vector

$$\mathbf{s}_i = (s_{i_0}, s_{i_1}, ..., s_{i_{N-1}}), \quad i = 0, ..., M-1, \tag{2.18}$$

and this vector is called the signal constellation point corresponding to the signal $u_i(t)$. There is a one-to-one correspondence between the transmitted signal $u_i(t)$ and its constellation point $\mathbf{s}_i$.

We can see that the energy of the signal $u_i(t)$ in (2.16) is:

$$E_i = \int_{-\infty}^{\infty} \left| \sum_{n=0}^{N-1} s_{i_n}\phi_n(t) \right|^2 dt = \sum_{n=0}^{N-1} |s_{i_n}|^2 = \|\mathbf{s}_i\|^2, \tag{2.19}$$

where we used the orthonormal property of the basis function in (2.14) and$\|\mathbf{s}_i\|^2 =$

$\sum_{n=0}^{N-1} s_{i_n}^2$ is the squared Euclidean norm of the vector $\mathbf{s}_i$. **Note that the squared norm of the vector $\mathbf{s}_i$ have the dimension of an energy**.

For example, with quadrature phase-shift-keying (QPSK), the constellation is shown in Fig. 2.3. The signal constellation is a plot of the permitted values for the complex envelope $u(t)$ and each constellation point is called a *symbol*. Each symbol is transmitted in a time duration T_s. The QPSK waveforms that are transmitted at each symbol time duration have complex envelopes

$$u_i(t) = s_i\phi_0(t), \quad i = 0, ..., 3, \tag{2.20}$$

where s_i is the constellation point of QPSK and $\phi_0(t)$ is the baseband pulse-shaping filter which satisfies (2.14).

The complex envelope of the QPSK signal is

$$u_i(t) = \Re\{s_i\}\phi_0(t) + j\Im\{s_i\}\phi_0(t) = \frac{1}{\sqrt{2}}[x_I(t) + jx_Q(t)], \tag{2.21}$$

where $x_I(t) = \pm\sqrt{2E}\phi_0(t)$ and $x_Q(t) = \pm\sqrt{2E}\phi_0(t)$. The pulse modulator reads in two bits of data at a time from the serial binary input stream, and maps the first of the two bits to $x_I(t)$ and the second bit to $x_Q(t)$.

2.1.3 Channel model

For the modelization of the channel parameters of $g(t, \tau)$ [46–49], there are many different methods. In wireless communication systems, the impulse response of a SISO channel $g(t, \tau)$ is caused by path loss, shadowing and multipath. The path loss and shadowing determine the large-scale fading, while the multipath effect determines the small-scale fading. In our study, we do not take into account the large-scale fading while just the small-scale multipath fading is considered.

If the transmitter sends a pulse, a series of pulses with different amplitudes and time delays will be received at the receiver. The first received pulse corresponds to the LOS (line of sight) component (if there is) and the other pulses correspond to a large number of reflectors.

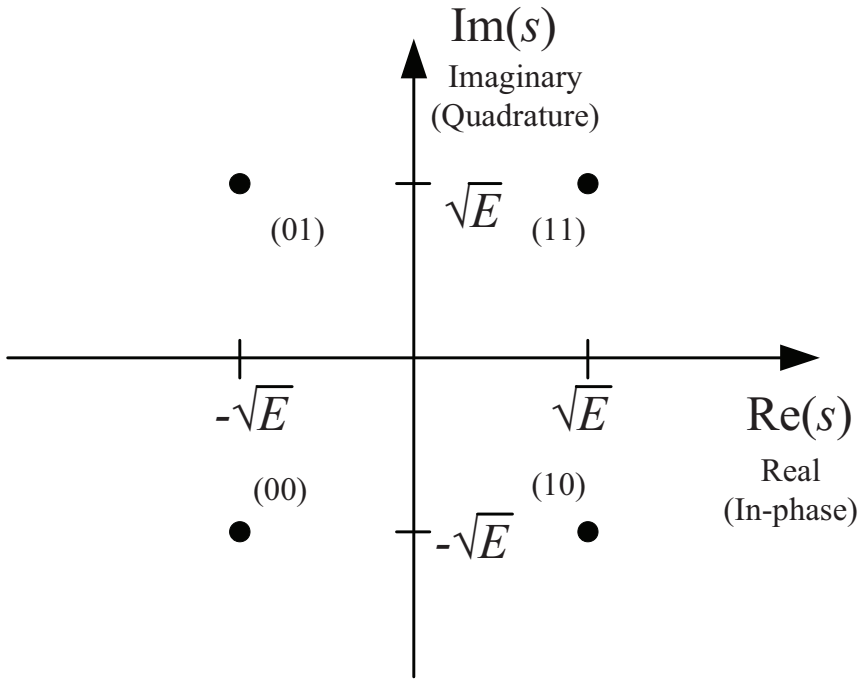

Figure 2.3: QPSK signal constellation.

An important characteristic of a multipath channel is the time *delay spread* that causes to the received signal. This delay spread (T_d) equals the time delay between the arrival of the first received signal component (LOS or multipath) and the last received signal component associated with a single transmitted pulse. The inverse of the root mean square (RMS) delay spread τ_{RMS} is an estimation of the *coherence bandwidth* (B_c) of the channel. For example, a typical delay spread is 5 μs (5×10^{-6} s) in cellular urban environments. If the delay spread is far less than the inverse of the signal bandwidth B, the time delay spread have little influence to the received signal, and we call this kind of channel *flat fading* channel. The channel impulse response $g(t, \tau)$ can be simplified to be $g(t)$ and $y(t) = g(t)x(t) + w(t)$.

However, when the delay spread is relatively large, there is significant time spreading of the received signal which can lead to substantial signal distortion. Under this condition, the received signal taking into account the multipath propagation is [50]:

$$y(t) = \int_0^\infty x(t-\tau)g(t,\tau)d\tau + w(t), \tag{2.22}$$

where $g(t, \tau)$ is the impulse response of the time-variant channel which can be in-

terpreted as the channel response at time t due to an impulse applied at time $t-\tau$. Since a physical channel cannot have an output before an input applied, therefore $g(t,\tau) = 0$ for $\tau < 0$. This kind of channel is called *frequency selective fading* channel.

Normally, for mobile communication systems, the channel is time-varying due to the movement of the transmitter or receiver. Furthermore, the locations of reflectors in the transmission path, which give rise to multipath, also change over time. Thus, if we repeatedly transmit pulses from a moving transmitter, we will observe changes in the amplitudes, delays, and the number of multipath components corresponding to each transmitted pulse. These changes will cause another important characteristic of wireless channel – the *Doppler shift*.

The maximum Doppler shift is also called *Doppler spread* which is defined as $f_d = \frac{V}{\lambda}$, where V is the relative velocity between the transmitter and receiver, and λ is the signal wavelength. The *coherence time* T_c which means during this time interval the channel characteristics do not change significantly corresponds to the Doppler spread. Clearly, a slow-changing channel has a large coherence time.

There is no exact relationship between coherence time and Doppler spread. A popular definition of T_c is: $T_c = \sqrt{\frac{9}{16\pi f_d^2}} = \frac{0.423}{f_d}$ [48]. In practice, for simplicity, people usually use it as $T_c \approx 0.5/f_d$. We define L equal to the normalized coherence time T_c/T_s, where T_s is the symbol duration. For example, with velocity $V = 120$ km/h, and carrier frequency $f = 900$ MHz, the Doppler spread is approximately 100 Hz and the coherence time is approximately 5 ms. For a symbol rate of 30 kHz, during the transmission of $L = 150$ symbols, the channel can be considered quasi time-invariant. For high speed vehicular $V = 350$ km/h channels [5], and carrier frequency $f = 1.8$ GHz, the Doppler spread is approximately 583 Hz and the coherence time is approximately 0.7 ms. For a symbol rate of 30 kHz, during the transmission of $L = 21$ symbols, the channel can be considered quasi time-invariant.

With these conditions, consider a general time-variant channel, the received sig-

nal can be written as follows:

$$\begin{aligned} y(t) &= r(t) + w(t) \\ &= \Re\left\{\sum_{n=1}^{N_p} \alpha_n u(t-\tau_n) e^{j\left[2\pi(f_c+f_{d,n})(t-\tau_n)\right]}\right\} + w(t) \\ &= \Re\left\{\left[\sum_{n=1}^{N_p} \alpha_n e^{-j\phi_n(t)} u(t-\tau_n)\right] e^{j2\pi f_c t}\right\} + w(t), \end{aligned} \tag{2.23}$$

where N_p is the number of multipath, $0 < \alpha_n < 1$ is the attenuation of the nth path, the length of each path component is l_n and $\tau_n = l_n/c$ is the corresponding delay, $f_{d,n} = f_d \cos\theta_n$ is Doppler frequency shift, θ_n is the angle of incidence between the nth plane wave with the speed vector of the mobile, α_n is amplitude based on the path loss and shadowing and $\phi_n(t) = 2\pi f_c \tau_n + 2\pi f_{d,n}(\tau_n - t)$.

As mentioned before, for flat fading channel or narrowband channel, the delay spread is far less than the inverse of the signal bandwidth B, i.e. $T_d \ll B^{-1}$. The symbol duration is far greater than the delay spread which means that $u(t-\tau_n) \approx u(t), \forall n$. The received signal can be rewritten as:

$$\begin{aligned} y(t) &= \Re\left\{u(t) e^{j2\pi f_c t}\left(\sum_n \alpha_n e^{-j\phi_n(t)}\right)\right\} + w(t) \\ &= \Re\left\{h(t) u(t) e^{j2\pi f_c t}\right\} + w(t). \end{aligned} \tag{2.24}$$

If the transmitted signal is an unmodulated constant signal (which means quite narrow, in fact it is a δ function, in frequency domain), i.e. $x(t) = \Re\left\{1 \times e^{j2\pi f_c t}\right\}$, the received signal becomes:

$$\begin{aligned} y(t) &= \Re\left\{e^{j2\pi f_c t}\left(\sum_n \alpha_n e^{-j\phi_n(t)}\right)\right\} + w(t) \\ &= r_I(t)\cos 2\pi f_c t + r_Q(t)\sin 2\pi f_c t + w(t), \end{aligned} \tag{2.25}$$

where

$$r_I(t) = \sum_n \alpha_n \cos\phi_n(t), \tag{2.26}$$

$$r_Q(t) = \sum_n \alpha_n \sin \phi_n(t), \tag{2.27}$$

and

$$\phi_n(t) = 2\pi f_c \tau_n + 2\pi f_{d,n}(\tau_n - t). \tag{2.28}$$

We assume that the number of path is large and there is not a LOS component, if α_n and $\phi_n(t)$ are stationary and ergodic, according to the Central Limit Theorem, $r_I(t)$ and $r_Q(t)$ are jointly Gaussian random processes. With the reasonable assumption that $\phi_n(t)$ is uniformly distributed on $[-\pi, \pi]$, we can see that the expectation of $r_I(t)$ is 0. Similarly, $\mathbb{E}[r_Q(t)] = 0$. The variance of $r_I(t)$ and $r_Q(t)$ are also the same: $\sigma_r^2 = 0.5 \sum_n E[\alpha_n^2]$. Therefore the variance of $r(t) = r_I(t) \cos 2\pi f_c t + r_Q(t) \sin 2\pi f_c t$ is $\mathbb{E}[r^2(t)] = \sigma_r^2 = 0.5 \sum_n E[\alpha_n^2]$. The autocorrelation of $r(t)$ is

$$\begin{aligned} R_r(\tau) &= \mathbb{E}[r(t)r(t+\tau)] \\ &= \mathbb{E}[r_I(t)r_I(t+\tau)] \cos(2\pi f_c \tau) - [r_Q(t)r_I(t+\tau)] \sin(2\pi f_c \tau) \\ &= R_{r_I}(\tau) \cos(2\pi f_c \tau) - R_{r_Q r_I}(\tau) \sin(2\pi f_c \tau), \end{aligned} \tag{2.29}$$

where

$$\begin{aligned} R_{r_I}(\tau) &= R_{r_Q}(\tau), \\ R_{r_I r_Q}(\tau) &= R_{r_Q r_I}(-\tau). \end{aligned}$$

In fact

$$\begin{aligned} R_{r_I}(\tau) &= \mathbb{E}[r_I(t)r_I(t+\tau)] = \sigma_r^2 \mathbb{E}_{\theta_n}[\cos 2\pi f_{d,n} \tau] \\ &= \sigma_r^2 \mathbb{E}_\theta[\cos 2\pi \tau f_d \cos\theta]. \end{aligned} \tag{2.30}$$

Similarly, the cross-correlation $R_{r_I r_Q}$ is

$$R_{r_I r_Q} = \sigma_r^2 \mathbb{E}_\theta[\sin 2\pi \tau f_d \cos\theta]. \tag{2.31}$$

Assume that the 2-D plane waves arrive at the mobile from all directions with equal probability, i.e., $p(\theta) = 1/(2\pi)$, $\theta \in [-\pi, \pi]$. With 2-D isotropic scattering and an isotropic receiver antenna with gain $G(\theta) = 1$, the expectation in (2.30) and (2.31)

become

$$\begin{aligned} R_{r_I}(\tau) &= \sigma_r^2 \int_{-\pi}^{\pi} \cos(2\pi\tau f_d \cos\theta) p(\theta) G(\theta) d\theta \\ &= \sigma_r^2 \frac{1}{\pi} \int_{0}^{\pi} \cos(2\pi\tau f_d \cos\theta) d\theta. \\ &= \sigma_r^2 J_0(2\pi f_d \tau) \end{aligned} \tag{2.32}$$

and

$$R_{r_I r_Q}(\tau) = \sigma_r^2 \int_{-\pi}^{\pi} \sin(2\pi\tau f_d \cos\theta) p(\theta) G(\theta) d\theta = 0, \tag{2.33}$$

where $J_0(x)$ is the zero-order Bessel function of the first kind. Therefore the autocorrelation of the received signal $r(t)$ is

$$R_r(\tau) = \mathbb{E}[r(t)r(t+\tau)] = \sigma_r^2 \cos(2\pi f_c \tau) J_0(2\pi f_d \tau). \tag{2.34}$$

The autocorrelation of the received complex envelope $h(t) = r_I(t) + j r_Q(t)$ is

$$R_h(\tau) = \mathbb{E}[h^*(t)h(t+\tau)] = 2[R_{r_I}(\tau) + j R_{r_I r_Q}(\tau)] = 2\sigma_r^2 J_0(2\pi f_d \tau). \tag{2.35}$$

For any two independent Gaussian random variables X and Y, both with mean zero and equal variance, it is shown that $Z = \sqrt{X^2 + Y^2}$ is Rayleigh-distributed. Thus the received signal envelope $z(t) = |h(t)| = \sqrt{r_I^2(t) + r_Q^2(t)}$ is Rayleigh-distributed with distribution:

$$p_Z(z) = \frac{z}{\sigma_z^2} \exp[-z^2/(2\sigma_z^2)], z \geq 0. \tag{2.36}$$

The average received signal power is $P_z = \mathbb{E}[|h|^2] = \sum_n \mathbb{E}[\alpha_n^2] = 2\sigma_r^2$. In our research, we assume that $P_z = \mathbb{E}[|h|^2] = \sum_n \mathbb{E}[\alpha_n^2] = 1$, which means that the average received signal power is equal to the transmitted signal power. Thus $|r_I(t)|$ and $|r_Q(t)|$ are $\mathcal{N}(0, 0.5)$ distributed respectively, where $\mathcal{N}(\mu, \sigma^2)$ denotes the Gaussian distribution with expectation μ and variance σ^2. This narrowband Rayleigh channel model is used through our research. For wide-band channels, OFDM technique is supposed to be used and the sub-channel is considered to be narrowband.

However, if there is a LOS path between the transmitter and the receiver, the distribution of the envelope of the received signal becomes Rician:

$$p_Z(z) = \frac{z}{\sigma_z^2} \exp\left(-\frac{z^2 + D^2}{2\sigma_z^2}\right) I_0\left(\frac{Dz}{\sigma_z^2}\right), z \geq 0, D \geq 0, \tag{2.37}$$

where D is the peak amplitude of the LOS signal and $I_0(\cdot)$ is the modified zero-order Bessel function of the first kind. Obviously, the Ricean distribution converges to Rayleigh distribution when the LOS signal disappears, i.e. $D = 0$, as expected. In our study, we don't consider this situation.

The additive noise $w(t)$ is modeled as zero-mean *Gaussian* wide-sense stationary random process. A Gaussian process $w(t)$ is a random function whose value w at any arbitrary time t is statistically characterized by the Gaussian probability density function:

$$p(w) = \frac{1}{\sigma\sqrt{2\pi}} \exp\left[-\frac{1}{2}\left(\frac{w}{\sigma}\right)^2\right], \tag{2.38}$$

where σ^2 is the variance of w.

The power spectral density is $P_w(f) = N_0/2$ (W/Hz) for all f, where the factor of 2 indicates that $P_w(f)$ is a two-sided power spectral density. When the noise has such a uniform spectral density we refer to it as *white noise*. Furthermore, the noise is assumed to be ergodic in the mean and the autocorrelation function. The autocorrelation function of the noise is given by the inverse Fourier transform of the noise power spectral density, denoted as follows:

$$\begin{aligned} R_w(\tau) =& \mathbb{E}\left[w(t)w(t+\tau)\right] = \lim_{T\to\infty} 1/T \int_{-T/2}^{T/2} w(t)w(t+\tau)dt \\ =& F^{-1}P_w(f) = \frac{N_0}{2}\delta(\tau). \end{aligned} \tag{2.39}$$

The average power P_w of white noise is infinite because its bandwidth is infinite:

$$P_w = \mathbb{E}\left[w^2(t)\right] = R_w(0) = \int_{-\infty}^{\infty} \frac{N_0}{2} df = \infty. \tag{2.40}$$

However, in practice, the signal we deal with is bandpass and thus the corresponding noise is seen as bandpass noise with bandwidth B ($B << f_c$ as before).

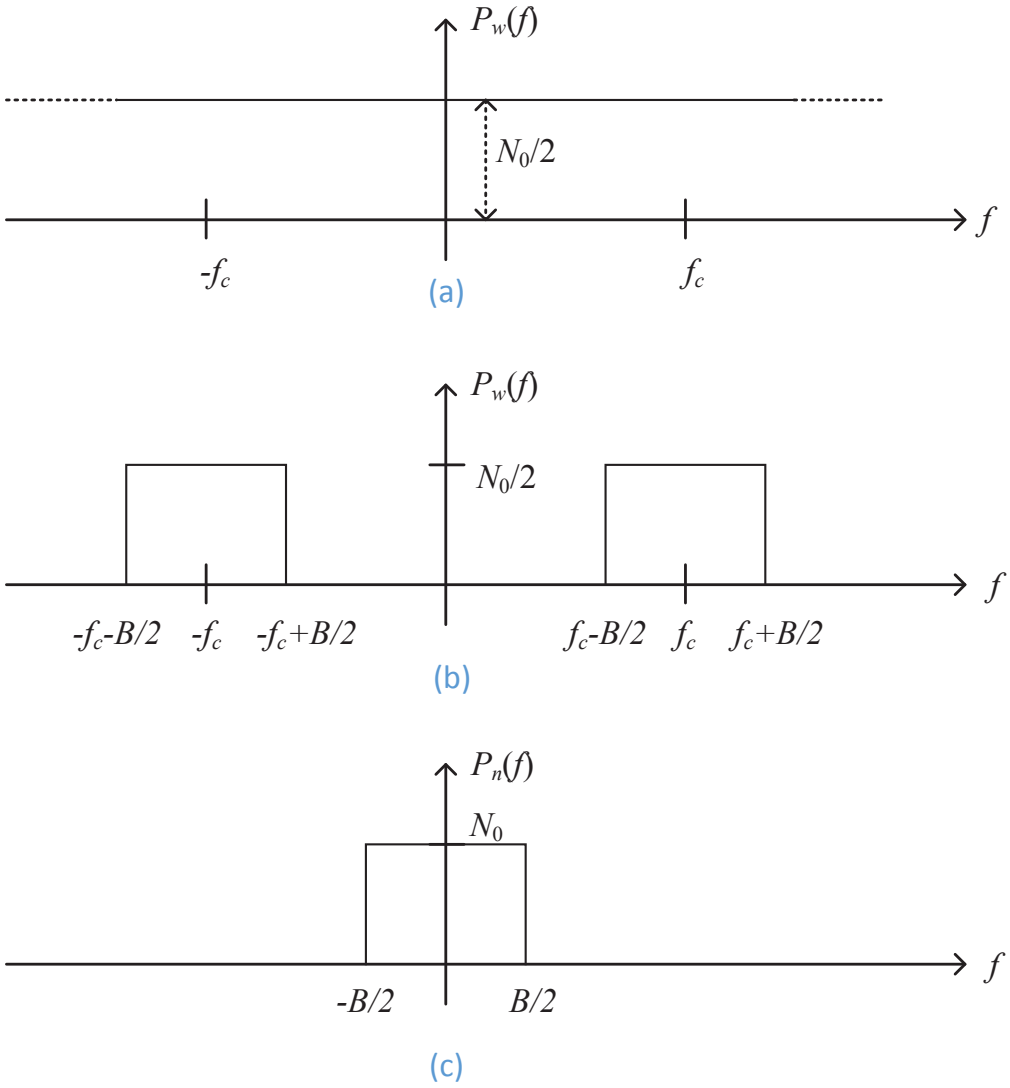

Figure 2.4: Power spectral density of AWGN. (a) The original AWGN. (b) Bandpass AWGN. (c) Baseband representation of bandpass AWGN.

The power spectral density of bandpass AWGN $w(t)$ is nonzero only in the pass-band, as shown in Fig. 2.4. Generally the system is analyzed in equivalent complex baseband. In this case, the baseband representation $n(t)$ and $w(t)$ have the relation:

$$w(t) = \Re\{n(t)e^{j2\pi f_c t}\} = w_I(t)\cos 2\pi f_c t - w_Q(t)\sin 2\pi f_c t, \tag{2.41}$$

where $n(t) = \frac{1}{\sqrt{(2)}}[w_I(t) + jw_Q(t)]$. To obtain the power spectrum $P_n(f)$ of $n(t)$, we need to analyse the corresponding autocorrelation function $R_n(\tau)$ which is the Fourier transform of $P_n(f)$. The autocorrelation function of $w_I(t)$ and $w_Q(t)$ is given

by [51]

$$R_{w_I}(\tau) = \mathbb{E}[w_I(t)w_I(t+\tau)] = R_w(\tau)\cos(2\pi f_c\tau) + \hat{R}_w(\tau)\sin(2\pi f_c\tau) \tag{2.42}$$

$$R_{w_Q}(\tau) = \mathbb{E}[w_Q(t)w_Q(t+\tau)] = R_w(\tau)\cos(2\pi f_c\tau) + \hat{R}_w(\tau)\sin(2\pi f_c\tau) \tag{2.43}$$

Taking Fourier transform of both sides of (2.42), the power spectral density for $w_I(t)$ and $w_Q(t)$ is obtained as:

$$P_{w_I}(f) = P_{w_Q}(f) = \begin{cases} P_w(f+f_c) + P_w(f-f_c), & |f| \le f_c \\ 0, \quad otherwise. \end{cases} = \begin{cases} N_0, & |f| \le B/2 \\ 0, \quad otherwise. \end{cases} \tag{2.44}$$

The cross-spectral density of $w_I(t)$ and $w_Q(t)$ is given by

$$P_{w_I w_Q} = \begin{cases} j[P_w(f+f_c) - P_w(f-f_c)], & |f| \le f_c \\ 0, \quad otherwise \end{cases} = 0. \tag{2.45}$$

Under this condition, $R_{w_I w_Q} = 0$, implying that $w_I(t)$ and $w_Q(t)$ are uncorrelated. Further, because $w(t)$ is Gaussian, $w_I(t)$ and $w_Q(t)$ are independent processes. The autocorrelation function of $n(t)$ is

$$\begin{aligned} R_n(\tau) &= \mathbb{E}[n^*(t)n(t+\tau)] = R_{w_I}(\tau) = R_{w_Q}(\tau) \\ &= \int_{-B/2}^{B/2} N_0 e^{j2\pi f\tau} df = \frac{N_0 \sin(B\tau\pi)}{\tau\pi}. \end{aligned} \tag{2.46}$$

Thus $n(t)$ is a complex AWGN random process with real and imaginary parts independent, the power spectral density is

$$P_n(f) = \begin{cases} N_0, & |f| \le B/2 \\ 0, \quad otherwise. \end{cases} \tag{2.47}$$

In this case,the variance (i.e. power) of $n(t)$ is:

$$\begin{aligned}\sigma^2 &= \mathbb{E}\left\{[n(t) - \mathbb{E}n(t)]^*[n(t) - \mathbb{E}n(t)]\right\} = \mathbb{E}[|n(t)|^2] \\ &= R_n(0) = \int_{-\infty}^{\infty} P_n(f)df = N_0 B.\end{aligned} \tag{2.48}$$

Now, we analyze the vector space representation of the additive white Gaussian noise. When the bandwidth B of the signals is high enough, the autocorrelation function of the noise in (2.46) can be seen as

$$R_n(\tau) = \delta(\tau). \tag{2.49}$$

With this assumption and the same basis function used in (2.16) and (2.17), we get the noise vector

$$\mathbf{n} = (n_0, n_1, ..., n_{N-1}), \tag{2.50}$$

where

$$n_i = \int_{-\infty}^{\infty} n(t)\phi_i^*(t)dt, \quad i = 0, ..., N-1. \tag{2.51}$$

It is clear that

$$\mathbb{E}[n_i] = 0, \tag{2.52}$$

and

$$\mathbb{E}[n_i n_k^*] = N_0 \delta_{ik}. \tag{2.53}$$

Thus, the elements of the noise vector are identically independent Gaussian distributed with mean zero and **variance** $\sigma^2 = N_0$. The probability density function of complex n_i is given by:

$$p(n_i) = \frac{1}{\pi\sigma^2} e^{-|n_i|^2/\sigma^2}, \tag{2.54}$$

and the probability density function of the noise vector $\mathbf{n}$ is given by:

$$p(\mathbf{n}) = (\pi\sigma^2)^{-N} \exp\left\{-\frac{\mathbf{n}^H\mathbf{n}}{\sigma^2}\right\}. \tag{2.55}$$

We say the elements of the noise vector are circularly symmetric and $n_i \sim \mathcal{CN}(0, \sigma^2)$, $\mathbf{n} \sim \mathcal{CN}(0, \sigma^2 I_N)$. Appendix A gives more details of Gaussian random variables,

vectors and matrices.

2.2 Brief presentation of the history of MIMO systems

It is accepted that modern electrical information theory is established by Shannon in the famous paper [52] in 1948, where the information was quantized and analyzed in strict mathematics and channel capacity for single-antenna system was defined. Multiple antennas are originally called antenna arrays which are mainly used in the fields of sonar [53], radar [54], and seismic [55] signal processing. The concept of multiple-input and multiple-output (MIMO) was raised in 1970s, which was used for multipair telephone cable or multiple-terminal systems to mitigate inter-symbol interference or inter-channel interference, such as [56–60].

With the first generation of mobile communication systems entered the commercial market around the 1980s, where multiple antennas can be installed at the base station, the concept of adaptive antennas which had been successfully used in radar technology was introduced to cellular systems [61]. Adaptive antennas are used to obtain *space diversity* [62] in cellular systems. Antennas arrays at the base station provide receive diversity to combat the effect of multipath fading [63,64] and later transmit diversity technique was studied [65,66]. Meanwhile, the beamforming technique was brought in [67,68].

Winters analysed the channel capacity of MIMO systems in 1987 [69] and get some interesting results. However, with the limitations of the capability of computation, MIMO systems didn't attract much attention until the late 1990s.

In 1995 and 1996, Telatar [13] and Foschini [14] evaluated the channel capacity and error performance of multiple-antenna wireless communication systems with the assumption that the channel coefficients are perfectly estimated in the receiver end. They found that the channel capacity increases almost linearly with the minimum of the number of transmit antennas and the number of receive antennas. Foschini indicated that, at a 12-dB SNR (signal-to-noise power ratio) and with the numbers of

antenna elements 8 or 12, capacity about 21 and 32 bps/Hz is available respectively [23]. This result displayed the great advantage of multiple-antenna systems and ignited magnificent interest in this division.

From then on, much work has been done on generalizing and improving their results on the capacity of MIMO systems. First, more realistic channel models are considered. For example, instead of assuming that the channels have rich scattering, so that the propagation coefficients between transmit and receive antennas are independent, it was assumed that correlation can exist between the channels [70–72]. The cochannel interference is also considered in [73]. Moreover, the line of sight (LOS) component which makes the channel to be Rician is also considered in [12,74]. Second, with the background of cellular systems, the capacity of multi-user MIMO systems is studied [75–77]. And third, recently, theoretic capacity results with very low SNR have been obtained due to the research of *green* systems which consume much less power [78–80].

These results indicate that multiple-antenna systems have much higher Shannon capacity than single-antenna ones. However, since Shannon capacity can only be achieved by codes with unbounded complexity and delay, the above results do not reflect the performance of real transmission systems. A possible method is proposed by Foschini in 1996 [23] which is later called BLAST (Bell Labs layered space-time) [81, 82]. Although the throughput is pretty high, this scheme does not use transmit diversity and the error performance without using error correcting codes is not sufficient to apply. The schemes that can improve the error performance of BLAST have been widely studied since then [83–86].

The techniques that exploit the space diversity at the transmitter end are widely investigated since 1998 when Alamouti presented his initiative work in [18]. Later, Tarokh et al. expanded the transmit diversity scheme to MIMO systems with any number of transmit antennas and named this kind of coding as space-time block codes (STBC) [21]. Since then, the coding techniques which are appropriate to multiple transmit antennas are called space-time coding. Space-time coding is a method used in multiple antenna systems to not only increase the reliability of the communication link, but also increase their throughput. This is accomplished

by encoding multiple streams of data across the spatial domain (i.e., antennas) and across the time domain. Tarokh et al. derived the design criteria of space-time codes in the sense of minimizing the upper bound of average probability of error in [22] and proposed a code scheme using the so called space-time trellis code (STTC). The number of states in the trellis codes grows exponentially with either the rate or the number of transmit antennas which limit it to expand to MIMO systems with large number of transmit or receive antennas. Alamouti's scheme is also called orthogonal space-time block code (O-STBC) due to the structure of the transmission matrix and can achieve full rate and full diversity gain for two transmit antennas. However, when the number of the antenna exceeds 2, the system cannot achieve full rate with this structure. Jafarkhani proposed QO-STBC (quasi-orthogonal space-time block code) scheme [87] to achieve full rate with the sacrificing of the maximum diversity gain. A lot of other improved space-time block codes are proposed such as (linear dispersion) LD-STBC [88], STBC from division algebras [89], the so-called perfect STBC [90] and so on.

The above systems are also called point-to-point MIMO systems because two devices with multiple antennas communicate with each other. In wireless or cellular systems, it is difficult to install multiple antennas at the user device due to the size, cost or hardware limitations, which can not sufficiently exert the advantages of MIMO techniques. Thus, Sendonaris et al. proposed a new cooperative communication scheme [91, 92] for cellular systems where the in-cell users can share their antennas. Extensive work have been done in this background [93–97]. This kind of scheme is also called virtual or distributed MIMO. Recently, Marzetta proposed a noncooperative large-scale antenna systems or so called Massive MIMO systems [11] where the base station is equipped with hundreds of antennas while the remote end which is limited in size and cost can have only one antenna. This scheme have some extraordinary advantages compared with point-to-point MIMO systems. Under line-of-sight propagation conditions (i.e., Rician channel), the multiplexing effect will reduce dramatically in point-to-point MIMO systems while retained in the multiuser MIMO systems [12]. As the number of antennas at the base station grows to infinity, the effects of uncorrelated noise and small-scale fading can be ignored,

the number of users per cell are independent of the size of the cell, and the required transmitted energy per bit vanishes. Furthermore, simple linear signal processing approaches can be used in massive MIMO systems to achieve these advantages [10].

While massive MIMO renders many traditional research problems irrelevant, it uncovers entirely new problems that urgently need attention: the challenge of making many low-cost low-precision components that work effectively together, acquisition and synchronization for newly joined terminals, the exploitation of extra degrees of freedom provided by the excess of service antennas, reducing internal power consumption to achieve total energy efficiency reduction, and finding new deployment scenarios [9].

However, all of the above systems require the receiver or transmitter end have perfect estimation of the channel coefficients. The CSI is difficult to obtain when the number of antennas is large. In fact, the number of channel coefficients to be estimated by the receiver is equal to the product of the number of transmit antennas by the number of receive antennas. In massive MIMO systems, there are hundreds of antennas at the base station and tens of subscribers, which makes the estimation of channel coefficients complicated. Furthermore, the length of the training sequences is proportional to the number of transmit antennas [24], which reduces the overall system throughput. When the channel state changes rapidly, the estimation of channel coefficients is even not achievable before they change to other values. Since outdoor wireless systems strive to accommodate higher user mobility and indoor wireless communication systems such as BlueTooth rely on frequency hopping spread spectrum technology, these issues necessitate further research into MIMO systems in the absence of CSI. Therefore, MIMO systems that do not need CSI are attractive.

Marzetta and Hochwald analysed the channel capacity of MIMO systems without perfect channel coefficients in [25]. In fact, they assumed that the channel distribution information (CDI) is known by both the transmitter and the receiver, the channel mean is zero and the channel coefficient of each pair of transmit antenna and receive antenna are assumed to be i.i.d. random variables. This kind of channel model in [25] is called zero-mean spatially white (ZMSW) channel in [75]. Under

the zero-mean spatially white (ZMSW) model, the channel mean is zero and the channel covariance is modeled as white, i.e., the channel elements are assumed to be i.i.d. random variables. They found that, under this channel assumption, in order to achieve the channel capacity, the transmission symbol vectors of different antennas should be orthogonal to each other. There is no help for increasing the channel capacity to install more transmit antennas than the normalized coherence time. Zheng and Tse also analysed the channel capacity for ZMSW channel in [98]. They showed that at high SNRs capacity is achieved using no more than $M^\star = \min\{M, N, \lfloor T/2 \rfloor\}$, where M, N and T are the number of transmitter antennas, the number of receiver antennas and the normalized coherence time respectively. Lapidoth and Moser indicated that at high SNR without the block fading assumption, the channel capacity grows only double-logarithmically with the SNR [99]. Jafar and Goldsmith made an extended assumption of the ZMSW model, they considered that the channel coefficients were spatially correlated and the correlations between the channel coefficients are assumed to be known at the transmitter and the receiver. They indicated that channel capacity increases surely with the number of transmit antennas when the transmit antenna fades are spatially correlated [100].

Based on the analysis of channel capacity with ZMSW model, Hochwald and Marzetta introduced the unitary space-time modulation (USTM) scheme which does not need CSI in [26]. However, the problem of how to design constellations systematically that have low probability of error and low demodulation complexity remains open. Hochwald et al. proposed a possible systematic design based on discrete Fourier transform (DFT) in [101] and provided some transmission schemes for $M = 1, 2, 3$ transmitter antennas and data rate $R = 1$ bps/Hz. This scheme requires a complicated brute force maximum-likelihood (ML) decoder at the receiver, making it difficult to implement for large constellation sizes. Tarokh et al. designed specific unitary space-time constellations that are simple to decode in [102], however the error performance is worse than [101]. Leus et al. proposed a space-time frequency-shift keying (ST-FSK) scheme in [103] based on the orthogonal design in [21] and this scheme is easier to design compared to [101] while they have a comparable performance. Kim et al. designed a novel class of unitary space-time constellations in [104]

based on the quaternary quasi-orthogonal sequence (QOS) [105] which is used for designing the Walsh sequences in code-division multiple-access (CDMA) systems. This scheme has less decode complexity than ST-FSK [103] and has slightly better error performance.

Another class of space-time code/modulation schemes that do not need CSI are differential schemes. Hochwald and Sweldens presented the differential unitary space-time modulation (DUSTM) scheme [27] which is directly designed from the USTM scheme. Tarokh and Jafarkhani proposed the differential space-time block coding (DSTBC) scheme [28, 29] based on Alamouti's transmit diversity scheme [18]. Hughes introduced a differential space-time modulation in [106] where the information matrices are selected from a group designed from phase-shift keying (PSK) signals.

In [30,31], the authors invented a new kind of non-coherent space-time modulation scheme–matrix coded modulation (MCM) based on Weyl group for 2×2 MIMO systems. This scheme combines the error-correcting coding and space-time signal design together.

2.3 MIMO system model

In our study, we express signals in signal space, i.e., signals are represented by complex symbols. We consider narrowband MIMO systems with M transmit antennas and N receive antennas. At a general time t, the antenna n detects the symbol:

$$y_n = \sum_{m=1}^{M} h_{nm} x_m + w_n, n = 1, \ldots, N \tag{2.56}$$

where h_{nm} is the path gain of the quasi-static channel from the transmit antenna m to the receive antenna n. The channel coefficients h_{nm} are independent and identically distributed (iid), they are Gaussian distributed, i.e., $h_{nm} \sim \mathcal{CN}(0, 1)$. For a narrowband MIMO channel, corresponding to low data rate wireless systems [107] or for each sub-channel of OFDM (Orthogonal Frequency Division Multiplexing) MIMO systems [108], the frequency response of the propagation channel can be considered

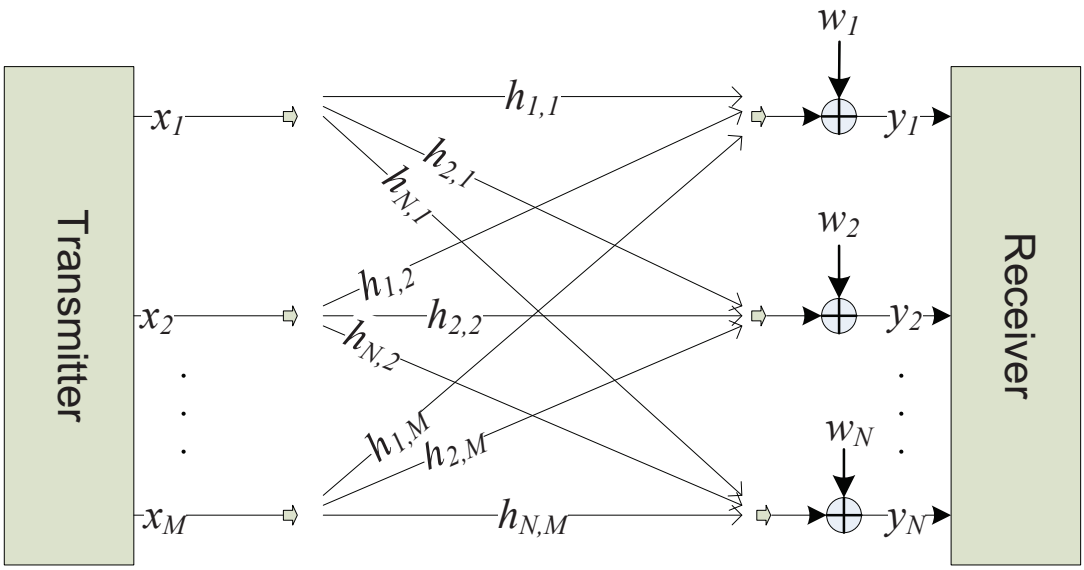

Figure 2.5: A general MIMO system model.

constant within the frequency bandwidth of the system, i.e., the channel is frequency non-selective or flat fading. Therefore, the coefficients h_{nm} of the channel matrix are usually considered constant over the frequency bandwidth but time-variant due to Doppler shift. x_m is the symbol transmitted from antenna m at time t. w_n is the additive white Gaussian noise at the receive antenna n at time t, $w_n \sim \mathcal{CN}(0, \sigma^2)$ and σ^2 is also the power of the noise. This system model is shown in Fig. 2.5.

If we define the vector of the transmitted signals as $\mathbf{x} = [x_1, x_2, ..., x_M]^T$, the vector of the received signals as $\mathbf{y} = [y_1, y_2, ..., y_N]^T$, the vector of noises as $\mathbf{w} = [w_1, w_2, ..., w_N]^T$ and the channel matrix as:

$$H = \begin{pmatrix} h_{11} & h_{12} & \cdots & h_{1M} \\ h_{21} & h_{22} & \cdots & h_{2M} \\ \vdots & \vdots & \ddots & \vdots \\ h_{N1} & h_{N2} & \cdots & h_{NM} \end{pmatrix}, \tag{2.57}$$

the system equation can be written in vector form as

$$\mathbf{y} = H\mathbf{x} + \mathbf{w}. \tag{2.58}$$

Moreover, if the coherence time T_c is much greater than the symbol period T_s (i.e., the Doppler shift effect can be ignored during the transmission of $L = T_c/T_s$ symbols), we can use the matrix form to analyze a MIMO system. Therefore, the system can be expressed in matrix form as:

$$Y = HX + W \tag{2.59}$$

where Y is the $N \times T$ received matrix, T denotes the number of symbols of each matrix for each transmit antenna and $T \leq L$. H is the channel matrix and its size is $N \times M$ as in (2.57). X is the $M \times T$ transmission matrix and W is the $N \times T$ additive white Gaussian noise matrix.

Furthermore, the expectation of the total power over M transmit antennas at each transmit time is set to be 1:

$$\sum_{m=1}^{M} \mathbb{E}\left[|x_{mt}|^2\right] = 1, t = 1, \ldots, T. \tag{2.60}$$

As analysed before, the squared discrete symbols have the dimension of an energy. Therefore, people usually indicate the above equation as power constraint conventionally.

For each receive antenna, the SNR is defined as follows:

$$\begin{aligned} SNR &= \frac{\mathbb{E}[|y_{nt} - w_{nt}|^2]}{\mathbb{E}[|w_{nt}|^2]} = \frac{\mathbb{E}\left[|\sum_{m=1}^{M} h_{nm}x_{mt}|^2\right]}{\mathbb{E}\left[|w_{nt}|^2\right]} \\ &= \frac{\sum_{m=1}^{M} \mathbb{E}\left[|h_{nm}x_{mt}|^2\right]}{\sigma^2} = \frac{\sum_{m=1}^{M} \mathbb{E}\left[|x_{mt}|^2\right]}{\sigma^2} = \frac{1}{\sigma^2} \end{aligned} \tag{2.61}$$

where $\mathbb{E}[\cdot]$ denotes the mathematical expectation.

2.4 Fundamentals of information theory

In this section, the terms concerning the channel capacity are shown. They are entropy and mutual information.

The entropy of $\mathcal{H}(x)$ of a continuous random variable x is defined as [109]:

$$\mathcal{H}(x) = -\int p(x)\log p(x)dx, \tag{2.62}$$

where $p(x)$ is the probability density function of x. We can see that this parameter measures the uncertainty of a random variable. The entropy of a typical circularly symmetric complex Gaussian random vector $\mathbf{z} \sim \mathcal{CN}(\mu, Q)$ with mean μ and covariance Q is:

$$H(\mathbf{z}) = \mathbb{E}[-\log p(\mathbf{z})] = \log\det(\pi e Q) \tag{2.63}$$

The joint entropy $\mathcal{H}(x, y)$ of a pair of continuous random variables (x, y) is defined as:

$$\mathcal{H}(x, y) = -\iint p(x, y)\log p(x, y)dxdy, \tag{2.64}$$

where $p(x, y)$ is the joint probability density function of x and y.

The conditional entropy $\mathcal{H}(y|x)$ is defined as:

$$\mathcal{H}(y|x) = -\iint p(x, y)\log p(y|x)dxdy, \tag{2.65}$$

where $p(y|x)$ is the probability density function of y conditioned on x.

The *mutual information* $\mathcal{I}(x, y)$ between two continuous random variables is given by:

$$\begin{aligned}\mathcal{I}(x; y) &= \iint p(x, y)\log\frac{p(x, y)}{p(x)p(y)}dxdy \\ &= \mathcal{H}(x) - \mathcal{H}(x|y) \\ &= \mathcal{H}(y) - \mathcal{H}(y|x).\end{aligned} \tag{2.66}$$

The capacity of a noisy channel is defined as the maximum mutual information of input x and output y over all possible values of input distribution $p(x)$:

$$C = \max_{p(x)} \mathcal{I}(x; y). \tag{2.67}$$

For example, consider the communication system with one transmit antenna and

one receive antenna in the presence of AWGN narrowband fading channel $y = hx+n$. Assume that the fading coefficient h is constant (non-fading Gaussian channel), the capacity of is given by [52]:

$$\begin{aligned} C &= \max_{p(x)} \mathcal{I}(x;y) = \max_{p(x)} \mathcal{H}(y) - \mathcal{H}(y|x) \\ &= \max_{p(x)} \mathcal{H}(y) - \mathcal{H}(n), \end{aligned} \tag{2.68}$$

From (2.63), we can get $\mathcal{H}(n) = \log(\pi e \sigma^2)$. To maximize $\mathcal{I}(x;y)$, we should maximize $\mathcal{H}(y)$. It is proved that [52] for a continuous distributed random variable, the Gaussian distribution with mean zero maximize the entropy. Thus $\mathbb{E}[y] = 0$ which indicates $\mathbb{E}[x] = 0$ and the variance of y

$$\mathbb{E}\left[y^2\right] = \mathbb{E}\left[(hx+n)^2\right] = h^2\mathbb{E}\left[x^2\right] + \mathbb{E}\left[n^2\right] = h^2P + \sigma^2, \tag{2.69}$$

where P is the average power constraint on the transmitted signal and with our power constraint (2.60), it is $P = 1$. Thus the maximized entropy $\mathcal{H}(y) = \log[\pi e(h^2+\sigma^2)]$. Finally, we get the channel capacity of SISO system:

$$C = \log[\pi e(h^2+\sigma^2)] - \log(\pi e\sigma^2) = \log\left(1 + \frac{|h|^2}{\sigma^2}\right). \tag{2.70}$$

When the fading coefficient h is a random variable, then the capacity above becomes

$$C = \mathbb{E}\left[\log\left(1 + \frac{|h|^2}{\sigma^2}\right)\right]. \tag{2.71}$$

2.5 Capacity of MIMO communication channels

The channel capacity of multiple-antenna communication systems is analyzed by many researchers [13, 14, 25]. The theoretical results show that the communication systems with multiple antennas can enlarge the channel capacity significantly compared to SISO systems.

Generally, people call the capacity obtained with the assumption of perfect knowledge of fading coefficients H at the receiver end as the *coherent capacity* of

the multiple-antenna channel, while the channel capacity obtained with no prior knowledge of H is called *non-coherent capacity* [98].

2.5.1 H is known to the receiver

Like the procedure to get the channel capacity of SISO system in (2.71), the channel capacity for MIMO system is given by [13, 25]:

$$\begin{aligned} C &= \max_{p(X)} \mathcal{I}(X;Y) \\ &= T \cdot \mathbb{E}\left[\log\det(I_M + \frac{1}{M\sigma^2} H^H H)\right] \\ &= T \cdot \mathbb{E}\left[\log\det(I_N + \frac{1}{M\sigma^2} H H^H)\right]. \end{aligned} \tag{2.72}$$

Here we use the matrix form of the MIMO system as in (2.59). This capacity is achieved with transmitted signal matrix X whose elements are independent and $\mathcal{CN}(0,1)$ distributed. This means that the transmit power is divided equally among all the transmit antennas and independent symbols are sent over different antennas.

In [13], Telatar evaluated the expectation in the equation (2.72). The capacity is obtained as:

$$C = \int_0^\infty \log\left(1 + \frac{\lambda}{M\sigma^2}\right) \sum_k^{K-1} \frac{k!}{(k+J-K)!} \left[L_k^{J-K}(\lambda)\right]^2 \lambda^{J-K} e^{-\lambda} d\lambda \tag{2.73}$$

where $K = \min\{M, N\}$, $J = \max\{M, N\}$ and L_j^i are the associated Laguerre polynomials:

$$L_j^i(x) = \frac{1}{j!} e^x x^{-i} \frac{d^n}{dx^n}(e^{-x} x^{i+j}). \tag{2.74}$$

Fig. 2.6 and Fig. 2.7 show that for fixed SNR, the coherent capacity increases almost linearly with K, i.e., the minimum of M and N.

2.5.2 H is unknown to the receiver

When both transmitter and receiver haven't the channel coefficients matrix H, Marzetta and Hochwald evaluated the channel capacity in [25] with the assumption

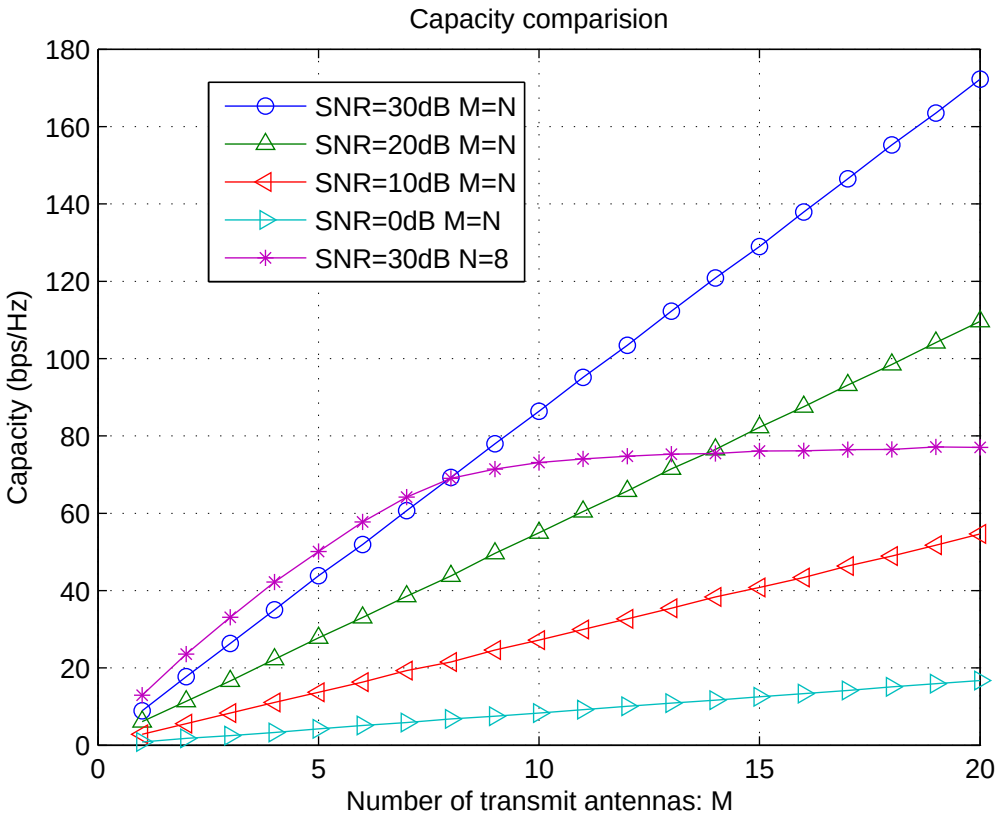

Figure 2.6: The normalized capacity C/T with independent Rayleigh fading, H is known to the receiver. The SNR is fixed to 0, 10, 20 and 30 dB respectively.

that the elements of H are zero-mean spatially white (ZMSW). Zheng and Tse also analysed the channel capacity under this kind of channel model in [98] and got some useful results for special cases.

Lapidoth and Moser indicated that at high SNR, without the block fading assumption, the channel capacity grows only double-logarithmically with the SNR [99], which makes communication at high SNR power inefficient. Jafar and Goldsmith made an extended assumption of the ZMSW model. They considered that the channel coefficients were spatially correlated and the correlations between the channel coefficients are assumed to be known at the transmitter and the receiver. They indicated that channel capacity increases surely with the number of transmit antennas when the transmit antenna fades are spatially correlated [100].

We know that the mutual information between the transmitted matrix (X) and

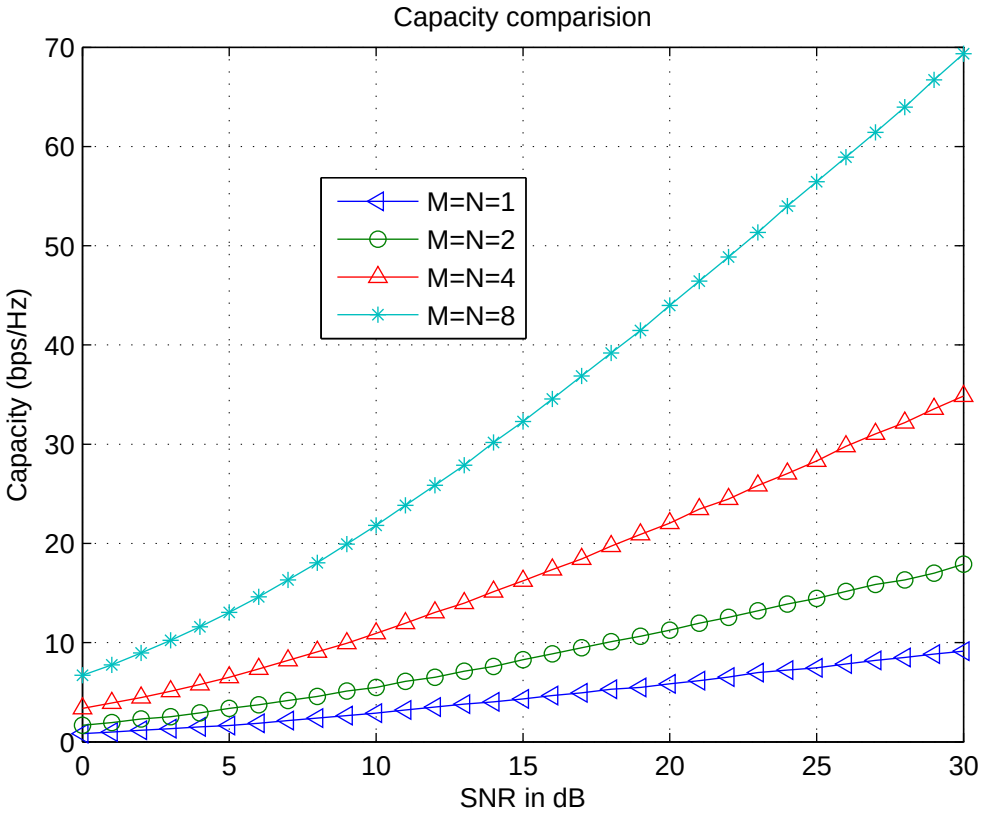

Figure 2.7: The normalized capacity C/T with independent Rayleigh fading, H is known to the receiver. The numbers of transmit antennas and receive antennas are fixed to 1, 2, 4 and 8 respectively.

the received matrix ($Y = HX + W$) is:

$$\begin{aligned} \mathcal{I}(X;Y) &= \iint p(X,Y) \log \frac{p(X,Y)}{p(X)p(Y)} dX dY \\ &= \iint p(Y|X)p(X) \log \frac{p(Y|X)}{p(Y)} dX dY. \end{aligned} \tag{2.75}$$

We now examine the properties of the function $p(Y|X)$. With the assumption that the channel coefficients are independent identically distributed: $h_{nm} \sim \mathcal{CN}(0,1)$ and the additive white Gaussian noise obeys: $w_{nt} \sim \mathcal{CN}(0,\sigma^2)$, the probability distribution function (PDF) of the received matrix Y conditioned on the transmit matrix X is also Gaussian. We have

$$\mathbb{E}[Y|X] = \mathbb{E}[HX + W|X] = 0, \tag{2.76}$$

and

$$\mathbb{E}[Y^H Y|X] = \mathbb{E}[X^H H^H H X + W^H W|X] = X^H X + \sigma^2 I_T. \tag{2.77}$$

Thus the PDF of Y conditioned on X can be written as:

$$p(Y|X) = \frac{1}{\pi^{TN} \det^N(\Lambda)} \exp\{-\mathrm{Tr}[\Lambda^{-1} Y^H Y]\}, \tag{2.78}$$

where $\Lambda = X^H X + \sigma^2 I_T$. It is clear that for any $M \times M$ unitary matrix Φ, $p(Y|\Phi X) = p(Y|X)$. In mathematics, a complex square matrix Φ is *unitary* if

$$\Phi^H \Phi = \Phi \Phi^H = I,$$

where I is the identity matrix and Φ^H is the conjugate transpose of Φ.

Marzetta and Hochwald proved [25] that for any T and any number of receiver antennas N, the capacity obtained with $M > T$ transmitter antennas is the same as the capacity obtained with $M = T$ transmitter antennas.

They also proved that the signal matrix that achieves capacity can be written as $X = V\Psi$, where V is an $M \times T$ real diagonal matrix and Ψ is an $T \times T$ isotropically distributed unitary matrix. Moreover, Ψ and V are independent of each other.

An *isotropically distributed* unitary matrix has a probability density that is unchanged when the matrix is multiplied by any deterministic unitary matrix. We denote the M real diagonal elements of V as $v_1, \ldots, v_M$, and it is proved that

$$\mathbb{E}[v_m^2] = \frac{T}{M}. \tag{2.79}$$

We rewrite the signal matrix in an equivalent form, that is:

$$X = A\Theta. \tag{2.80}$$

where A is an $M \times M$ diagonal matrix with the M diagonal elements $a_1 = v_1, \ldots, a_M = v_M$ and Θ is an $M \times T$ matrix with the M row vectors equal to the first M row vectors of the matrix Ψ. The row vectors of Θ are orthogonal to each other ($\Theta\Theta^H = I_M$). The ith row θ_i of Θ represents the direction of the transmitted signal from antenna

i, i.e., $\theta_i = x_i/\|x_i\|$. The ith diagonal entry of A, $a_i = \|x_i\|$, represents the norm of that signal.

Marzetta and Hochwald obtained a lower bound of the channel capacity as $T \to \infty$ with $a_1 = \cdots = a_M = \sqrt{T/M}$. The exact noncoherent channel capacity seems unattainable by now.

Zheng and Tse [98] gave some results with special cases. They showed that at high SNRs capacity is achieved using no more than $M^\star = \min\{M, N, \lfloor T/2 \rfloor\}$ transmit antennas. They also indicated that for large MIMO systems, where both $M = N$ and T increase to infinity and M/T is fixed, the channel capacity increases linearly with the number of antennas M. However, for noncoherent channel at high SNR, having more transmit antennas than receive antennas takes no benefit to the channel capacity.

2.6 Error performance of MIMO systems

In communication systems, the error occurs when the receiver recovers a signal that is not sent by the transmitter.

The *pair-wise error probability* (PEP) conditioned on H is the probability that the decoder selects the estimated matrix $\hat{X}$ as the transmitted matrix while in fact the transmitted matrix is X. We examine the PEP performances of MIMO systems and hereby get some design criteria for space-time codes.

2.6.1 H is known to the receiver

With the assumption that the elements of the noise matrix W are independent identically Gaussian distributed, i.e. $w_{nt} \sim \mathcal{CN}(0, N_0)$, when the channel coefficients are correctly estimated by the receiver, the maximum likelihood detection is:

$$X_{ml} = \arg\min_{X_l} D(Y, HX_l), \tag{2.81}$$

where $D(Y, HX_l)$ is the distance between the received matrix Y and HX_l. The distance between two matrices A and B is defined as follows:

$$D(A, B) = \|A - B\|, \tag{2.82}$$

and $\|\cdot\|$ denotes the Frobinius norm of a matrix, i.e.,

$$\|A\| = \sqrt{\sum_{i,j} |a_{ij}|^2} = \sqrt{\mathrm{Tr}\{A^H A\}} = \sqrt{\mathrm{Tr}\{AA^H\}}. \tag{2.83}$$

If the transmitted matrix is X, the pair-wise error occurs when:

$$D(Y, HX) > D(Y, H\hat{X}), \tag{2.84}$$

where $\hat{X}$ is any other possible transmission matrix.

When the receiver estimates the channel state information perfectly, the PEP of this case can be written as [22, 110]:

$$P(X, \hat{X}|H) = Q\left(\sqrt{\frac{1}{2N_0}} D(XH, \hat{X}H)\right), \tag{2.85}$$

where

$$Q(x) = \frac{1}{\sqrt{2\pi}} \int_x^\infty e^{\frac{-y^2}{2}} dy, \tag{2.86}$$

and N_0 is the complex noise variance. The signal-to-noise power ratio (SNR) is $\gamma = 1/N_0$ in this case.

We can see that Q function is a *monotonically decreasing* function, thus, to make the pair-wise error probability as less as possible, we should make D as larger as possible. The Q function has an upper bound:

$$Q(x) \leq \frac{1}{2} e^{\frac{-x^2}{2}}, x \geq 0, \tag{2.87}$$

which is shown in Fig. 2.8. This upper bound is the Chernoff bound of the tail of Gaussian PDF [49].

Obviously, $\sqrt{\frac{1}{2N_0}} D(XH, \hat{X}H) \geq 0$, therefore, the upper bound of the pairwise

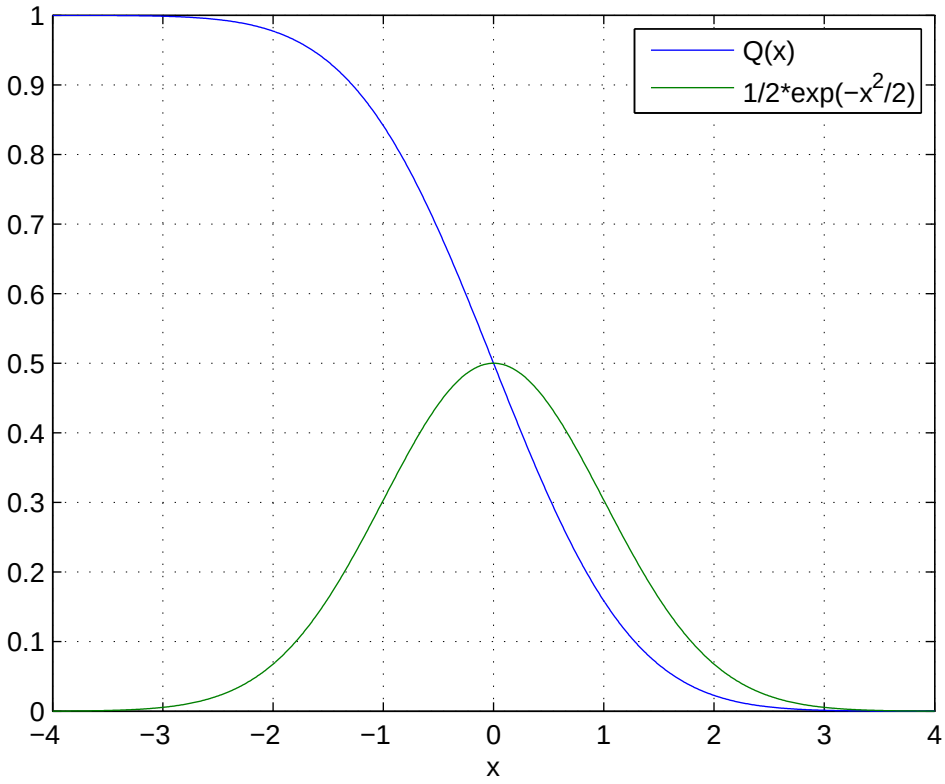

Figure 2.8: The upper bound of Q function.

error probability is:

$$P(X, \hat{X}|H) \leq \frac{1}{2} \exp\left[-\frac{1}{4N_0} D^2(XH, \hat{X}H)\right]. \tag{2.88}$$

Now we analyse the inequality above and get some design criteria for space-time codes. Define $A(X, \hat{X}) = (X - \hat{X})(X - \hat{X})^H$. We can see that $\mathrm{Tr}\{A(X, \hat{X})\} = D^2(X, \hat{X})$. The eigenvalues of $A(X, \hat{X})$ are denoted by λ_m, $m = 1, 2, ..., M$ and $\lambda_1 \geq \lambda_2 \geq ... \geq \lambda_M \geq 0$. Using the singular value decomposition (SVD) theorem, we have

$$A(X, \hat{X}) = V \Lambda V^H, \tag{2.89}$$

where $\Lambda = \mathrm{diag}(\lambda_1, \lambda_2, ..., \lambda_M)$ and V is a unitary matrix. Therefore

$$D^2(XH, \hat{X}H) = \mathrm{Tr}\{HA(X, \hat{X})H^H\} = \mathrm{Tr}\{HV\Lambda V^H H^H\}. \tag{2.90}$$

Denote the (n, m)th element of HV as β_{nm}, then

$$D^2(XH, \hat{X}H) = \sum_{n=1}^{N} \sum_{m=1}^{M} \lambda_m |\beta_{nm}|^2. \tag{2.91}$$

Attention that

$$D^2(X, \hat{X}) = \sum_{m=1}^{M} \lambda_m. \tag{2.92}$$

As β_{nm} is a linear combination of Gaussian random variables, it is also Gaussian distributed and its magnitude $|\beta_{nm}|$ is Rayleigh distributed:

$$p(|\beta_{nm}|) = 2|\beta_{nm}| \exp(-|\beta_{nm}|^2). \tag{2.93}$$

The expected value of PEP can then be evaluated as:

$$P(X, \hat{X}) = \mathbb{E}[P(X, \hat{X})|H] \leq \prod_{m=1}^{M} [1 + (\gamma \lambda_m / 4)]^{-N}. \tag{2.94}$$

If the matrix $A(X, \hat{X})$ has rank $r < M$, i.e., $\lambda_{r+1} = ... = \lambda_M = 0$, then, at high SNR, the above inequality can be written as:

$$P(X, \hat{X}) \leq \gamma^{-rN} 4^{rN} \prod_{m=1}^{r} \lambda_m^{-N}, \tag{2.95}$$

where the component 1 in (2.94) is neglected due to high SNR. We know that the diversity gain is defined as:

$$G_d = -\lim_{\gamma \to \infty} \frac{\log(P_e)}{\log(\gamma)}. \tag{2.96}$$

Thus the diversity gain of space-time code is rN. Therefore, a good design criterion to guarantee full diversity is to make sure that for all possible codewords X_i and X_j, $i \neq j$, the matrix $A(X_i, X_j)$ has full rank M, i.e., $(X_i - X_j)$ has full rank $\forall i, j$ with $i \neq j$.

If the space-time code has full diversity gain MN, next we should maximize the minimum value of $\prod_{m=1}^{M} \lambda_m$ in (2.95) which is the determinant of $A(X_i, X_j)$. This

criterion set is referred to as rank & determinant criterion.

Furthermore, as mentioned before, the transmitted signals have a power constraint (2.60). Therefore, we have:

$$\mathbb{E}\|X\|^2 = \mathbb{E}\left[\sum_{m,t} |x_{m,t}|^2\right] = T. \tag{2.97}$$

For simplicity, as a special case, we set $\|X\|^2 = T$. In this case $D^2(X, \hat{X}) \leq (\|X\| + \|\hat{X}\|)^2 = 4T$, i.e., $\sum_{m=1}^{M} \lambda_m \leq 4T$. In fact, if $\hat{X} = -X$, $D^2(X, \hat{X}) = 4T$.

The design criteria for other channel models such as Rician channels and rapid fading channels can be found in [22]. The exact value of $P(X, \hat{X})$ is also evaluated in [26, 111–113].

In order to better understand the pair-wise error probability of coherent space-time codes, we show some Chernoff bounds (2.94) for special cases in Fig. 2.9 and Fig. 2.10.

Fig. 2.9 is obtained with $\lambda = \lambda_1 = ... = \lambda_M = 1$ and 1 receive antenna. The number of transmit antennas is 2, 4 and 8 respectively. This figure shows that increase the number of transmit antennas can significantly improve the PEP performance. Fig. 2.10 shows the PEP as a function of λ ($\lambda = \lambda_1 = ... = \lambda_M$). It is obtained with 4 transmit antennas and 1 receive antenna, and SNR = 0, 10, 20 dB respectively. This figure show that, increase the distance between any pair of the transmission matrices can also improve the PEP performance especially for large SNR which leads people to design good space-time codes.

2.6.2 H is unknown to the receiver

If H is unknown to the receiver, the maximum likelihood detector has to select the matrix that maximizes the conditioned probability:

$$X_{ml} = \arg\max_{X_l} p(Y|X_l) = \arg\max_{X_l} \frac{\exp\{-\mathrm{Tr}[\Lambda^{-1} Y^H Y]\}}{\pi^{TN} \det^N(\Lambda)}, \tag{2.98}$$

where $\Lambda = X_l^H X_l + \sigma^2 I_T$.

In this case (without CSI), the transmitted matrices have specific structure, as

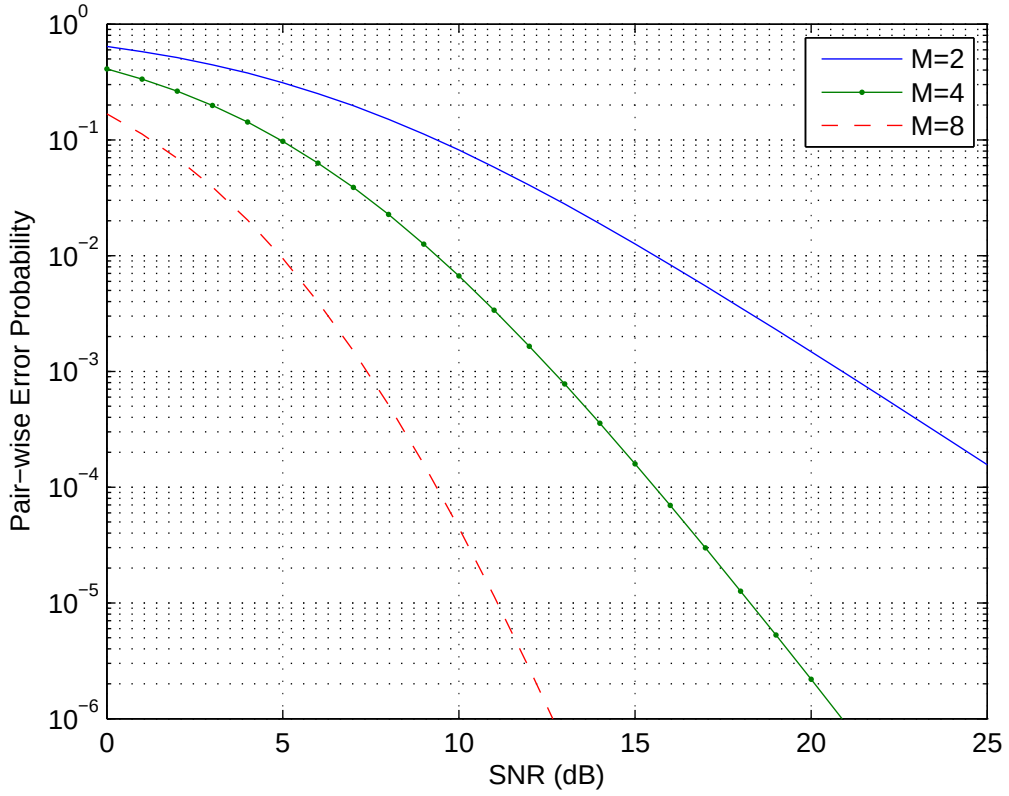

Figure 2.9: The Chernoff bound of PEP of coherent space-time codes. Number of transmit antennas $M = 2, 4, 8$ respectively and the number of receive antenna is 1. $\lambda_m = 1$, $m = 1, .., M$.

discussed in Section 2.5.2. The transmission matrix can be written as $X = A\Theta$. Marzetta and Hochwald [25, 26] proved that when the duration of the coherence interval is significantly greater than the number of transmit antennas ($T \gg M$) or SNR is high and $T > M$, setting $a_1 = ... = a_M = \sqrt{T/M}$ attains capacity. Thus, we fix the transmission matrix as $X = \sqrt{T/M}\Theta$ and this kind of scheme is called unitary space-time modulation (USTM) in [26] because the rows of Θ are orthonormal, i.e., $\Theta\Theta^H = I_M$. With this structure, the detector in (2.98) becomes:

$$\Theta_{ml} = \arg\max_{\Theta_l} p(Y|\Theta_l) = \arg\max_{\Theta_l} \frac{\exp\{-\mathrm{Tr}[\Lambda^{-1}Y^H Y]\}}{\pi^{TN}\det^N(\Lambda)}, \tag{2.99}$$

where $\Lambda = X_l^H X_l + \sigma^2 I_T = \frac{T}{M}\Theta_l^H\Theta_l + \sigma^2 I_T = \sigma^2(\frac{T}{M\sigma^2}\Theta_l^H\Theta_l + I_T)$. With the matrix formulas

$$\det(I + AB) = \det(I + BA)$$

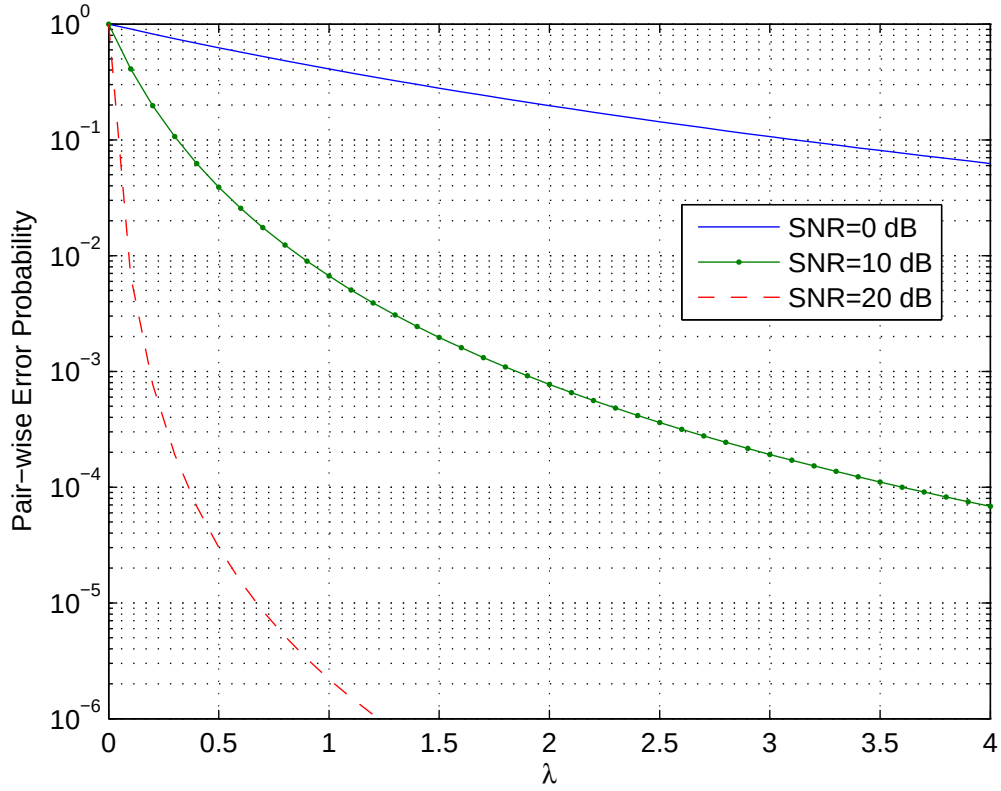

Figure 2.10: The Chernoff bound of PEP for coherent space-time codes. Number of transmit antennas $M = 4$ and number of receive antenna is 1.

and

$$(A + BCD)^{-1} = A^{-1} - A^{-1}B(C^{-1} + DA^{-1}B)^{-1}DA^{-1},$$

(2.99) can be further simplified as:

$$\begin{aligned}\Theta_{ml} &= \arg\max_{\Theta_l} p(Y|\Theta_l) = \arg\max_{\Theta_l} \frac{\exp\{-\mathrm{Tr}[\frac{1}{\sigma^2}(I_T - \frac{\Theta_l^H\Theta_l}{1+M\sigma^2/T})Y^HY]\}}{\pi^{TN}\sigma^{2NT}[1+T/(M\sigma^2)]^{NT}} \\ &= \arg\max_{\Theta_l} \mathrm{Tr}[Y\Theta_l^H\Theta_l Y^H].\end{aligned} \tag{2.100}$$

Now we examine the pair-wise error probability when the transmitter sends Θ_1 and the receiver detected Θ_2 incorrectly. We denote the probability as:

$$P(\Theta_1, \Theta_2) = P\left\{\mathrm{Tr}[Y(\Theta_2^H\Theta_2 - \Theta_1^H\Theta_1)Y^H] > 0|\Theta_1\right\}. \tag{2.101}$$

Hochwald and Marzetta gave an exact expression of PEP with the help of char-

acteristic function and Chernoff upper bound is given by:

$$P(\Theta_1, \Theta_2) \leq \frac{1}{2} \prod_{m=1}^{M} \left[1 + \frac{(\frac{T}{M\sigma^2})^2 (1 - d_m^2)}{4(1 + \frac{T}{M\sigma^2})} \right]^{-N}, \tag{2.102}$$

where $1 \geq d_1 \geq ... \geq d_M \geq 0$ are the singular values of the $M \times M$ matrix $\Theta_1 \Theta_2^H$. $\Theta_1 \Theta_2^H$ can be seen as the correlation between the matrices Θ_1 and Θ_2. The less correlation between Θ_1 and Θ_2, the better the MIMO system performs. Obviously, when $\Theta_1 \Theta_2^H = 0$, i.e., $d_1 = ... = d_M = 0$, the Chernoff bound is minimized. It seems that we should make the transmission matrices Θ_l orthogonal to each other. However, as T is limited, the number of vectors that are orthogonal to each other in the T dimension vector space is limited to T, which in turn makes the number of matrices that are orthogonal to each other limited to $\lfloor T/M \rfloor$. Nevertheless, it is still a criterion to make the correlation of each pair of the matrices as small as possible.

Furthermore, when the SNR is pretty high, i.e., $\sigma^2 \ll 1$, the Chernoff bound can be written as:

$$P(\Theta_1, \Theta_2) \leq \frac{1}{2} \left(\frac{T}{4M\sigma^2} \right)^{-MN} \prod_{m=1}^{M} \left(1 - d_m^2 \right)^{-N}, \tag{2.103}$$

which is similar to (2.95). The exact pair-wise error probability of USTM is also studied in [114].

Fig. 2.11 displays the Chernoff bound of PEP (2.102) as a function of SNR for different numbers of transmit antennas. This figure is obtained with $d_1 = ... = d_M = 0.8$, $T = 2M$ and 1 receive antenna. The number of transmit antennas are $M = 2$, 4 and 8 respectively. We can see that with these values of d_m, noncoherent space-time codes have comparable PEP performance as coherent space-time codes. However, the time duration of the transmission matrices in this figure is $T = 2M$, which reduces the overall throughput of the systems. Fig. 2.12 shows the Chernoff bound of PEP (2.102) as a function of d for different values of SNR. The number of transmit antennas is 4 and the number of receive antennas is 1. The time duration of each transmission matrix is $T = 2M = 8$. We can see that reducing d below 0.4 approximately does not reduce the error by much.

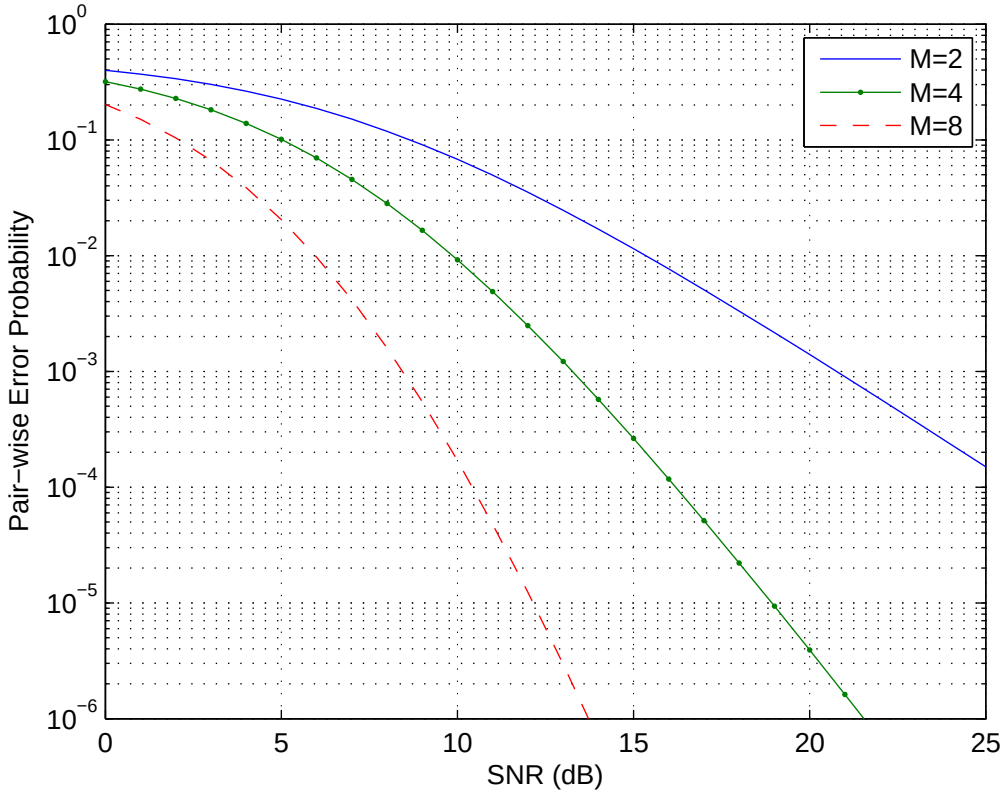

Figure 2.11: The Chernoff bound of PEP of noncoherent space-time codes. Number of transmit antennas $M = 2, 4, 8$ respectively and the number of receive antenna is 1. $d_m = 0.8$.

2.7 Conclusion

In this chapter, we presented the general model of modern wireless digital communication systems which includes the baseband representation of bandpass signals and further the vector space representation of signals. The channel model was also presented in this section. The history of MIMO communication systems were briefly reviewed. MIMO systems have been widely studied from the late 1990s. Space-time coding or modulation schemes for point-to-point MIMO systems are studied to enlarge the spectrum efficiency and to improve the communication robust. Recently, multi-user MIMO systems have been analyzed to further improve the spectrum efficiency. Then, we gave the MIMO system model which was used through our research. Finally, the channel capacities of MIMO systems with or without CSI were analyzed and the error performance of MIMO systems were also examined.

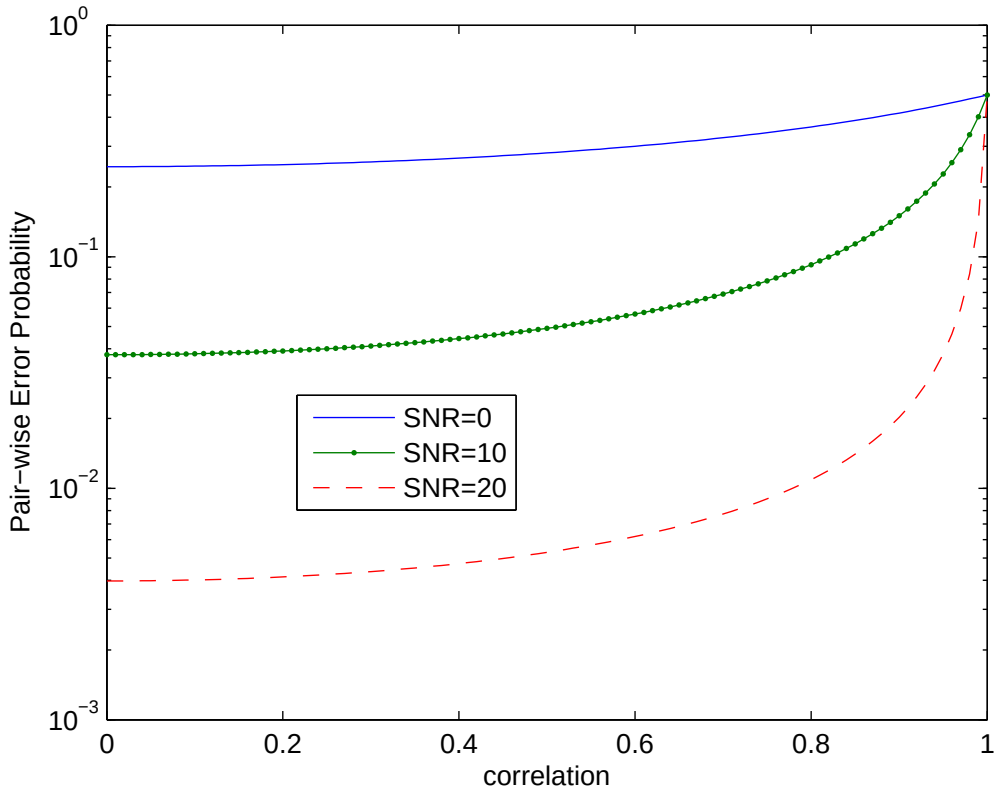

Figure 2.12: The Chernoff bound of PEP for noncoherent space-time codes. Number of transmit antennas $M = 4$ and number of receive antenna is 1 $N = 1$. SNR $= 0$, 10, 20 dB respectively.

3 Non-coherent space-time coding

In this chapter, we present some existing non-coherent space-time coding schemes. A non coherent communication system is a communication system where Channel State Information (CSI) is not known at the receiver end.

Some well-known space-time coding schemes are unitary space-time modulation (USTM) scheme [25, 26], differential unitary space-time modulation (DUSTM) [27], differential space-time block coding (DSTBC) [28, 29], differential space-time modulation (DSTM) [106] and matrix coded modulation (MCM) [30,31]. In fact, the basic idea behind DSTM and DUSTM is the same. Therefore, without special statement, DSTM and DUSTM are equivalents. The transmit and receive principles of each scheme are presented briefly.

3.1 Unitary space-time modulation

During the analysis of the capacity of MIMO systems without CSI [25], Marzetta and Hochwald found that the transmitted matrices must have special structure to achieve the capacity. They called the MIMO schemes with this special structure unitary space-time modulation (USTM) [26]. The structure of this scheme is obtained in Chapter 2, Section 2.5.2.

3.1.1 Transmission scheme

Hochwald and Marzetta proved the transmission matrix has the structure $X = A\Theta$ where A is an $M \times M$ diagonal matrix and Θ is an $M \times T$ matrix. The row

vectors of Θ are orthogonal one to each other ($\Theta\Theta^H = I_M$). When the duration of the normalized coherence interval is significantly greater than the number of transmitter antennas ($T \gg M$) or for any fixed $T > M$ as $\rho \to \infty$, setting $a_1 = a_2 = \cdots = a_M = \sqrt{\frac{T}{M}}$ attains capacity. In this case, the transmit matrix becomes $X = \sqrt{\frac{T}{M}}\Theta$ and Θ is an $M \times T$ isotropically distributed matrix. Furthermore, in this scheme, setting $T = M$ results $X^H X = \Theta^H\Theta = I_M$. The conditional probability will be $p(Y|X) = p(Y)$, which leads the mutual information $\mathcal{I}(X;Y)$ to be zero and the channel capacity is zero.

The information matrix is selected by a bit stream with RM bits from a set containing $K = 2^{MR}$ matrices, i.e., $\Theta \in \{\Theta_1, ..., \Theta_K\}$, where R is spectral efficiency with unit bps/Hz or bits/(channel use).

3.1.2 Detection scheme and design criteria of USTM constellations

At the receiver end, $Y = HX+W$ of dimension $N\times T$ is detected by the antennas. As presented in Chapter 2, Section 2.6.2, the maximum likelihood detector of this scheme must to determine the matrix that maximizes the conditional probability. That is

$$\begin{aligned}\Theta_{ml} &= \arg \max_{\Theta_k \in \{\Theta_1,...,\Theta_K\}} p(Y|\Theta_k) \\ &= \arg \max_{\Theta_k \in \{\Theta_1,...,\Theta_K\}} \mathrm{Tr}[Y\Theta_k^H\Theta_k Y^H].\end{aligned} \tag{3.1}$$

With this ML detector, the pairwise error probability (PEP) between Θ_k and Θ'_k is:

$$\begin{aligned}P_e =& \frac{1}{2}P\left(\mathrm{Tr}[Y\Theta_{k'}^H\Theta_{k'}Y^H] > \mathrm{Tr}[Y\Theta_k^H\Theta_k Y^H]|\Theta_k\right) \\ &+ \frac{1}{2}P\left(\mathrm{Tr}[Y\Theta_k^H\Theta_k Y^H] > \mathrm{Tr}[Y\Theta_{k'}^H\Theta_{k'}Y^H]|\Theta_{k'}\right),\end{aligned} \tag{3.2}$$

where Θ_k and $\Theta_{k'}$ are assumed to be transmitted with equal probability.

It is proved that the Chernoff upper bound of the above PEP is [26, 106]:

$$P_e \leq \frac{1}{2}\prod_{m=1}^{M}\left[1+\frac{(\frac{T}{M\sigma^2})^2(1-d_{kk',m}^2)}{4(1+\frac{T}{M\sigma^2})}\right]^{-N}, \tag{3.3}$$

where $d_{kk',1},\ldots,d_{kk',M}$ are singular values of $\Theta_k\Theta_{k'}^H$.

To minimize the pairwise error probability, we should make the singular values of the products $\Theta_k\Theta_{k'}^H$ as small as possible. The probability of error (and Chernoff bound) is lowest when $d_{kk',1}=\cdots=d_{kk',M}=0$ and highest when $d_{kk',1}=\cdots=d_{kk',M}=1$. As analyzed in Sec. 2.6.2, $d_{kk',1}=\cdots=d_{kk',M}=0$ indicates that $\Theta_k\Theta_{k'}^H=0$. However, as T is limited, the number of vectors that are orthogonal to each other in the T dimension vector space is limited to T, which in turn makes the number of matrices that are orthogonal to each other limited to $\lfloor T/M\rfloor$.

There are mainly two different criteria for designing USTM constellations. The first one is to minimize the maximum sum of squares of the singular values. For a given constellation, we define

$$\delta=\max_{1\leq k<k'\leq K}\frac{1}{\sqrt{M}}\|\Theta_k\Theta_{k'}^H\|=\max_{1\leq k<k'\leq K}\sqrt{\frac{1}{M}\sum_{m=1}^{M}d_{kk',m}^2}, \tag{3.4}$$

where the factor $\frac{1}{\sqrt{M}}$ is used to ensure $0\leq\delta\leq 1$. Then the design of USTM constellations is to find K matrices that minimize δ.

The second design criterion is obtained directly from the Chernoff upper bound of PEP(3.3). For high SNR, i.e., $\sigma^2\ll 1$, the Chernoff upper bound depends mainly on the product

$$\prod_{m=1}^{M}(1-d_{kk',m}^2).$$

As shown in [115], we can think of $d_{kk',m}$ as the cosine of the principal angle $\phi_{kk',m}$ between the subspaces spanned by the columns of Θ_k and $\Theta_{k'}$. The above expression can therefore be interpreted as the product of the squares of the sines of the m principal angles. To obtain a quantity that can be compared for different M, we

define $\zeta_{kk'}$ as the geometric mean of the sines of the principal angles

$$\zeta_{kk'} = \left[\prod_{m=1}^{M} \sin(\phi_{kk',m})\right]^{1/M} = \left[\prod_{m=1}^{M} (1 - d^2_{kk',m})\right]^{\frac{1}{2M}}. \tag{3.5}$$

Because $0 \leq d^2_{kk',m} \leq 1$, we have $0 \leq \zeta_{kk'} \leq 1$, and if $\zeta_{kk'}$ is large, the PEP is small. Thus, we need to maximize the *diversity product* defined as

$$\zeta = \min_{1 \leq k < k' \leq K} \zeta_{kk'}. \tag{3.6}$$

In particular, any constellation with nonzero diversity product is said to have full transmitter diversity. For small $d_{kk',m}$,

$$\zeta^2_{kk'} = 1 - \frac{1}{M}\sum_{m=1}^{M} d^2_{kk',m} + O(d^4_{kk',m}) = 1 - \frac{1}{M}\|\Theta_k \Theta^H_{k'}\|^2 + O(d^4_{kk',m}). \tag{3.7}$$

Thus, $\zeta^2 \approx 1 - \delta^2$ and small δ implies large ζ.

However, there is no special way to minimize these singular values $d_{kk',m}$, and the properties of a good signal constellation are not obvious. Hochwald and Marzetta analyzed the special case where $M = 1$, $R = 1$, $T = 5$ and $M = 2$, $R = 1$, $T = 5$ in [26]. However the transmission matrices are not given in the paper. In [101], a Fourier-based construction is proposed. This scheme is easy to realize, but it is not proved whether it is optimal. A USTM scheme via Cayley transform is presented in [116].

3.2 Differential unitary space-time modulation

Motivated by differential phase-shift keying (DPSK) scheme and based on unitary space-time modulation, Hochwald and Sweldens proposed Differential Unitary Space-Time Modulation (DUSTM) in [27].

3.2.1 Classical differential phase-shift keying

DPSK [46,49] is a technique used for single antenna communication system where the receiver end does not need to estimate the carrier phase. PSK modulation requires coherent demodulation, i.e., the phase of the receiver must match to the phase of the transmitted carrier. Techniques for phase recovery typically require more complexity and cost in the receiver and they are also susceptible to phase drift of the carrier.

DPSK is traditionally used when the channel changes the phase of the symbol in an unknown, but consistent or slowly varying way. The data information is sent in the difference of the phases of two consecutive symbols. For a date rate of R bits/(channel use) ($R \in \mathbb{N}$), the transmitted signal is selected from a constellation containing $K = 2^R$ signals. Normally, the constellation is:

$$\mathcal{A} = \{e^{2\pi jk/2^R} | k = 0, 1, \ldots, 2^R - 1\}. \tag{3.8}$$

In differential modulation scheme, we must transmit a reference signal first, for example, $x_0 = 1$. Suppose we want to send R bits and they are mapped to a symbol φ_t in the constellation. By differential transmission, the transmitted signal should be:

$$x_t = \varphi_t x_{t-1}, \quad t = 1, 2, \ldots \tag{3.9}$$

At the receiver end, the detected signals will be:

$$y_t = h_t x_t + w_t, \quad t = 0, 1, 2, \ldots, \tag{3.10}$$

where h_t is the fading coefficient which varies slowly with t and w_t is the additive white Gaussian noise. The symbol φ_t carries information and we use differential detection to recover the information bits. The signal received at time $t + 1$ is:

$$y_{t+1} = h_{t+1} x_{t+1} + w_{t+1} = h_{t+1} \varphi_{t+1} x_t + w_{t+1}. \tag{3.11}$$

With the approximation $h_{t+1} \approx h_t$, and the relation (3.10), the above equation can

be further simplified as:

$$y_{t+1} = \varphi_{t+1} y_t + (w_{t+1} - \varphi_{t+1} w_t). \tag{3.12}$$

Thus, the maximum likelihood demodulation is:

$$\hat{\varphi}_{t+1} = \arg \min_{k=1,\ldots,K} |y_{t+1} - \varphi_k y_t|. \tag{3.13}$$

Differentially encoded PSK can be demodulated coherently or noncoherently. Moreover, the noncoherent receiver has a simple form and performs within 3 dB of the coherent receiver on Rayleigh fading channels

Differential modulation is less sensitive to a random drift in the carrier phase. However, if the channel has a nonzero Doppler frequency, the signal phase can decorrelate between two successive symbols, making the previous symbol a very noisy phase reference. This decorrelation gives rise to an irreducible error floor for differential modulation over time-varying wireless channels which introduces a Doppler shift to the carrier frequency.

3.2.2 Multiple-antenna differential modulation

Hochwald and Sweldens [27] expanded the DPSK scheme to multiple-antenna system.

As we know, the transmitted signal of USTM scheme is a matrix with the rows orthogonal to each other, i.e., the vector of T signals transmitted by one antenna is orthogonal to the vector of T signals corresponding to another transmit antenna. The signals of DUSTM also constrain this rule. In order to fit the differential transmission scheme, the signals have some new properties.

Like DPSK, at time $t = 0$, a reference matrix, e.g., $X_0 = I_M$ is transmitted. Suppose at time $t-1$, X_{t-1} is transmitted. At time t, RM information bits are mapped to an $M \times M$ unitary matrix V_t selected from the set $\{V_1, ..., V_K\}$, $K = 2^{RM}$. The transmission matrix at time t is differentially obtained as: $X_t = X_{t-1} V_t$. At the

receiver end, the received matrices corresponding to time $t-1$ and t are:

$$Y_{t-1} = H_{t-1}X_{t-1} + W_{t-1} \tag{3.14}$$

and

$$Y_t = H_t X_t + W_t. \tag{3.15}$$

With the assumption that the channel is approximately constant during the transmission of two matrices, i.e., $H_{t-1} \approx H_t$, the received matrices at time t (Y_t) can be represented by the received matrix at time $t-1$ (Y_{t-1}):

$$\begin{aligned} Y_t &= H_{t-1}X_{t-1}V_t + W_t = (Y_{t-1} - W_{t-1})V_t + W_t \\ &= Y_{t-1}V_t + \sqrt{2}W_t'. \end{aligned} \tag{3.16}$$

Thus, V_t can be demodulated by the maximum likelihood detector:

$$\begin{aligned} \hat{V}_t &= \arg \min_{V_k \in \{V_1,\ldots,V_k\}} \|Y_t - Y_{t-1}V_k\| \\ &= \arg \min_{V_k \in \{V_1,\ldots,V_k\}} \mathrm{Tr}\{(Y_t - Y_{t-1}V_k)(Y_t - Y_{t-1}V_k)^H\} \\ &= \arg \max_{V_k \in \{V_1,\ldots,V_k\}} \Re\{\mathrm{Tr}[Y_{t-1}V_k Y_t^H]\} \\ &= \arg \max_{V_k \in \{V_1,\ldots,V_k\}} \Re\{\mathrm{Tr}[Y_t^H Y_{t-1}V_k]\}. \end{aligned} \tag{3.17}$$

As Hochwald and Swelden indicated, this scheme can be seen as a special case of USTM. In fact, the transmission matrices can be written as:

$$\Phi_t = \sqrt{\frac{T}{M}}\Theta_t = \sqrt{\frac{T}{M}}\frac{1}{\sqrt{2}}[I_M, V_t] = [I_M, V_t] \tag{3.18}$$

for USTM, where $\Theta_t = \frac{1}{\sqrt{2}}[I_M, V_t]$. We can see that the coherence interval here is $T = 2M$ and the factor $\sqrt{2}$ ensures $\Theta_t\Theta_t^H = I_M$.

At the receiver end, at time t, the detected matrix is:

$$\Upsilon_t = H_t[I_M, V_t] + \mathcal{N}_t = [Y_{t1}, Y_{t2}]. \tag{3.19}$$

The maximum likelihood detector in (3.1) becomes:

$$\begin{aligned} V_{ml} &= \arg \max_{V_k \in \{V_1,\ldots,V_K\}} \mathrm{Tr}[\Upsilon_t \Theta_k^H \Theta_k \Upsilon_t^H] \\ &= \arg \max_{\Theta_k \in \{V_1,\ldots,V_K\}} \mathrm{Tr}[(Y_{t1} + Y_{t2}V_k^H)(Y_{t1} + Y_{t2}V_k^H)^H] \\ &= \arg \max_{V_k \in \{V_1,\ldots,V_k\}} \Re\{\mathrm{Tr}[Y_{t1}V_k Y_{t2}^H]\}, \end{aligned} \tag{3.20}$$

which is the same as (3.17). Here we can see that the effect of the first half part Y_{t1} of Υ_t can be seen as a not so perfect estimation of the channel coefficients matrix H with a noise $\mathcal{N}_{t1}$ which is the first half part of $\mathcal{N}_t$.

Therefore, the differential scheme is a special case of USTM where the first half part of the transmission matrix is a reference. (3.16) is the fundamental differential receiver equation where Y_{t-1} can be seen as the channel response at time t which is known to the receiver. The sacrifice is that the noise has twice the variance which makes the error performance slightly worse. This corresponds to the well-known result that standard single-antenna differential modulation suffers from approximately a 3-dB performance loss in effective SNR when the channel is unknown versus when it is known.

Now we analyse the pair-wise error probability of DUSTM and get the design criteria. From (3.3), we know that the PEP performance of USTM depends on the singular values of $\Theta_k \Theta_{k'}^H$ and here $\Theta_k = \frac{1}{\sqrt{2}}[I_M, V_k]$. Then

$$\Theta_k \Theta_{k'}^H = \frac{1}{2}(I_M + V_k V_{k'}^H).$$

We denote the mth singular value of a matrix A as $\sigma_m(A)$ and the mth eigenvalue of matrix A as $\lambda_m(A)$. We know that $\sigma_m^2(A) = \lambda_m(AA^H)$. Then we have the relation

$$\begin{aligned} \sigma_m^2(\Theta_k \Theta_{k'}^H) &= \frac{1}{4}\sigma_m^2(I_M + V_k V_{k'}^H) \\ &= \frac{1}{4}\lambda_m(2I_M + V_k V_{k'}^H + V_{k'} V_k^H). \end{aligned} \tag{3.21}$$

The term $(1 - d^2_{kk',m})$ in (3.3) can be written as:

$$\begin{aligned} 1 - d^2_{kk',m} &= 1 - \frac{1}{4}\lambda_m(2I_M + V_k V_{k'}^H + V_{k'} V_k^H) \\ &= \frac{1}{4}\lambda_m(2I_M - V_k V_{k'}^H - V_{k'} V_k^H) \\ &= \frac{1}{4}\sigma_m^2(I_M - V_k V_{k'}^H) = \frac{1}{4}\sigma_m^2(V_k - V_{k'}). \end{aligned} \tag{3.22}$$

This equation says that minimizing the singular values of the correlations of the unknown-channel signals is equivalent to maximizing the singular values of the differences of the known channel signals.

From this analysis, we can see that there are also two design criteria for DUSTM. The first one is to maximize the sum of the square singular values of the differences of V_k and $V_{k'}$. We define

$$\delta_{kk'} = \sqrt{\frac{1}{M}\sum_{m=1}^{M}\left(1 - d^2_{kk',m}\right)} = \sqrt{\frac{1}{4M}\sum_{m=1}^{M}\sigma_m^2(V_k - V_{k'})} = \frac{1}{\sqrt{4M}}\|V_k - V_{k'}\|. \tag{3.23}$$

Thus the first design criterion is to maximize the minimum value of $\delta_{kk'}$ for all k. This criterion can be interpreted by maximizing the the minimum Frobinius distance between any two matrices V_k and $V_{k'}$.

The second design criterion is derived from (3.5) which is suitable for high SNRs. For DUSTM, $\zeta_{kk'}$ in (3.5) becomes:

$$\begin{aligned} \zeta_{kk'} &= \left[\prod_{m=1}^{M}(1 - d^2_{kk',m})\right]^{\frac{1}{2M}} = \frac{1}{2}\left[\prod_{m=1}^{M}\sigma_m(V_k - V_{k'})\right]^{\frac{1}{M}} \\ &= \frac{1}{2}\left|\det(V_k - V_{k'})\right|^{\frac{1}{M}}. \end{aligned} \tag{3.24}$$

The diversity product for differential modulation can now be written as

$$\zeta = \frac{1}{2}\min_{1\le k<k'\le K}\zeta_{kk'} = \frac{1}{2}\min_{1\le k<k'\le K}\left|\det(V_k - V_{k'})\right|^{\frac{1}{M}}. \tag{3.25}$$

Therefore, this design criterion is to maximize ζ of the constellation.

Hochwald and Sweldens proposed a cyclic group structure of the constellation

M	R	K	ζ	$[u_1, u_2, ..., u_M]$
1	1	2	1	[1](standard DBPSK)
2	1	4	0.7071	[1, 1]
3	1	8	0.5134	[1, 1, 3]
4	1	16	0.5453	[1, 3, 5, 7]
5	1	32	0.4095	[1, 5, 7, 9, 11]
1	2	4	0.7071	[1] (standard DQPSK)
2	2	16	0.3826	[1, 7]
3	2	64	0.2765	[1, 11, 27]
4	2	256	0.2208	[1, 25, 97, 107]
5	2	1024	0.1999	[1, 157, 283, 415, 487]

Table 3.1: DUSTM constellations [27] for $M = 1, 2, 3, 4, 5$ transmit antennas and spectral efficiency $R = 1, 2$ bps/Hz. The number of signals in the constellation is $K = 2^{RM}$.

where V_k has the form

$$V_k = V_1^k, \quad k = 0, ..., K-1$$

where the generator matrix V_1 is a Kth root of the unity, i.e., $V_1^K = I_M$. The matrix V_1 is diagonal and can be written as

$$V_1 = \text{diag}[e^{i(2\pi/K)u_1}, ..., e^{i(2\pi/K)u_M}], \quad u_m \in \{0, ..., K-1\}; \quad m = 1, ..., M.$$

At any time, only one transmitter antenna is active and transmitting a phase-shifted symbol. When $M = 1$, the signals reduce to standard DPSK. Now consider the design of $\{u_1, ..., u_M\}$. People should try to find $\{u_1, ..., u_M\}$ that maximizes ζ:

$$\begin{aligned} \zeta &= \frac{1}{2} \min_{0 \le k < k' \le K-1} |\det(V_k - V_{k'})|^{\frac{1}{M}} = \frac{1}{2} \min_{0 \le k \le K-1} |\det(V_k - I_M)|^{\frac{1}{M}} \\ &= \min_{0 \le k \le K-1} \left| \prod_{m=1}^{M} \sin(\pi u_m k / K) \right|^{\frac{1}{M}}. \end{aligned} \tag{3.26}$$

Hochwald and Sweldens got the $\{u_1, ..., u_M\}$s for $M = 1, 2, 3, 4, 5$ and $R = 1, 2$ respectively with exhaustive computer searches and we show them in Table 3.1.

We present the bit error rate (BER) performance of this scheme in Fig. 3.1 and

Fig. 3.2 for $R = 1$ and $R = 2$ respectively with the number of transmit antenna $M = 1, 2, 3, 4, 5$ and the number of receive antenna $N = 1$. The Rayleigh channel is assumed to be block-constant. In these simulations, the channel H is constant during the transmission of one block of 100 matrices and changes to other values randomly for the next block. From Fig. 3.1 we can see that for $R = 1$ systems, using multiple transmit antennas can significantly improve the error performance. However, in low SNR regime, the benefits of using multiple antennas more than 2 are not so clear. This phenomenon can also be seen for $R = 2$ systems, as shown in Fig. 3.2. This is because the scheme of Hochwald and Sweldens [27] is designed for high SNR.

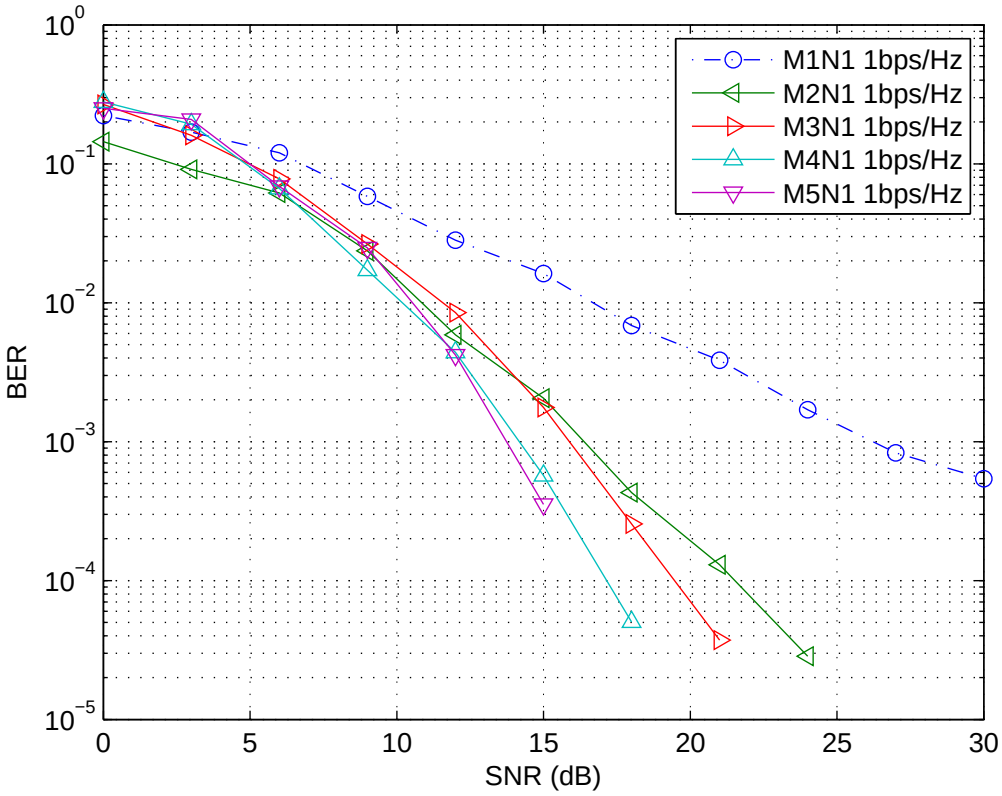

Figure 3.1: BER performance of DUSTM [27], $R = 1$.

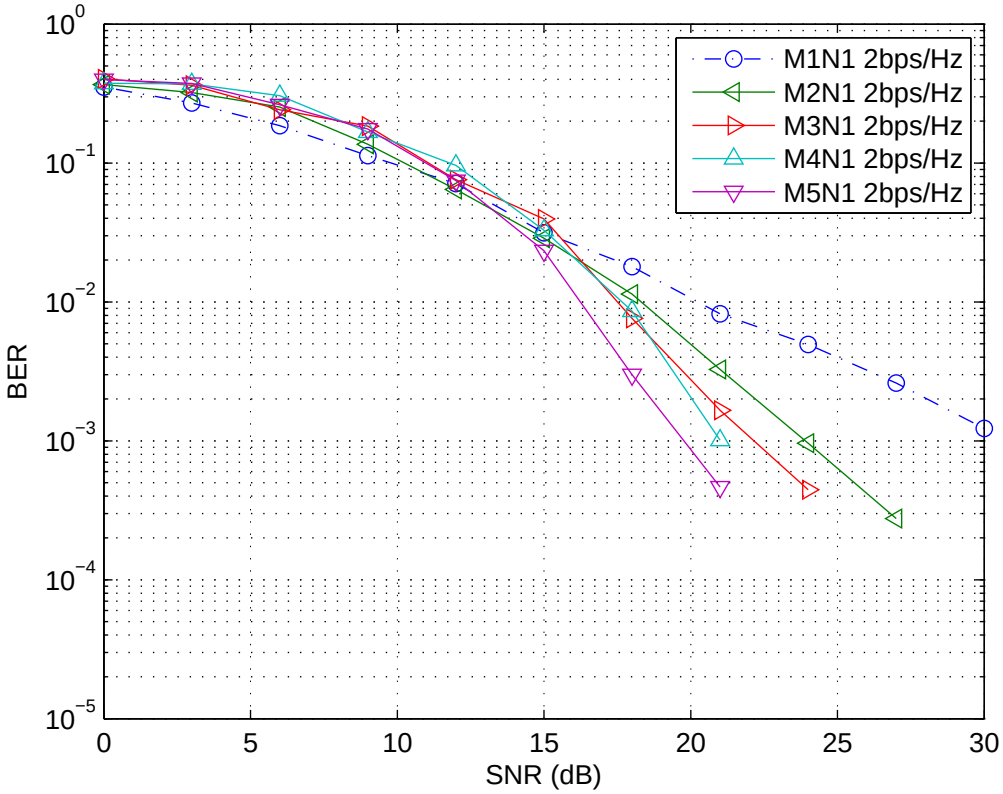

Figure 3.2: BER performance of DUSTM [27], $R = 2$.

3.3 Differential space-time block code

In [28, 29], Tarokh and Jafarkhani proposed a differential scheme (DSTBC) for STBC based on Alamouti's scheme [18]. This scheme is designed directly from Alamouti's STBC scheme and is easy to apply. In this scheme, the channel is assumed to be constant during two successive transmission matrices as in DPSK.

3.3.1 Alamouti's STBC scheme

Consider a MIMO system with 2 transmit antennas and 1 receive antenna. The channel coefficients are perfectly estimated by the receiver. The transmission matrix

of Alamouti's scheme is:

$$X = \begin{pmatrix} x_{11} & x_{12} \\ x_{21} & x_{22} \end{pmatrix} = \begin{pmatrix} s_1 & -s_2^* \\ s_2 & s_1^* \end{pmatrix}, \tag{3.27}$$

and the received matrix is:

$$\begin{aligned} Y &= (y_{11}, y_{12}) = HX + W \\ &= (h_{11}, h_{12}) \begin{pmatrix} s_1 & -s_2^* \\ s_2 & s_1^* \end{pmatrix} + (w_{11} \quad w_{12}), \end{aligned} \tag{3.28}$$

where s_i is the signal selected from a signal set, for example, PSK signal set according to the incoming information bits. Due to the orthogonal structure of transmission matrix, if the channel coefficients are perfectly obtained by the receiver, the estimated signal of (s_1, s_2) are:

$$\begin{aligned} (\widetilde{s}_1, \widetilde{s}_2) =& (y_{11}, y_{12}^*) \begin{pmatrix} h_{11}^* & h_{12}^* \\ h_{12} & -h_{11} \end{pmatrix} \\ =& \big((|h_{11}|^2 + |h_{12}|^2)s_1 + h_{11}^* w_{11} + h_{12} w_{12}^*, \\ & (|h_{11}|^2 + |h_{12}|^2)s_2 - h_{11} w_{12}^* + h_{12}^* w_{11}\big). \end{aligned} \tag{3.29}$$

When the estimated signals above are obtained, the transmitted signal can be recovered as in the SISO communication systems, which is pretty simple.

3.3.2 Differential transmission of Alamouti's STBC scheme

Now we consider the differential transmission of Alamouti's scheme. Any two dimensions vector $S = (s_3, s_4)$ can be uniquely represented by the orthonormal basis

given by Alamouti's scheme:

$$\begin{pmatrix} s_3 \\ \\ s_4 \end{pmatrix} = XP = \begin{pmatrix} s_1 & -s_2^* \\ \\ s_2 & s_1^* \end{pmatrix} \begin{pmatrix} p_1 \\ \\ p_2 \end{pmatrix}, \tag{3.30}$$

where s_i are PSK signals selected from the set $\mathcal{A} = \left\{ \frac{e^{2\pi kj/2^b}}{\sqrt{2}} | k = 0, 1, ..., 2^b - 1 \right\}$ and b is the number of bits that each signal can represent. $P = (p_1, p_2)^T$ is the coefficients vector. In this case, the transmission matrix X of Alamouti's scheme is unitary matrix, i.e., $X^{-1} = X^H$ and

$$P = \begin{pmatrix} p_1 \\ \\ p_2 \end{pmatrix} = X^H \begin{pmatrix} s_3 \\ \\ s_4 \end{pmatrix} = \begin{pmatrix} s_1^* & s_2^* \\ \\ -s_2 & s_1 \end{pmatrix} \begin{pmatrix} s_3 \\ \\ s_4 \end{pmatrix}. \tag{3.31}$$

Let $(s_1, s_2) = \frac{1}{\sqrt{2}}(1, 1)$ and given all the possible combinations of (s_3, s_4), the set $\mathcal{P}$ that contains all column vectors P can be determined. The set $\mathcal{P}$ has 2^{2b} column vectors and $2b$ information bits are mapped onto P. Suppose that at time $\tau - 1$, $X_{\tau-1}$ is transmitted. Then at time τ, $2b$ information bits are mapped onto P_τ and the signals to be transmitted are determined by (3.30), i.e.:

$$\begin{pmatrix} s_{2\tau+1} \\ \\ s_{2\tau+2} \end{pmatrix} = X_{\tau-1} P_\tau = \begin{pmatrix} s_{2\tau-1} & -s_{2\tau}^* \\ \\ s_{2\tau} & s_{2\tau-1}^* \end{pmatrix} \begin{pmatrix} p_{1\tau} \\ \\ p_{2\tau} \end{pmatrix}, \tag{3.32}$$

and

$$X_\tau = \begin{pmatrix} s_{2\tau+1} & -s_{2\tau+2}^* \\ \\ s_{2\tau+2} & s_{2\tau+1}^* \end{pmatrix} = X_{\tau-1} \begin{pmatrix} p_{1\tau} & -p_{2\tau}^* \\ \\ p_{2\tau} & p_{1\tau}^* \end{pmatrix} \tag{3.33}$$

At the receiver side, with 2 transmit antennas and 1 receive antenna, we have the relation:

$$\begin{aligned} Y_\tau &= \begin{pmatrix} y_{2\tau+1} & y_{2\tau+2} \end{pmatrix} = HX_\tau + W_\tau \\ &= \begin{pmatrix} h_{11} & h_{12} \end{pmatrix} \begin{pmatrix} s_{2\tau+1} & -s^*_{2\tau+2} \\ s_{2\tau+2} & s^*_{2\tau+1} \end{pmatrix} + \begin{pmatrix} w_{2\tau+1} & w_{2\tau+2} \end{pmatrix}. \end{aligned} \tag{3.34}$$

This relation can be rewritten in the forms as followed:

$$\begin{pmatrix} y_{2\tau+1} & y^*_{2\tau+2} \end{pmatrix} = (s_{2\tau+1}, s_{2\tau+2}) \begin{pmatrix} h_{11} & h^*_{12} \\ h_{12} & -h^*_{11} \end{pmatrix} + (w_{2\tau+1}, w^*_{2\tau+2}), \tag{3.35}$$

$$\begin{pmatrix} y_{2\tau} & y^*_{2\tau-1} \end{pmatrix} = (s_{2\tau-1}, s_{2\tau}) \begin{pmatrix} h_{11} & h^*_{12} \\ h_{12} & -h^*_{11} \end{pmatrix} + (w_{2\tau-1}, w^*_{2\tau}), \tag{3.36}$$

and

$$\begin{pmatrix} y_{2\tau} & -y^*_{2\tau-1} \end{pmatrix} = \begin{pmatrix} -s^*_{2\tau} & s^*_{2\tau-1} \end{pmatrix} \begin{pmatrix} h_{11} & h^*_{12} \\ h_{12} & -h^*_{11} \end{pmatrix} + (w_{2\tau-1}, w^*_{2\tau}). \tag{3.37}$$

From (3.32), we know that:

$$\begin{aligned} \begin{pmatrix} p_{1\tau} \\ p_{2\tau} \end{pmatrix} &= \begin{pmatrix} s_{2\tau-1} & -s^*_{2\tau} \\ s_{2\tau} & s^*_{2\tau-1} \end{pmatrix}^H \begin{pmatrix} s_{2\tau+1} \\ s_{2\tau+2} \end{pmatrix} \\ &= \begin{pmatrix} s^*_{2\tau-1} & s^*_{2\tau} \\ -s_{2\tau} & s_{2\tau-1} \end{pmatrix} \begin{pmatrix} s_{2\tau+1} \\ s_{2\tau+2} \end{pmatrix}. \end{aligned} \tag{3.38}$$

Combine the above four relations, we get the estimation of P_τ as

$$\begin{aligned}\widetilde{P}_\tau &= \begin{pmatrix} y^*_{2\tau-1} & y_{2\tau} \\ y_{2\tau} & -y^*_{2\tau-1} \end{pmatrix} \begin{pmatrix} y_{2\tau+1} \\ y^*_{2\tau+2} \end{pmatrix} \\ &= (|h_{11}|^2 + h_{12}|^2) \begin{pmatrix} s^*_{2\tau-1}s_{2\tau+1} + s^*_{2\tau}s_{2\tau+2} \\ -s_{2\tau+1}s_{2\tau} + s_{2\tau+2}s_{2\tau-1} \end{pmatrix} + W',\end{aligned} \tag{3.39}$$

where W' is the noise component. The closest vector of $\mathcal{P}$ to $\widetilde{P}_\tau$ is believed to be the information vector and the inverse mapping let us obtain the information bits. Jafarkhani and Tarokh expanded the scheme above to MIMO systems with 4 transmit antennas in [29] and the transmit and receive procedure is similar.

The bit error rate (BER) performances of DSTBC and STBC are shown in Fig. 3.3.

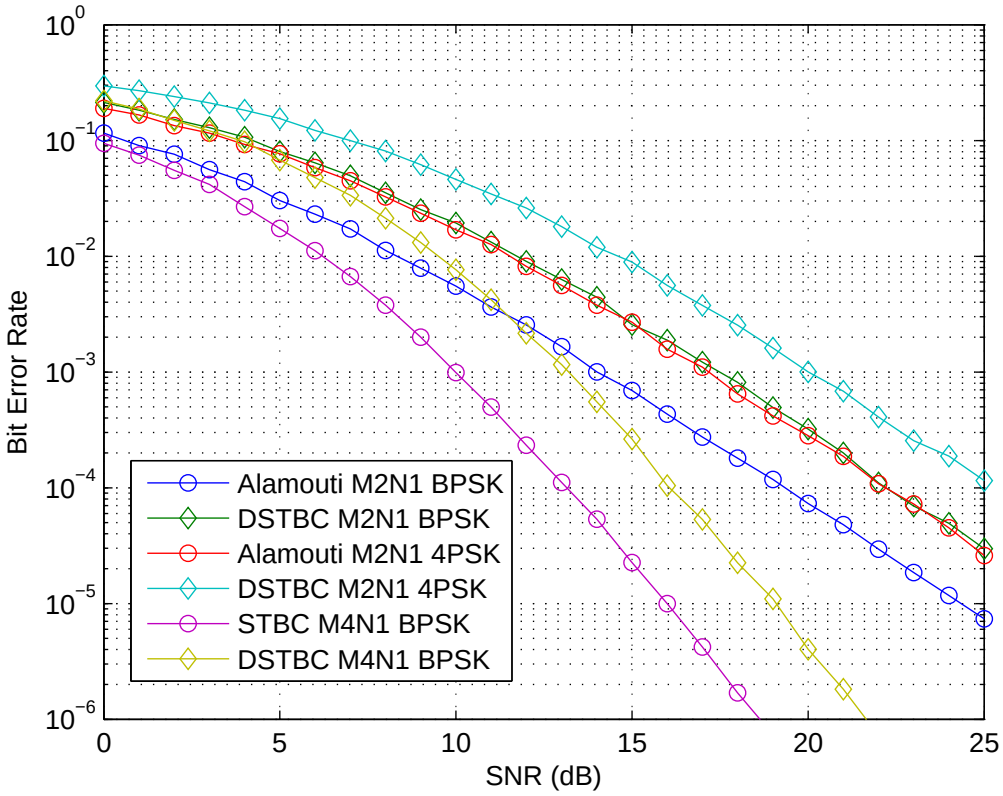

Figure 3.3: BER performance of STBC and DSTBC.

The fading is assumed to be constant over each frame and vary from one frame to another. We can see from this figure that the BER performance of differential space-time coding scheme is about 3 dB worse than the corresponding coherent detection STBC scheme. Furthermore, the STBC and DSTBC schemes in the figure achieve full diversity gain which is represented by the slope of the BER curve.

DSTBC schemes are suitable for MIMO systems with up to 4 transmit antennas.

3.4 Matrix coded modulation

Matrix coded modulation or MCM is a kind of MIMO system that proposed by A. El Arab, J-C. Carlach and M. Hélard [30, 31]. This scheme combines channel coding, modulation and space-time coding into one function, and it is dedicated to non-coherent systems.

Fig. 3.4 shows a general model of the MCM scheme.

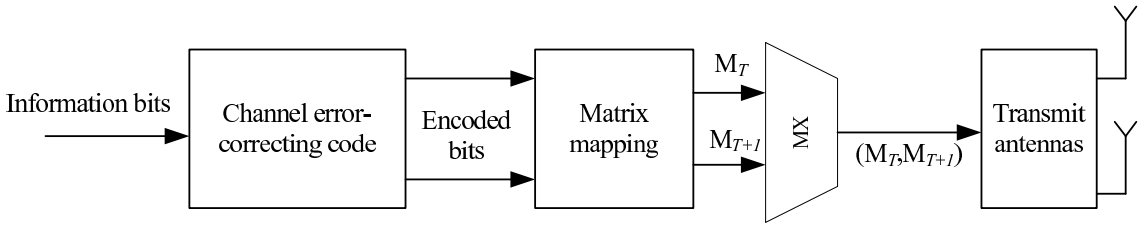

Figure 3.4: MIMO-MCM system model.

Information bits are encoded with a channel error-correcting code and then divided into streams to be mapped directly onto matrices of complex symbols. Take 2×2 non-coherent MIMO-MCM scheme as an example. Information bits, b_{0-3}, are coded by an error correcting code ($H(8,4,4)$ Hamming code) and generates two streams of coded bits c_{0-3} and c_{4-7}, where $c_{0-3} = b_{0-3}$ are the information bits and c_{4-7} are 4 control bits.

These two bit-streams are interleaved with (π_p, π_q) and mapped directly into a pair of invertible matrices (V_α, V_β) of size $M \times M$. These two matrices are consecutively transmitted over the M antennas by $X_t = V_\alpha$ and $X_{t+1} = V_\beta$. The invertible matrices should be chosen from a multiplicative group G such that: $(V_\alpha, V_\beta) \in$

(C_p, C_q) where (C_p, C_q) are two different cosets of G. The choice of (π_p, π_q) and (C_p, C_q) is not arbitrary. In fact, for a given pair (V_α, V_β), the couple $(V_a, V_b) \in (C_p, C_q)$ which verify the equation

$$V_\alpha V_a^{-1} - V_\beta V_b^{-1} = 0$$

must be unique. At the receiver end, this relation will be used to detect the transmitted matrices.

3.4.1 The transmission group of MCM

The transmitted matrices are selected from the Weyl group G_w [117]. The Weyl group G_w is a set that contains 12 cosets $(C_0, C_1, ..., C_{11})$. Each coset contains 16 invertible matrices. The first coset is defined as:

$$C_0 = \alpha \left\{ \begin{pmatrix} 1 & 0 \\ 0 & 1 \end{pmatrix}, \begin{pmatrix} 1 & 0 \\ 0 & -1 \end{pmatrix}, \begin{pmatrix} 0 & 1 \\ 1 & 0 \end{pmatrix}, \begin{pmatrix} 0 & 1 \\ -1 & 0 \end{pmatrix} \right\} \tag{3.40}$$

with $\alpha \in \{1, -1, i, -i\}$. The 12 cosets of G_w are derived from C_0 as follows:

$$C_k = A_k C_0, \quad k = 0, 1, \ldots, 11, \tag{3.41}$$

where the matrices $A_k, k = 0, 1, \ldots, 5$ are respectively:

$$A_0 = \begin{pmatrix} 1 & 0 \\ 0 & 1 \end{pmatrix}, A_1 = \begin{pmatrix} 1 & 0 \\ 0 & i \end{pmatrix}, A_2 = \frac{1}{\sqrt{2}} \begin{pmatrix} 1 & 1 \\ 1 & -1 \end{pmatrix},$$
$$A_3 = \frac{1}{\sqrt{2}} \begin{pmatrix} 1 & 1 \\ i & -i \end{pmatrix}, A_4 = \frac{1}{\sqrt{2}} \begin{pmatrix} 1 & i \\ 1 & -i \end{pmatrix}, A_5 = \frac{1}{\sqrt{2}} \begin{pmatrix} 1 & i \\ i & 1 \end{pmatrix},$$

and the matrices $A_k, k = 6, 7, \ldots, 11$ are given by:

$$A_{k+6} = \eta A_k, \quad with \quad \eta = (1+i)/\sqrt{2}, \quad k = 0, 1, \ldots, 5. \tag{3.42}$$

3.4.2 MCM with Hamming block coding

Consider a MCM system with $M = 2$ transmit antennas and $N = 2$ (also, we can set $N = 1, 3, ...$) receive antennas, and each transmit matrix is sent during $T = M = 2$ symbols. The systematic Hamming code $H(8, 4, 4)$ is used to encode the information bits. The code rate is $r = 1/2$ and its minimum Hamming distance is $d_{min} = 4$. The generation equation of Hamming code is: $c = bG$, where c is the generated codeword $(c_0, c_1, ..., c_7)$, b is a block of 4 information bits and G is the generation matrix. For this special scheme, the generation matrix is:

$$G = \begin{pmatrix} 1 & 0 & 0 & 0 & 1 & 1 & 1 & 0 \\ 0 & 1 & 0 & 0 & 0 & 1 & 1 & 1 \\ 0 & 0 & 1 & 0 & 1 & 0 & 1 & 1 \\ 0 & 0 & 0 & 1 & 1 & 1 & 0 & 1 \end{pmatrix}$$

The codeword $(c_0, c_1, ..., c_7)$ is mapped onto 2 $M \times M$ matrices (V_α, V_β). The mapping rule is defined as follows:

1. With the encoded bits $(c_0, c_1, ..., c_7)$, the first 4 information bits (c_0, c_1, c_2, c_3) are permuted with π_0: $(0, 1, 2, 3) \rightarrow (0, 1, 2, 3)$, i.e., $(c_0, c_1, c_2, c_3) \rightarrow (c_0, c_1, c_2, c_3)$ and then mapped to a matrix V_α in the coset C_0. The other 4 redundant bits (c_4, c_5, c_6, c_7) are permuted with π_2: $(0, 1, 2, 3) \rightarrow (1, 0, 3, 2)$, i.e., $(c_4, c_5, c_6, c_7) \rightarrow (c_5, c_4, c_7, c_6)$ and then mapped to a matrix V_β in the coset C_2.

2. The choice of the 2 permutations (π_0, π_2) and the 2 cosets (C_0, C_2) is not arbitrary. In fact, they are obtained by exhaustive search. With the matrices (V_α, V_β) generated above, there must be a unique solution to the equation:

$$V_\alpha V_a^{-1} - V_\beta V_b^{-1} = 0,$$

where $(V_a, V_b) \in (C_p, C_q)$.

In fact, there are $A_4^4 = 24$ different kinds of permutations for π_0 and π_2 respectively, and 24×24 pairs of (π_0, π_2). But the pairs which satisfy the solution

of the equation above are rare. For π_0: $(0,1,2,3) \to (0,1,2,3)$, there are only 3 permutations π_2 which satisfy the condition. They are: $(0,1,2,3) \to (1,0,3,2)$, $(0,1,2,3) \to (1,2,3,0)$ and $(0,1,2,3) \to (3,2,1,0)$.

For example, four information bits 0001 feed into the encoder, according to the generation matrix, the codeword is 00011101. With the permutation $(0,1,2,3) \to (0,1,2,3)$, we compute the label (i_0, i_2) of the matrices (V_α, V_β) in the cosets C_0 and C_2:

$$i_0 = 0 \cdot 2^3 + 0 \cdot 2^2 + 0 \cdot 2^1 + 1 \cdot 2^0 = 1$$
$$i_2 = 1 \cdot 2^3 + 1 \cdot 2^2 + 1 \cdot 2^1 + 0 \cdot 2^0 = 14.$$

The pair of matrices $(X_t, X_{t+1}) = (V_\alpha, V_\beta) = (V_{i_0}, V_{i_2})$ is transmitted successively during 4 time slots on the two transmit antennas. The 2 $M \times M$ matrices $(X_t, X_{t+1}) = (V_\alpha, V_\beta)$ are received successively by the N transmit antennas:

$$Y_t = HX_t + W_t$$
$$Y_{t+1} = HX_{t+1} + W_{t+1}$$

According to the mapping rule (the solution to the equation $V_\alpha V_a^{-1} - V_\beta V_b^{-1} = 0$ is unique), we get the decoding algorithm as follows:

$$(\hat{V}_a, \hat{V}_b) = \arg \min_{(V_a, V_b) \in (C_0, C_2)} \| Y_t V_a^{-1} - Y_{t+1} V_b^{-1} \|.$$

With the estimated matrices and the bijective mapping rule, the 4 information bits are recovered.

In the study of this scheme, we found that the matrices of the Weyl group are perfectly suitable for the differential transmission scheme. Therefore we study the performance of Weyl group in the differential MIMO systems and get some interesting results.

3.5 Conclusion

In this chapter, we presented the non-coherent space-time coding/modulation schemes which are related to our research. Marzetta and Hochwald proposed USTM scheme [26] when they tried to analyze the capacity of MIMO systems without CSI [25]. Then they expanded this scheme to differential unitary space-time modulation [27]. However, how to generate good performing constellations of unitary matrices for both of these two schemes is not clear, especially for systems with large number of transmit antennas. Tarokh and Jafarkhani proposed DSTBC schemes in [28] based on Alamouti's STBC scheme for MIMO systems with 2 transmit antennas and expanded the differential scheme to MIMO systems with 4 transmit antennas in [29]. This scheme is suitable for MIMO systems with less than 4 transmit antennas. A. El Arab, J-C. Carlach and M. Hélard [30, 31] presented a new kind of modulation scheme (MCM) for MIMO systems without using CSI. This scheme is just suitable for MIMO systems with 2 transmit antennas. The expansion of this scheme to MIMO systems with more than 2 transmit antennas is not clear and the spectral efficiency is limited. In the study of MCM, we found that the Weyl group can be used in DSTM schemes.

4

New differential space-time modulation with 2 transmit antennas

In this chapter, we propose our new differential space-time modulation scheme based on the Weyl group and the simulation results are analyzed. This scheme can be used for MIMO systems with $2^n, n = 1, 2, ...$ transmit antennas. We present here DSTM schemes with 2 transmit antennas in this chapter. For MIMO systems with 2 transmit antennas, the information matrices are elements of the Weyl group which is a special case of Lie group with finite order. Gray mapping is used to improve the BER performance. Furthermore, the BER performance can be improved by selecting the set with the best distance spectrum, which is a design criterion of DSTM schemes. The second design criterion which is based on the diversity product is also analysed. We compare our schemes with DSTBC in [28, 29] and DUSTM schemes in [27] and show the advantages of our schemes.

4.1 General Model of Differential Space-Time Modulation System

The differential MIMO system model is based on the fundamental equation (2.59) discussed in Chapter 2 and the scheme discussed in Section 3.2. In the differential space-time modulation systems, one vector of information bits is mapped onto a matrix V in the candidate set P according to a mapping rule. The dimension of the transmitted matrix X is $M \times T$. For simplicity, we assume that $T = M$. Of course,

this scheme can be extended to MIMO systems with $T > M$ or $T < M$. However, this extension introduces some complications and we will not discuss this situation here. For example, the transmitter sends a reference matrix $X_0 = V_0$ at time τ_0. The first vector of the information bits is mapped onto the information matrix V_{τ_1} and the second block is mapped onto V_{τ_2} etc. The fundamental differential transmission relation is:

$$X_{\tau+1} = X_\tau V_{i_{\tau+1}}, \quad \tau = 0, 1, \ldots \tag{4.1}$$

Therefore, at the transmitter end, the sequence of transmitted matrices is:

$$\begin{aligned}
&X_0 = V_0,\\
&X_1 = X_0 V_{i_1} = V_0 V_{i_1},\\
&X_2 = X_1 V_{i_2} = V_0 V_{i_1} V_{i_2},\\
&\ldots\\
&X_\tau = X_{\tau-1} V_{i_\tau} = V_0 V_{i_1} \ldots V_{i_\tau},\\
&\ldots
\end{aligned}$$

At the receiver side, the N antennas receive a matrix stream $Y_0, \ldots, Y_\tau, Y_{\tau+1}, \ldots$. We know that

$$Y_\tau = H_\tau X_\tau + W_\tau \tag{4.2}$$

and

$$Y_{\tau+1} = H_{\tau+1} X_{\tau+1} + W_{\tau+1} \tag{4.3}$$

Based on the differential transmission equation (4.1) and with the assumption that the fading coefficients are constant during the transmission of two successive matrices,i.e., $H_\tau = H_{\tau+1} = H$, we get

$$\begin{aligned}
Y_{\tau+1} &= H X_{\tau+1} + W_{\tau+1} = H X_\tau V_{i_{\tau+1}} + W_{\tau+1}\\
&= (Y_\tau - W_\tau) V_{i_{\tau+1}} + W_{\tau+1} = Y_\tau V_{i_{\tau+1}} + W_{\tau+1} - W_\tau V_{i_{\tau+1}}\\
&= Y_\tau V_{i_{\tau+1}} + W'_{\tau+1},
\end{aligned} \tag{4.4}$$

where $W'_{\tau+1} = W_{\tau+1} - W_\tau V_{i_{\tau+1}}$.

Therefore, to estimate the information matrix, the maximum likelihood demodulator is

$$\begin{aligned}\hat{V}_{i_{\tau+1}} &= \arg\min_{V\in P}\|Y_{\tau+1} - Y_\tau V\| \\ &= \arg\min_{V\in P}\mathrm{Tr}\{(Y_{\tau+1} - Y_\tau V)^H(Y_{\tau+1} - Y_\tau V)\} \\ &= \arg\max_{V\in P}\mathrm{Tr}\{\mathrm{Re}(Y_{\tau+1}^H Y_\tau V)\}.\end{aligned} \tag{4.5}$$

Once the information matrix is obtained, the information bits can be recovered by the inverse mapping rule.

4.2 The constellation for MIMO systems with 2 transmit antennas

In our scheme, the information matrices are derived from the Weyl group used in [30, 31]. The Weyl group G_w is a set that contains 12 cosets $\big(C_0, C_1, \ldots, C_{11}\big)$. Each coset contains 16 invertible matrices. The first coset is defined as:

$$C_0 = \alpha\left\{M_0 = \begin{pmatrix}1 & 0\\ 0 & 1\end{pmatrix}, M_1 = \begin{pmatrix}1 & 0\\ 0 & -1\end{pmatrix}, M_2 = \begin{pmatrix}0 & 1\\ 1 & 0\end{pmatrix}, M_3 = \begin{pmatrix}0 & 1\\ -1 & 0\end{pmatrix}\right\}, \tag{4.6}$$

with $\alpha \in \{1, -1, i, -i\}$. The 12 cosets of G_w are derived from C_0 as follows:

$$C_k = A_k C_0, \quad k = 0, 1, \ldots, 11, \tag{4.7}$$

where the matrices A_k, $k = 0, 1, \ldots, 5$ are respectively:

$$A_0 = \begin{pmatrix}1 & 0\\ 0 & 1\end{pmatrix}, A_1 = \begin{pmatrix}1 & 0\\ 0 & i\end{pmatrix}, A_2 = \frac{1}{\sqrt{2}}\begin{pmatrix}1 & 1\\ 1 & -1\end{pmatrix},$$

$$A_3 = \frac{1}{\sqrt{2}}\begin{pmatrix}1 & 1\\ i & -i\end{pmatrix}, A_4 = \frac{1}{\sqrt{2}}\begin{pmatrix}1 & i\\ 1 & -i\end{pmatrix}, A_5 = \frac{1}{\sqrt{2}}\begin{pmatrix}1 & i\\ i & 1\end{pmatrix},$$

and the matrices $A_k, k = 6, 7, \ldots, 11$ are given by:

$$A_{k+6} = \eta A_k, \quad with \quad \eta = (1+i)/\sqrt{2}, \forall k = 0, 1, \ldots, 5. \tag{4.8}$$

There are 192 matrices in this group, and we number the matrices as $M_0, M_1, \ldots, M_{191}$:

$$\begin{aligned} M_{k+4} &= -M_k,\ M_{k+8} = iM_k,\ M_{k+12} = -iM_k,\ k = 0, ..., 3. \\ M_{16l+j} &= A_l \times M_j,\ l = 0, ..., 11.\ j = 0, ..., 16. \end{aligned} \tag{4.9}$$

Furthermore, they are all *unitary* matrices, i.e., the inverse of the matrix is equal to the conjugate transpose of the matrix and the matrix obeys the power constraint (2.60).

The matrices of the Weyl Group can be seen as 192 points distributed in the complex matrices sphere.

We define the distance between two matrices M_a and M_b as in (2.82):

$$D(M_a, M_b) = \|M_a - M_b\|. \tag{4.10}$$

We can see that $D(M_a, M_b) = D(M_b, M_a)$. Therefore, there are $191 \times 192/2 = 18336$ values $D(M_a, M_b)$ with $0 \leq a < b \leq 191$. However, for any value a, the distribution of the 191 values $D(M_a, M_b)$ with $b \neq a$ is the same, as shown in Fig. 4.1 and Table 4.1. For C_0, this distribution is given in Fig. 4.2.

Remark If A is an $n \times n$ unitary matrix, i.e., $AA^H = A^H A = I_n$, the Frobinous norm of A, $\|A\| = \sqrt{\mathrm{Tr}(AA^H)} = \sqrt{\mathrm{Tr}(A^H A)} = \sqrt{n}$. $\forall\ M_a, M_b \in C_0$, $\|M_a - M_b\| = \sqrt{\mathrm{Tr}[(M_a - M_b)^H (M_a - M_b)]}$. Since all the cosets are generated from C_0 by multiplying special unitary matrices A_k, the distance between $A_k M_a$ and $A_k M_b$ is $\|A_k M_a - A_k M_b\| = \sqrt{\mathrm{Tr}[(M_a - M_b)^H A_k^H A_k (M_a - M_b)]} = \sqrt{\mathrm{Tr}[(M_a - M_b)^H (M_a - M_b)]} = \|M_a - M_b\|$. Therefore, the distance spectrum of each coset of the Weyl group is exactly the same as the spectrum of C_0.

Consider a MIMO system with $M = 2$ transmit antennas and $N = 2$ receive antennas. Each transmit matrix is sent during $T = 2$ symbol durations. The

Distance	Occurrences
$\sqrt{4-2\sqrt{2}}$	8
$\sqrt{2}$	20
$\sqrt{4-\sqrt{2}}$	16
2	102
$\sqrt{4+\sqrt{2}}$	16
$\sqrt{6}$	20
$\sqrt{4+2\sqrt{2}}$	8
$2\sqrt{2}$	1

Table 4.1: The distance spectrum for an arbitrary matrix in G_w.

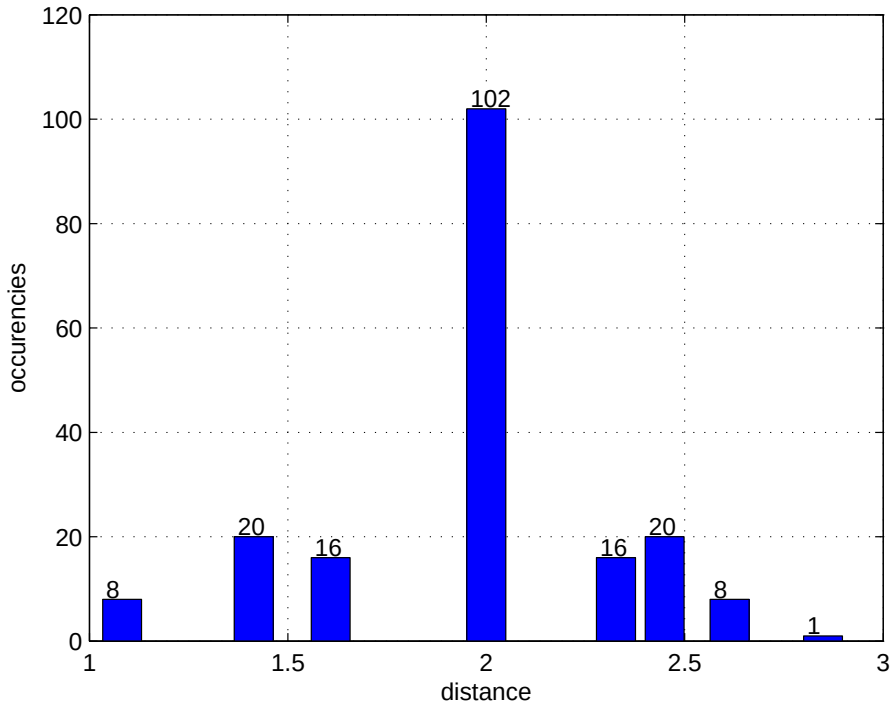

Figure 4.1: Distance spectrum of Weyl group.

number of receive antennas is arbitrary, i.e. we can set $N = 1, 2, 3, \ldots$. As there are $K = 192$ matrices in the Weyl group G_w, for MIMO systems with 2 transmit antennas, the maximum spectral efficiency we can get is $R = \frac{1}{M}\lfloor \log_2 K \rfloor = 3.5$ bps/Hz. We present the DSTM MIMO systems with $R = 2$ bps/Hz and $R = 1,\ 3$ bps/Hz respectively.

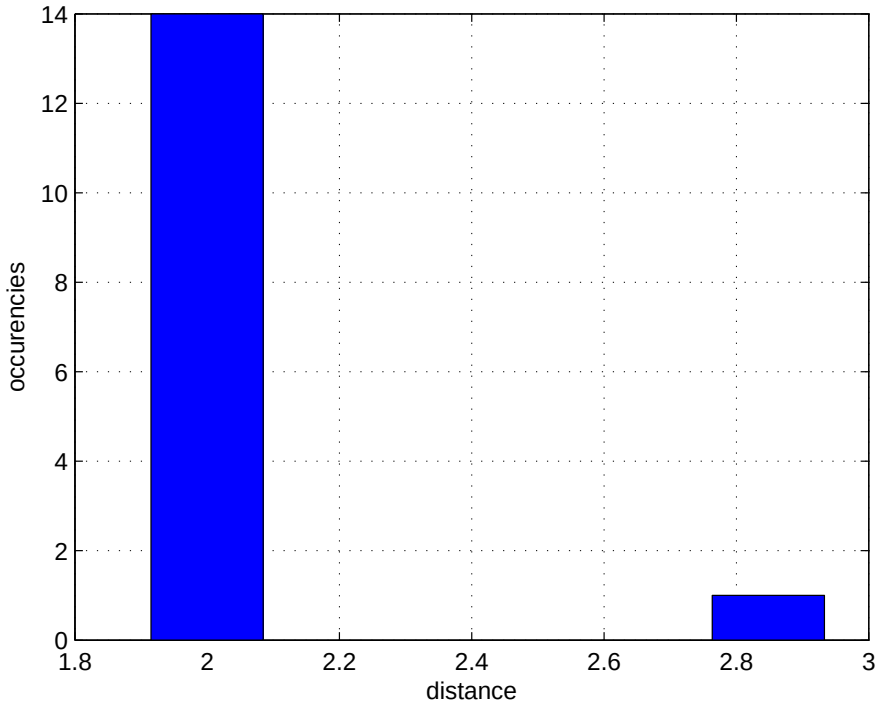

Figure 4.2: Distance spectrum of coset C_0

4.3 Spectral efficiency $R = 2$ bps/Hz

With the number of transmit antennas $M = 2$ and $T = M = 2$, for spectral efficiency $R = 2$ bps/Hz, each transmission matrix should carry $RT = 4$ bits and a set with $2^{RT} = 16$ matrices are needed. We select the set with the maximized minimum distance to map the information bits. Consider a group with K matrices $V_1, ..., V_K$, the minimum distance of the group is defined as:

$$\delta = \min_{1 \le k < k' \le K} \|V_k - V_{k'}\|. \tag{4.11}$$

The best group should have the maximized δ. We can see that the minimum distance of the matrices in C_0 is 2 which is maximized for all possible sets with 16 matrices in Weyl group. We say that C_0 is the best set. Since the other 11 cosets have exactly the same distance spectrum as C_0, they are also the best sets.

Furthermore, we can see that the constellation of the cosets C_0, C_1 is $4PSK \bigcup \{0\}$ and the constellation of C_6 and C_7 is 4PSK with a phase shift $\pi/4$ $\bigcup \{0\}$. At each

transmission time, only one of the antenna is active and transmit a symbol with energy 1. When the cosets $C_2, ..., C_5$ and $C_8, ..., C_{11}$ are used, the energy of the transmitted symbol is half of the energy of the transmitted symbol selected from the cosets C_0, C_1, C_6 and C_7. At each transmission time, both antennas are active. Therefore, in real systems, we prefer to use the cosets $C_2, ..., C_5$ and $C_8, ..., C_{11}$ as the information group so that the amplifier will work efficiently with low-power level signal.

In our research, for simplicity we use C_0 as the candidate information set. We use a general mapping rule from the information bits to the transmit matrices, as shown is Table 4.2. The distances between each of the matrix in C_0 are shown in Table. 4.3.

Information bits	Matrix in coset C_0
0000	$M_0 = \begin{pmatrix} 1 & 0 \\ 0 & 1 \end{pmatrix}$
0001	$M_1 = \begin{pmatrix} 1 & 0 \\ 0 & -1 \end{pmatrix}$
0010	$M_2 = \begin{pmatrix} 0 & 1 \\ 1 & 0 \end{pmatrix}$
0011	$M_3 = \begin{pmatrix} 0 & 1 \\ -1 & 0 \end{pmatrix}$
0100	$M_4 = \begin{pmatrix} -1 & 0 \\ 0 & -1 \end{pmatrix}$
0101	$M_5 = \begin{pmatrix} -1 & 0 \\ 0 & 1 \end{pmatrix}$
0110	$M_6 = \begin{pmatrix} 0 & -1 \\ -1 & 0 \end{pmatrix}$
0111	$M_7 = \begin{pmatrix} 0 & -1 \\ 1 & 0 \end{pmatrix}$
1000	$M_8 = \begin{pmatrix} i & 0 \\ 0 & i \end{pmatrix}$
1001	$M_9 = \begin{pmatrix} i & 0 \\ 0 & -i \end{pmatrix}$
1010	$M_{10} = \begin{pmatrix} 0 & i \\ i & 0 \end{pmatrix}$
1011	$M_{11} = \begin{pmatrix} 0 & i \\ -i & 0 \end{pmatrix}$
1100	$M_{12} = \begin{pmatrix} -i & 0 \\ 0 & -i \end{pmatrix}$
1101	$M_{13} = \begin{pmatrix} -i & 0 \\ 0 & i \end{pmatrix}$
1110	$M_{14} = \begin{pmatrix} 0 & -i \\ -i & 0 \end{pmatrix}$
1111	$M_{15} = \begin{pmatrix} 0 & -i \\ i & 0 \end{pmatrix}$

Table 4.2: The general mapping rule from the information bits to coset C_0.

Notice that:

$$\begin{aligned} \{M_4, M_5, M_6, M_7\} &= -\{M_0, M_1, M_2, M_3\} \\ \{M_8, M_9, M_{10}, M_{11}\} &= i\ \{M_0, M_1, M_2, M_3\} \\ \{M_{12}, M_{13}, M_{14}, M_{15}\} &= -i\ \{M_0, M_1, M_2, M_3\}. \end{aligned} \tag{4.12}$$

At time $\tau = 0$, we transmit a reference matrix $X_0 = M_0 = \left(\begin{smallmatrix} 1 & 0 \\ 0 & 1 \end{smallmatrix}\right)$.

Suppose that at time τ, X_τ is transmitted. At time $\tau+1$, a vector of 4 information bits arrives. These bits are mapped onto one of the matrices $M_{i_{\tau+1}} = M_a$ of the coset C_0, and then

$$X_{\tau+1} = X_\tau M_{i_{\tau+1}} \tag{4.13}$$

is transmitted.

The maximum likelihood demodulator is

$$\begin{aligned} \hat{M}_{i_{\tau+1}} &= \arg \min_{M \in C_0} \|Y_{\tau+1} - Y_\tau M\| \\ &= \arg \max_{M \in C_0} \mathrm{Tr}\{\mathrm{Re}(Y_{\tau+1}^H Y_\tau M)\}. \end{aligned} \tag{4.14}$$

as shown in the Section. 4.1.

We compare the performance of our new scheme with those of DSTBC [28] and DUSTM [27]. The simulation results are shown in Fig. 4.3. In these simulations, as in [28], the step channel model is used. In this model, the channel matrix is constant during the transmission of L ($L = T_c/T_s$) symbols, and change randomly to another constant channel matrix for the next L symbols.

We find that for MIMO systems with 2 transmit antennas, our new scheme performs worse than Tarokh's DSTBC scheme [28]. This is because the decoding method of our scheme is a general maximum likelihood decoding without any pre-process, while the variable used to decode in [28] is linearly scaled by the channel coefficients due to some pre-process. However, our new scheme performs better than the corresponding DUSTM scheme [27] when SNR is less than 14 dB. This is because the DUSTM scheme is designed for large SNR environments according to the second design criterion defined in (3.25).

Distances	M_0	M_1	M_2	M_3	M_4	M_5	M_6	M_7	M_8	M_9	M_{10}	M_{11}	M_{12}	M_{13}	M_{14}	M_{15}
M_0	0	2	2	2	$2\sqrt{2}$	2	2	2	2	2	2	2	2	2	2	2
M_1	2	0	2	2	2	$2\sqrt{2}$	2	2	2	2	2	2	2	2	2	2
M_2	2	2	0	2	2	2	$2\sqrt{2}$	2	2	2	2	2	2	2	2	2
M_3	2	2	2	0	2	2	2	$2\sqrt{2}$	2	2	2	2	2	2	2	2
M_4	$2\sqrt{2}$	2	2	2	0	2	2	2	2	2	2	2	2	2	2	2
M_5	2	$2\sqrt{2}$	2	2	2	0	2	2	2	2	2	2	2	2	2	2
M_6	2	2	$2\sqrt{2}$	2	2	2	0	2	2	2	2	2	2	2	2	2
M_7	2	2	2	$2\sqrt{2}$	2	2	2	0	2	2	2	2	2	2	2	2
M_8	2	2	2	2	2	2	2	2	0	2	2	2	$2\sqrt{2}$	2	2	2
M_9	2	2	2	2	2	2	2	2	2	0	2	2	2	$2\sqrt{2}$	2	2
M_{10}	2	2	2	2	2	2	2	2	2	2	0	2	2	2	$2\sqrt{2}$	2
M_{11}	2	2	2	2	2	2	2	2	2	2	2	0	2	2	2	$2\sqrt{2}$
M_{12}	2	2	2	2	2	2	2	2	$2\sqrt{2}$	2	2	2	0	2	2	2
M_{13}	2	2	2	2	2	2	2	2	2	$2\sqrt{2}$	2	2	2	0	2	2
M_{14}	2	2	2	2	2	2	2	2	2	2	$2\sqrt{2}$	2	2	2	0	2
M_{15}	2	2	2	2	2	2	2	2	2	2	2	$2\sqrt{2}$	2	2	2	0

Table 4.3: The distances between the matrices in C_0.

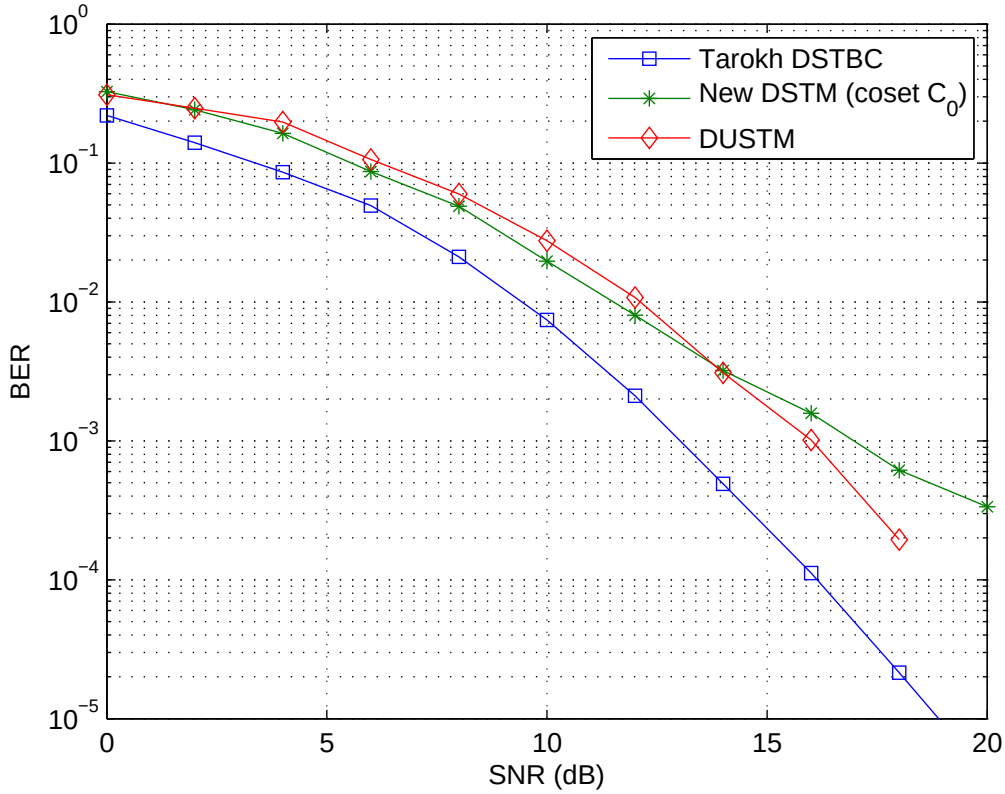

Figure 4.3: Comparison of performances of MIMO systems with 2 transmit antennas and 2 receive antennas. These three scheme are DSTBC [28] with 4PSK, our new DSTM with coset C_0 (general mapping rule) and DUSTM [27].

4.3.1 Gray mapping

In fact, according to our measure rule (Frobenius distance), the matrices of the Weyl group can be seen as the points distributed on the surface of a high dimension sphere. The distance between M_0 and M_4 is the largest (the diameter of the sphere, i.e., $2\sqrt{2}$), as shown in Fig.4.4. The distances between M_0 and all other 14 matrices in coset C_0 are equal, that is 2, as shown in Fig. 4.2 and Table 4.3.

We suppose to use a mapping rule like Gray mapping to improve the BER performance. As shown in Table 4.3 and (4.12), for each matrix, there is only 1 maximum distance and the others are the same. We map the pair of matrices with maximum distance to the pair of bit vectors that have the largest Hamming distance. The new mapping rule is shown in Table 4.4. The simulation result of this new mapping is shown in Fig. 4.5. We can see that the BER performance can be slightly improved

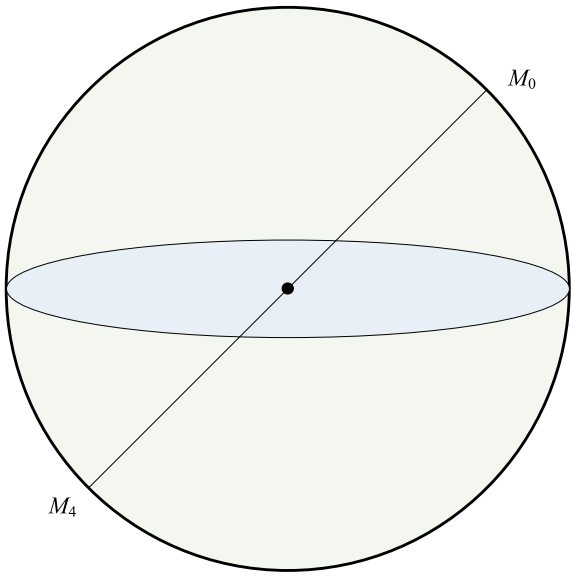

Figure 4.4: Position of the matrices M_0 and M_4 on the surface of a sphere.

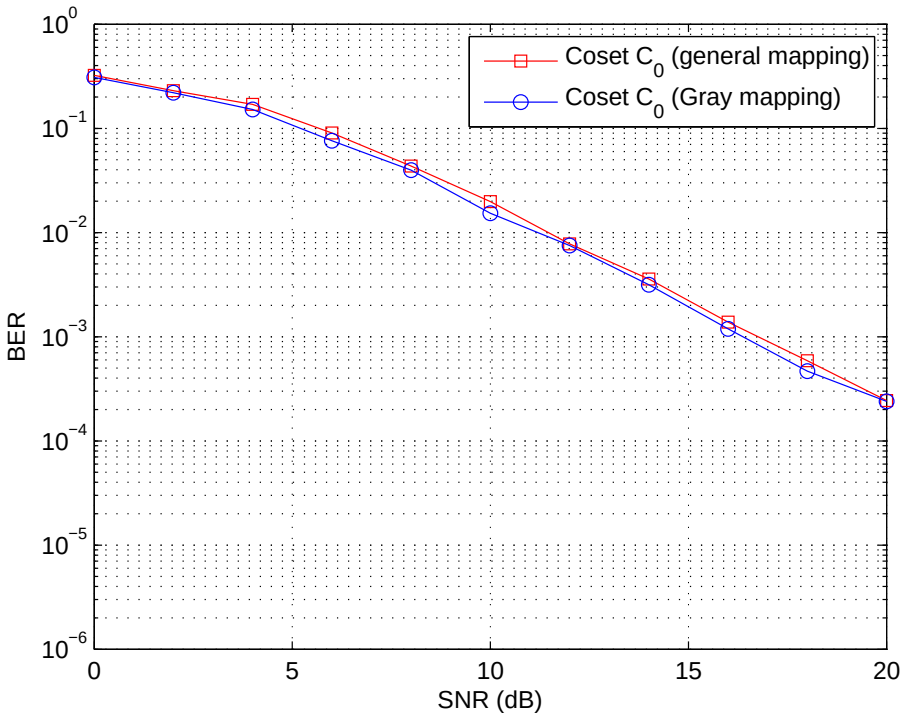

Figure 4.5: Simulation results of DSTM with coset C_0 (new mapping rule).

by Gray mapping.

Information bits	Matrix in coset C_0
0000	M_0
0001	M_1
0011	M_2
0010	M_3
1111	M_4
1110	M_5
1100	M_6
1101	M_7
0110	M_8
0100	M_9
0101	M_{10}
0111	M_{11}
1001	M_{12}
1011	M_{13}
1010	M_{14}
1000	M_{15}

Table 4.4: Gray mapping rule from the information bits onto the matrices in coset C_0.

4.3.2 Justification of the design criterion

4.3.2.1 The design criterion based on distance

In order to further investigate the effect of distance spectrum to the performance of DSTM MIMO systems, we construct a new set $S = C_0^r \cup A_1 C_0^r$ as an alternative to C_0. The set C_0^r contains the 8 real matrices of C_0 and $A_1 C_0^r$ is the set obtained by multiplying A_1 with the matrices of C_0^r. As the set C_0, the set S contains 8 couples (M_a, M_b) with $D(M_a, M_b) = ||M_a - M_b|| = 2\sqrt{2}$, the greatest distance between 2 matrices of G_W. If we consider 2 couples (M_a, M_b) and (M_c, M_d) of C_0, with $D(M_a, M_b) = D(M_c, M_d) = 2\sqrt{2}$, we have $D(M_a, M_c) = D(M_a, M_d) = D(M_b, M_c) = D(M_b, M_d) = 2$, while for the set S, if $D(M_a, M_b) = D(M_c, M_d) = 2\sqrt{2}$ with $M_a, M_b \in C_0^r$ and $M_c, M_d \in A_1 C_0^r$, then $[D(M_a, M_c)\ D(M_b, M_d)\ D(M_b, M_c)\ D(M_a, M_d)] = [\sqrt{2}\ \sqrt{2}\ \sqrt{6}\ \sqrt{6}]$. The distance table is shown in Table 4.5. We can see that the minimum distance of this set is $\sqrt{2}$ which is less than the minimum distance of the set C_0. As shown in Fig.4.6, the results obtained for S is slightly worse than that of C_0. This simulation justifies our first design criterion based on distance. Therefore,

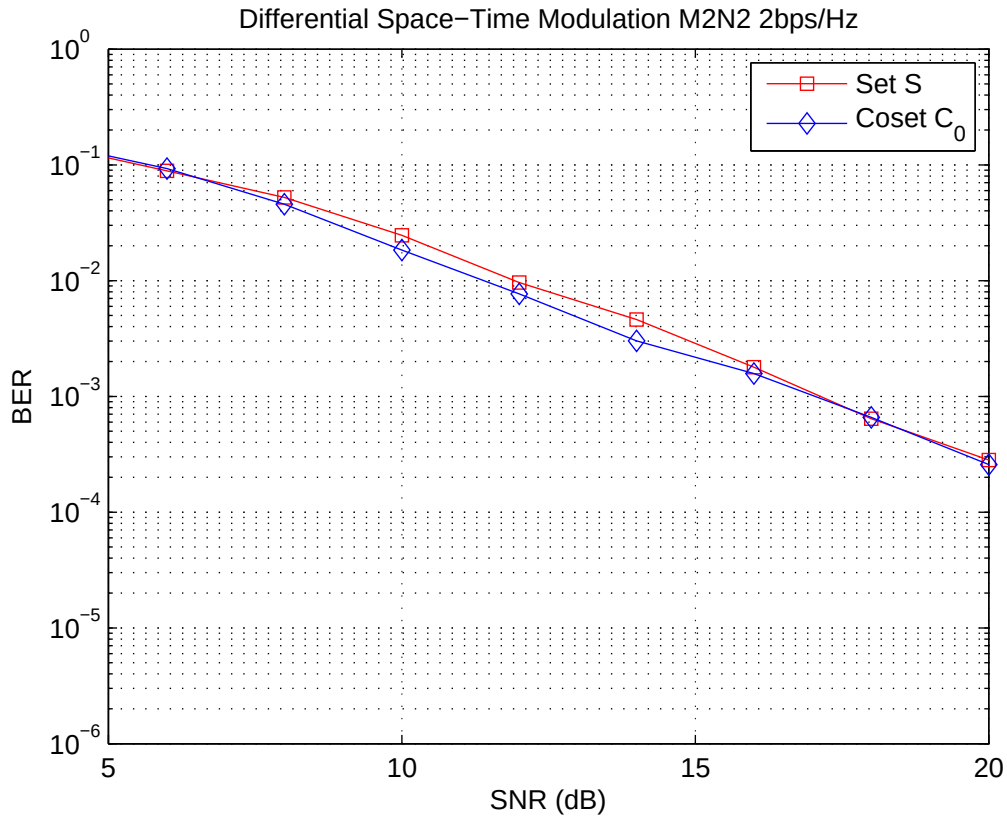

Figure 4.6: Comparison of differential space-time scheme for 2 transmit antennas and 2 receive antennas R = 2 with different set.

for $M = 2$ and $R = 2$ bps/Hz MIMO systems, we select one of the 12 cosets of Weyl group as the information group.

4.3.2.2 The design criterion based on diversity product

We know that there is a second design criterion called maximizing the diversity product as in (3.25). We select a set which has the maximized diversity product in the Weyl Group. The selected set S_d is:

$$\{M_0, M_4, M_3, M_7, M_9, M_{13}, M_{10}, M_{14}, M_{144}, M_{148}, M_{147}, M_{151}, M_{153}, M_{157}, M_{154}, M_{158}\}.$$

The diversity product of this set is 0.5 which is greater than the corresponding diversity product 0.3826 in DUSTM scheme [27]. We compare the BER performances of this set, C_0 and the DUSTM scheme. The simulation product is shown in Fig. 4.7. We can see that the BER performance with this new set S_d is better than the other

Distances	M_0	M_1	M_2	M_3	M_4	M_5	M_6	M_7	A_1M_0	A_1M_1	A_1M_2	A_1M_3	A_1M_4	A_1M_5	A_1M_6	A_1M_7
M_0	0	2	2	2	$2\sqrt{2}$	2	2	2	$\sqrt{2}$	$\sqrt{2}$	2	2	$\sqrt{6}$	$\sqrt{6}$	2	2
M_1	2	0	2	2	2	$2\sqrt{2}$	2	2	$\sqrt{2}$	$\sqrt{2}$	2	2	$\sqrt{6}$	$\sqrt{6}$	2	2
M_2	2	2	0	2	2	2	$2\sqrt{2}$	2	2	2	$\sqrt{2}$	$\sqrt{2}$	2	2	$\sqrt{6}$	$\sqrt{6}$
M_3	2	2	2	0	2	2	2	$2\sqrt{2}$	2	2	$\sqrt{2}$	$\sqrt{2}$	2	2	$\sqrt{6}$	$\sqrt{6}$
M_4	$2\sqrt{2}$	2	2	2	0	2	2	2	$\sqrt{6}$	$\sqrt{6}$	2	2	$\sqrt{2}$	$\sqrt{2}$	2	2
M_5	2	$2\sqrt{2}$	2	2	2	0	2	2	$\sqrt{6}$	$\sqrt{6}$	2	2	$\sqrt{2}$	$\sqrt{2}$	2	2
M_6	2	2	$2\sqrt{2}$	2	2	2	0	2	2	2	$\sqrt{6}$	$\sqrt{6}$	2	2	$\sqrt{2}$	$\sqrt{2}$
M_7	2	2	2	$2\sqrt{2}$	2	2	2	0	2	2	$\sqrt{6}$	$\sqrt{6}$	2	2	$\sqrt{2}$	$\sqrt{2}$
A_1M_0	$\sqrt{2}$	$\sqrt{2}$	2	2	$\sqrt{6}$	$\sqrt{6}$	2	2	0	2	2	2	$2\sqrt{2}$	2	2	2
A_1M_1	$\sqrt{2}$	$\sqrt{2}$	2	2	$\sqrt{6}$	$\sqrt{6}$	2	2	2	0	2	2	2	$2\sqrt{2}$	2	2
A_1M_2	2	2	$\sqrt{2}$	$\sqrt{2}$	2	2	$\sqrt{6}$	$\sqrt{6}$	2	2	0	2	2	2	$2\sqrt{2}$	2
A_1M_3	2	2	$\sqrt{2}$	$\sqrt{2}$	2	2	$\sqrt{6}$	$\sqrt{6}$	2	2	2	0	2	2	2	$2\sqrt{2}$
A_1M_4	$\sqrt{6}$	$\sqrt{6}$	2	2	$\sqrt{2}$	$\sqrt{2}$	2	2	$2\sqrt{2}$	2	2	2	0	2	2	2
A_1M_5	$\sqrt{6}$	$\sqrt{6}$	2	2	$\sqrt{2}$	$\sqrt{2}$	2	2	2	$2\sqrt{2}$	2	2	2	0	2	2
A_1M_6	2	2	$\sqrt{6}$	$\sqrt{6}$	2	2	$\sqrt{2}$	$\sqrt{2}$	2	2	$2\sqrt{2}$	2	2	2	0	2
A_1M_7	2	2	$\sqrt{6}$	$\sqrt{6}$	2	2	$\sqrt{2}$	$\sqrt{2}$	2	2	2	$2\sqrt{2}$	2	2	2	0

Table 4.5: The distances between the matrices in S.

two schemes. At the BER level of 10^{-3}, it is 2 dB better than the corresponding DUSTM scheme and 3 dB better than the DSTM scheme with set C_0.

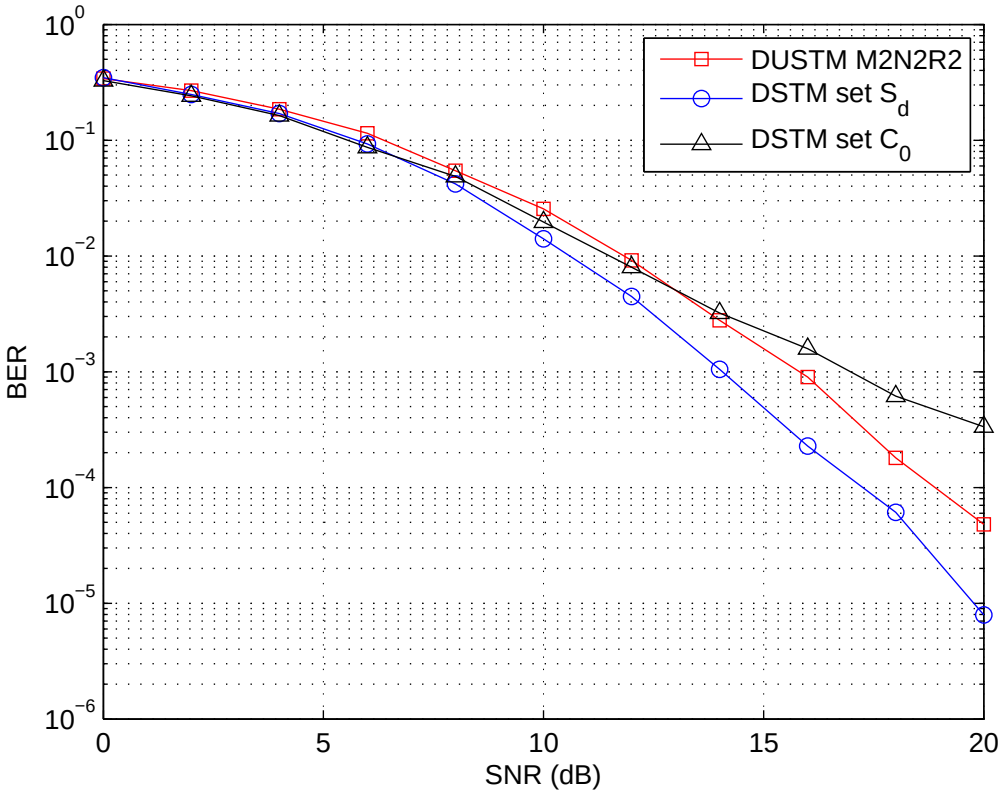

Figure 4.7: Comparison of DSTM for different sets from different design criteria. 2 transmit antennas, 2 receive antenna and $R = 2$ bps/Hz.

4.4 Spectral efficiency $R = 1$ and 3 bps/Hz

4.4.1 $R = 1$ bps/Hz

Now, we consider the group used for $R = 1$ bps/Hz. With the number of transmit antennas $M = 2$, $T = M$, $RT = 2$ bits are transmitted during 2 symbols time-durations and $2^{RT} = 4$ matrices are needed. According to the maximizing the minimum distance design criterion, we select the pair $M_0 = \left(\begin{smallmatrix} 1 & 0 \\ 0 & 1 \end{smallmatrix}\right)$ and $M_4 = -M_0$ which has the maximun distance as the first two matrices. Then we try to select the other two matrices that have the maximized minimum distance with M_0 and M_4. We suppose the two matrices are M_l and $-M_l$ (in our definition here, $M_{l+4} = -M_l$)

which has the maximun distance $2\sqrt{2}$. We find that, for a general matrix M_l, if the distance between M_0 and M_l is greater than 2, the distance between M_4 and M_l is less than 2. Therefore we should select the matrices that have distance 2 with M_0 and M_4. From the distance spectrum of G_w, such as Table 4.1, we know that there are 102 matrices (51 pairs) that have distance 2 with M_0 and M_4. Then we use the second design criterion (3.25), i.e. maximize the diversity product, to select the pair of matrices from the 51 pairs. We find 10 pairs of matrices in the 51 pairs that have the maximized diversity product $\frac{\sqrt{2}}{2}$ with M_0 and M_4. They are (M_3, M_7), (M_8, M_{12}), (M_9, M_{13}), (M_{10}, M_{14}), (M_{40}, M_{44}), (M_{43}, M_{47}), (M_{83}, M_{87}), (M_{89}, M_{93}), (M_{114}, M_{118}) and (M_{123}, M_{127}).

Based on the analysis above, we select the set $\{M_0, M_4, M_8, M_{12}\}$ as the information group for the spectrum $R = 1$ bps/Hz. This group is exactly the same as the group used in DUSTM scheme in Table 3.1. We compare the BER performances for different mapping rule, i.e., general mapping and Gray mapping. The two mapping rules are shown in Table 4.6. The BER performances for different mapping rules are

Information bits	Gray mapping	general mapping
00	M_0	M_0
01	M_8	M_4
11	M_4	M_{12}
10	M_{12}	M_8

Table 4.6: Mapping rules from the information bits onto the matrices in group $\{M_0, M_4, M_8, M_{12}\}$.

shown in Fig. 4.8. We can see that with Gray mapping the BER performance can be about 0.5 dB improved.

4.4.2 $R = 3$ bps/Hz

For DSTM scheme with $M = 2$ transmit antennas and spectral efficiency $R = 3$ bps/Hz, the information set should have $2^{RM} = 64$ matrices. We select the first 64 matrices in the Weyl group as the information group and the simulation result is shown in Fig. 4.9. For all possible sets with 64 matrices selected from G_w, the minimum diversity product is 0 and the minimum distance is $\sqrt{4 - 2\sqrt{2}} = 1.0824$.

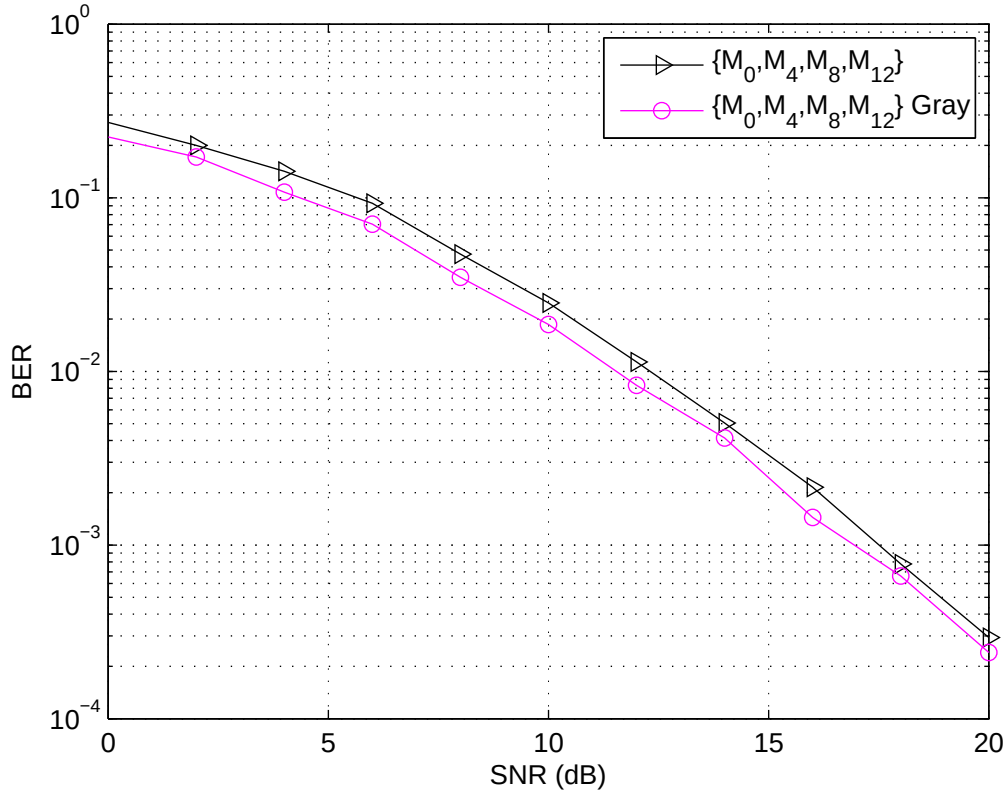

Figure 4.8: Comparison of DSTM for general mapping and Gray mapping. 2 transmit antennas, 1 receive antenna and $R = 1$ bps/Hz.

Therefore, all the sets with 64 matrices selected from G_w are best sets according the two design criteria.

4.5 Conclusion

In this chapter, we presented a new DSTM scheme based on the Weyl group. MIMO systems with 2 transmit antennas are considered.

For spectrum efficiency $R = 2$ bps/Hz, all of the the 12 cosets $\left(C_0, C_1, \ldots, C_{11}\right)$ of the Weyl group are the best sets if the first design criterion is considered. In real systems, we prefer to use the cosets $C_2, ..., C_5$ and $C_8, ..., C_{11}$ as the information group so that the amplifier will work efficiently with low-power level signal. Our scheme performs better than the corresponding DUSTM scheme with SNR less than 14 dB. We also examined this new scheme with Gray mapping and the simulation results

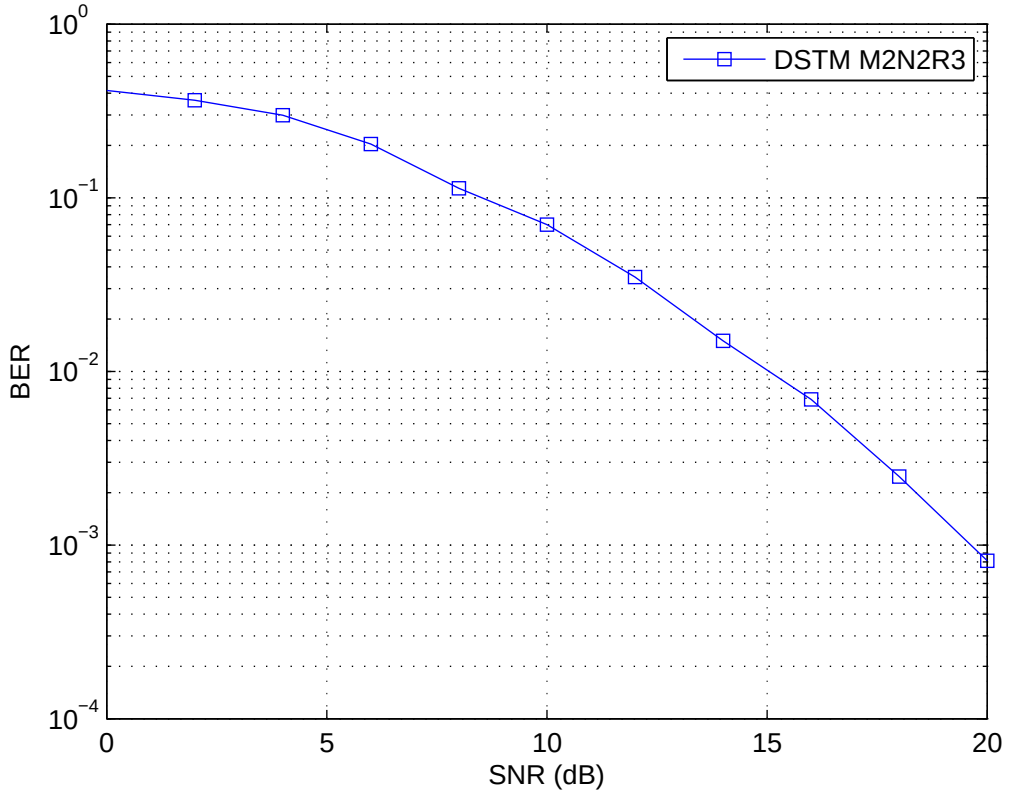

Figure 4.9: DSTM with 2 transmit antennas, 2 receive antenna and $R = 3$ bps/Hz.

show that the improvement for BER performance is negligible. Considering the second design criterion, we select a new best information set and simulation result shows that this set performs better than the best set selected from the first design criterion.

We aslo give the best sets for spectrum efficiencies $R = 1$ and $R = 3$ bps/Hz.

5 New DSTM with 4 and 8 transmit antennas

In this chapter, we expand our new DSTM scheme to MIMO systems with 4 and 8 transmit antennas. In fact, with Kronecker product, our scheme can be expanded to MIMO systems with 2^n $(n = 2, 3, ...)$ transmit antennas. The BER performance for MIMO systems with 4 and 8 transmit antennas is shown in this chapter.

5.1 Differential MIMO systems with 4 transmit antennas

To design a MIMO system with 4 transmit antennas, the *Kronecker product* is used to expand the Weyl group.

The Kronecker product of two arbitrary matrices A and B is defined as:

$$A \otimes B = \begin{pmatrix} a_{11}B & \cdots & a_{1n}B \\ \vdots & \ddots & \vdots \\ a_{m1}B & \cdots & a_{mn}B \end{pmatrix} \tag{5.1}$$

where A is an $m \times n$ matrix, B is a $p \times q$ matrix and the resulting matrix is an $mp \times nq$ matrix. In general, $A \otimes B \neq B \otimes A$. The Kronecker product has the properties:

1. $A \otimes B$ is invertible if and only if A and B are invertible:

$$(A \otimes B)^{-1} = A^{-1} \otimes B^{-1} \tag{5.2}$$

2. The operation of transposition is distributive over the Kronecker product:

$$(A \otimes B)^T = A^T \otimes B^T \tag{5.3}$$

3. The Kronecker product is linear and associative:

$$\begin{aligned} A \otimes (\alpha B + \beta C) &= \alpha A \otimes B + \beta A \otimes C, \\ (A \otimes B) \otimes C &= A \otimes (B \otimes C) \end{aligned} \tag{5.4}$$

4. The Kronecker product is not commutative:

$$A \otimes B \neq B \otimes A \tag{5.5}$$

If we combine the Kronecker product and the distance between two matrices, two theorems are stated and proved.

Theorem 5.1.1. *Consider the complex matrices A, B of size $p \times q$ and M a complex matrix of size $m \times n$. If $\|M\|$ is the Frobenius norm of the matrix M, i.e.,*

$$\|M\| = \sqrt{\sum_{i=1}^{m} \sum_{j=1}^{n} m_{ij} m_{ij}^*}$$

and $D(A, B) = \|A - B\|$, then:

$$D(M \otimes A, M \otimes B) = \|M\| \cdot D(A, B). \tag{5.6}$$

Proof. We have:

$$\begin{aligned} D(M \otimes A, M \otimes B) &= \|M \otimes A - M \otimes B\| = \|M \otimes (A - B)\| \\ &= \sqrt{\sum_{ij} \sum_{kl} [m_{ij}(a_{kl} - b_{kl})][m_{ij}(a_{kl} - b_{kl})]^*} \\ &= \sqrt{\sum_{ij} m_{ij} m_{ij}^* \sum_{kl} [(a_{kl} - b_{kl})][(a_{kl} - b_{kl})]^*} \\ &= \|M\| \cdot \|A - B\| = \|M\| \cdot D(A, B). \end{aligned}$$

□

Theorem 5.1.2. *If M is a non-null complex matrix of size $m \times n$ and A, B, C, D are complex matrices of size $p \times q$, then*

$$D(A, B) < D(C, D) \Rightarrow D(M \otimes A, M \otimes B) < D(M \otimes C, M \otimes D). \tag{5.7}$$

Proof. If $D(A, B) < D(C, D)$ and $\|M\| > 0$, using the first theorem, we have:

$$\begin{aligned} D(M \otimes C, M \otimes D) - D(M \otimes A, M \otimes B) &= \|M\| \cdot D(C, D) - \|M\| \cdot D(A, B) \\ &= \|M\|(D(C, D) - D(A, B)) > 0. \end{aligned}$$

□

With the assumption $M = T$, for MIMO systems with 4 transmit antennas, 4×4 transmit matrices should be used.

Using the Kronecker product between each couple of 2×2 matrices of the Weyl group, 4×4 matrices are obtained. There are 192×192 matrices in this set among which only $K = 4608$ matrices are distinct. They are denoted $N_0, N_1, \ldots, N_{4607}$. The set of these matrices is also a group denoted by G_{w4}. We have the definition $G_{w4} = G_w \otimes G_w$. The maximum spectral efficiency we can get with such 4 transmit antennas systems is then $R = \frac{1}{M}\lfloor \log_2 K \rfloor = \frac{1}{4}\lfloor \log_2 4608 \rfloor = 3$ bps/Hz.

5.1.1 Spectral efficiency $R = 1$ bps/Hz

To design a scheme for $R = 1$ bps/Hz, we need an information set with $2^{RM} = 16$ matrices. We consider the first design criterion. We know that coset C_0 is one of the best sets for MIMO systems with 2 transmit antennas. We make the Kronecker products between the first matrix $M_0 = \left(\begin{smallmatrix} 1 & 0 \\ 0 & 1 \end{smallmatrix}\right)$ of C_0 and all the matrices in C_0 to get a set C_{00}. According to the Theorem 5.1.2, C_{00} is a best set for MIMO systems with 4 transmit antennas because C_0 is the best set of 16 matrices in G_w.

$$C_{00} = M_0 \otimes C_0. \tag{5.8}$$

That is,

$$C_{00} = \alpha\{ \begin{pmatrix} 1 & 0 & 0 & 0 \\ 0 & 1 & 0 & 0 \\ 0 & 0 & 1 & 0 \\ 0 & 0 & 0 & 1 \end{pmatrix}, \begin{pmatrix} 1 & 0 & 0 & 0 \\ 0 & -1 & 0 & 0 \\ 0 & 0 & 1 & 0 \\ 0 & 0 & 0 & -1 \end{pmatrix}, \begin{pmatrix} 0 & 1 & 0 & 0 \\ 1 & 0 & 0 & 0 \\ 0 & 0 & 0 & 1 \\ 0 & 0 & 1 & 0 \end{pmatrix}, \begin{pmatrix} 0 & 1 & 0 & 0 \\ -1 & 0 & 0 & 0 \\ 0 & 0 & 0 & 1 \\ 0 & 0 & -1 & 0 \end{pmatrix} \}$$

where $\alpha \in \{1, -1, i, -i\}$. The minimum distance of the matrices in C_{00} is $2\sqrt{2}$ and the distance spectrum of C_{00} is shown in Table 5.1.

Remark We have $\|M_i\| = \sqrt{2}$, $\forall M \in G_w$ (Weyl group). Therefore, using $M_0 = \left[\begin{smallmatrix} 1 & 0 \\ 0 & 1 \end{smallmatrix}\right]$ in order to create $C_{00} \subset G_{w4}$ generate a set of matrices having the same distance spectrum like any other matrix $M \in G_w$. Hence, using M_0 is as good as using any other matrix of G_w.

Distances	N_0	N_1	N_2	N_3	N_4	N_5	N_6	N_7	N_8	N_9	N_{10}	N_{11}	N_{12}	N_{13}	N_{14}	N_{15}
N_0	0	$2\sqrt{2}$	$2\sqrt{2}$	$2\sqrt{2}$	4	$2\sqrt{2}$	$2\sqrt{2}$	$2\sqrt{2}$	$2\sqrt{2}$	$2\sqrt{2}$	$2\sqrt{2}$	$2\sqrt{2}$	$2\sqrt{2}$	$2\sqrt{2}$	$2\sqrt{2}$	$2\sqrt{2}$
N_1	$2\sqrt{2}$	0	$2\sqrt{2}$	$2\sqrt{2}$	$2\sqrt{2}$	4	$2\sqrt{2}$	$2\sqrt{2}$	$2\sqrt{2}$	$2\sqrt{2}$	$2\sqrt{2}$	$2\sqrt{2}$	$2\sqrt{2}$	$2\sqrt{2}$	$2\sqrt{2}$	$2\sqrt{2}$
N_2	$2\sqrt{2}$	$2\sqrt{2}$	0	$2\sqrt{2}$	$2\sqrt{2}$	$2\sqrt{2}$	4	$2\sqrt{2}$	$2\sqrt{2}$	$2\sqrt{2}$	$2\sqrt{2}$	$2\sqrt{2}$	$2\sqrt{2}$	$2\sqrt{2}$	$2\sqrt{2}$	$2\sqrt{2}$
N_3	$2\sqrt{2}$	$2\sqrt{2}$	$2\sqrt{2}$	0	$2\sqrt{2}$	$2\sqrt{2}$	$2\sqrt{2}$	4	$2\sqrt{2}$	$2\sqrt{2}$	$2\sqrt{2}$	$2\sqrt{2}$	$2\sqrt{2}$	$2\sqrt{2}$	$2\sqrt{2}$	$2\sqrt{2}$
N_4	4	$2\sqrt{2}$	$2\sqrt{2}$	$2\sqrt{2}$	0	$2\sqrt{2}$	$2\sqrt{2}$	$2\sqrt{2}$	$2\sqrt{2}$	$2\sqrt{2}$	$2\sqrt{2}$	$2\sqrt{2}$	$2\sqrt{2}$	$2\sqrt{2}$	$2\sqrt{2}$	$2\sqrt{2}$
N_5	$2\sqrt{2}$	4	$2\sqrt{2}$	$2\sqrt{2}$	$2\sqrt{2}$	0	$2\sqrt{2}$	$2\sqrt{2}$	$2\sqrt{2}$	$2\sqrt{2}$	$2\sqrt{2}$	$2\sqrt{2}$	$2\sqrt{2}$	$2\sqrt{2}$	$2\sqrt{2}$	$2\sqrt{2}$
N_6	$2\sqrt{2}$	$2\sqrt{2}$	4	$2\sqrt{2}$	$2\sqrt{2}$	$2\sqrt{2}$	0	$2\sqrt{2}$	$2\sqrt{2}$	$2\sqrt{2}$	$2\sqrt{2}$	$2\sqrt{2}$	$2\sqrt{2}$	$2\sqrt{2}$	$2\sqrt{2}$	$2\sqrt{2}$
N_7	$2\sqrt{2}$	$2\sqrt{2}$	$2\sqrt{2}$	4	$2\sqrt{2}$	$2\sqrt{2}$	$2\sqrt{2}$	0	$2\sqrt{2}$	$2\sqrt{2}$	$2\sqrt{2}$	$2\sqrt{2}$	$2\sqrt{2}$	$2\sqrt{2}$	$2\sqrt{2}$	$2\sqrt{2}$
N_8	$2\sqrt{2}$	$2\sqrt{2}$	$2\sqrt{2}$	$2\sqrt{2}$	$2\sqrt{2}$	$2\sqrt{2}$	$2\sqrt{2}$	$2\sqrt{2}$	0	$2\sqrt{2}$	$2\sqrt{2}$	$2\sqrt{2}$	4	$2\sqrt{2}$	$2\sqrt{2}$	$2\sqrt{2}$
N_9	$2\sqrt{2}$	$2\sqrt{2}$	$2\sqrt{2}$	$2\sqrt{2}$	$2\sqrt{2}$	$2\sqrt{2}$	$2\sqrt{2}$	$2\sqrt{2}$	$2\sqrt{2}$	0	$2\sqrt{2}$	$2\sqrt{2}$	$2\sqrt{2}$	4	$2\sqrt{2}$	$2\sqrt{2}$
N_{10}	$2\sqrt{2}$	$2\sqrt{2}$	$2\sqrt{2}$	$2\sqrt{2}$	$2\sqrt{2}$	$2\sqrt{2}$	$2\sqrt{2}$	$2\sqrt{2}$	$2\sqrt{2}$	$2\sqrt{2}$	0	$2\sqrt{2}$	$2\sqrt{2}$	$2\sqrt{2}$	4	$2\sqrt{2}$
N_{11}	$2\sqrt{2}$	$2\sqrt{2}$	$2\sqrt{2}$	$2\sqrt{2}$	$2\sqrt{2}$	$2\sqrt{2}$	$2\sqrt{2}$	$2\sqrt{2}$	$2\sqrt{2}$	$2\sqrt{2}$	$2\sqrt{2}$	0	$2\sqrt{2}$	$2\sqrt{2}$	$2\sqrt{2}$	4
N_{12}	$2\sqrt{2}$	$2\sqrt{2}$	$2\sqrt{2}$	$2\sqrt{2}$	$2\sqrt{2}$	$2\sqrt{2}$	$2\sqrt{2}$	$2\sqrt{2}$	4	$2\sqrt{2}$	$2\sqrt{2}$	$2\sqrt{2}$	0	$2\sqrt{2}$	$2\sqrt{2}$	$2\sqrt{2}$
N_{13}	$2\sqrt{2}$	$2\sqrt{2}$	$2\sqrt{2}$	$2\sqrt{2}$	$2\sqrt{2}$	$2\sqrt{2}$	$2\sqrt{2}$	$2\sqrt{2}$	$2\sqrt{2}$	4	$2\sqrt{2}$	$2\sqrt{2}$	$2\sqrt{2}$	0	$2\sqrt{2}$	$2\sqrt{2}$
N_{14}	$2\sqrt{2}$	$2\sqrt{2}$	$2\sqrt{2}$	$2\sqrt{2}$	$2\sqrt{2}$	$2\sqrt{2}$	$2\sqrt{2}$	$2\sqrt{2}$	$2\sqrt{2}$	$2\sqrt{2}$	4	$2\sqrt{2}$	$2\sqrt{2}$	$2\sqrt{2}$	0	$2\sqrt{2}$
N_{15}	$2\sqrt{2}$	$2\sqrt{2}$	$2\sqrt{2}$	$2\sqrt{2}$	$2\sqrt{2}$	$2\sqrt{2}$	$2\sqrt{2}$	$2\sqrt{2}$	$2\sqrt{2}$	$2\sqrt{2}$	$2\sqrt{2}$	4	$2\sqrt{2}$	$2\sqrt{2}$	$2\sqrt{2}$	0

Table 5.1: The distances between the matrices in C_{00}.

Four information bits are viewed as an information vector. The vector is mapped to one of the 16 matrices in C_{00} as an information matrix and the mapping rule is shown in Table 5.2. Once the matrix is obtained, it is used to differentially modulate the previous transmitted matrix to get the current transmission matrix.

Information bits	Matrix in coset C_{00}
0000	$N_0 = \begin{pmatrix} 1 & 0 & 0 & 0 \\ 0 & 1 & 0 & 0 \\ 0 & 0 & 1 & 0 \\ 0 & 0 & 0 & 1 \end{pmatrix}$
0001	$N_1 = \begin{pmatrix} 1 & 0 & 0 & 0 \\ 0 & -1 & 0 & 0 \\ 0 & 0 & 1 & 0 \\ 0 & 0 & 0 & -1 \end{pmatrix}$
0010	$N_2 = \begin{bmatrix} 0 & 1 & 0 & 0 \\ 1 & 0 & 0 & 0 \\ 0 & 0 & 0 & 1 \\ 0 & 0 & 1 & 0 \end{bmatrix}$
0011	$N_3 = \begin{pmatrix} 0 & 1 & 0 & 0 \\ -1 & 0 & 0 & 0 \\ 0 & 0 & 0 & 1 \\ 0 & 0 & -1 & 0 \end{pmatrix}$
0100	$N_4 = \begin{pmatrix} -1 & 0 & 0 & 0 \\ 0 & -1 & 0 & 0 \\ 0 & 0 & -1 & 0 \\ 0 & 0 & 0 & -1 \end{pmatrix}$
0101	$N_5 = \begin{pmatrix} -1 & 0 & 0 & 0 \\ 0 & 1 & 0 & 0 \\ 0 & 0 & -1 & 0 \\ 0 & 0 & 0 & 1 \end{pmatrix}$
0110	$N_6 = \begin{pmatrix} 0 & -1 & 0 & 0 \\ -1 & 0 & 0 & 0 \\ 0 & 0 & 0 & -1 \\ 0 & 0 & -1 & 0 \end{pmatrix}$
0111	$N_7 = \begin{pmatrix} 0 & -1 & 0 & 0 \\ 1 & 0 & 0 & 0 \\ 0 & 0 & 0 & -1 \\ 0 & 0 & 1 & 0 \end{pmatrix}$
1000	$N_8 = \begin{pmatrix} i & 0 & 0 & 0 \\ 0 & i & 0 & 0 \\ 0 & 0 & i & 0 \\ 0 & 0 & 0 & i \end{pmatrix}$
1001	$N_9 = \begin{pmatrix} i & 0 & 0 & 0 \\ 0 & -i & 0 & 0 \\ 0 & 0 & i & 0 \\ 0 & 0 & 0 & -i \end{pmatrix}$
1010	$N_{10} = \begin{pmatrix} 0 & i & 0 & 0 \\ i & 0 & 0 & 0 \\ 0 & 0 & 0 & i \\ 0 & 0 & i & 0 \end{pmatrix}$
1011	$N_{11} = \begin{pmatrix} 0 & i & 0 & 0 \\ -i & 0 & 0 & 0 \\ 0 & 0 & 0 & i \\ 0 & 0 & -i & 0 \end{pmatrix}$
1100	$N_{12} = \begin{pmatrix} -i & 0 & 0 & 0 \\ 0 & -i & 0 & 0 \\ 0 & 0 & -i & 0 \\ 0 & 0 & 0 & -i \end{pmatrix}$
1101	$N_{13} = \begin{pmatrix} -i & 0 & 0 & 0 \\ 0 & i & 0 & 0 \\ 0 & 0 & -i & 0 \\ 0 & 0 & 0 & i \end{pmatrix}$
1110	$N_{14} = \begin{pmatrix} 0 & -i & 0 & 0 \\ -i & 0 & 0 & 0 \\ 0 & 0 & 0 & -i \\ 0 & 0 & -i & 0 \end{pmatrix}$
1111	$N_{15} = \begin{pmatrix} 0 & -i & 0 & 0 \\ i & 0 & 0 & 0 \\ 0 & 0 & 0 & -i \\ 0 & 0 & i & 0 \end{pmatrix}$

Table 5.2: The general mapping rule from the information bits to subset C_{00}.

The constellation of the modulation of this scheme (i.e., the possible value of the matrices' elements) is $\{\pm 1, \pm i, 0\}$ which corresponds to $QPSK \cup 0$, and the spectral efficiency is 1 bps/Hz. The simulation result is shown in Fig.5.1.

The simulation parameters are similar to the parameters used for DSTM schemes with 2 transmit antennas. The channel matrix which is constant during the transmission of L ($L = T_c/T_s$) symbols, and change randomly to another constant channel matrix for the next L symbols is used. For comparison, the 4×1 DSTBC scheme [29] with modulation BPSK has the same spectral efficiency. The DUSTM scheme with 4 transmit antennas, 1 receive antenna and spectral efficiency $R = 1$ bps/Hz is also shown here. We can see that similar to the schemes shown in Fig. 4.3, our new scheme with the first design criterion is not better than the other two schemes.

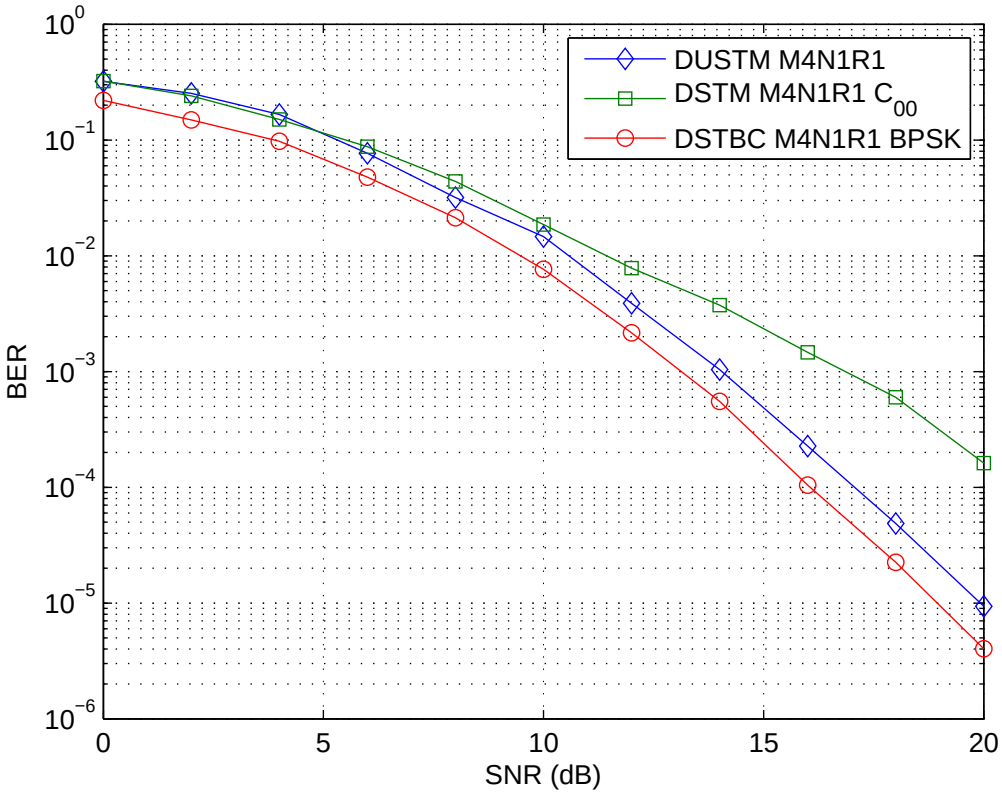

Figure 5.1: Comparison of DSTBC [29], DUSTM [27] and our new DSTM scheme (M=4, N=1, R=1).

Now, we analyze the second design criterion: maximizing the diversity product. The diversity product is defined based on the determinent of the difference of the

information matrices. Consider the complex matrices A, B of size $p \times p$ and M of size $q \times q$. The determinent of $M \otimes A$ is

$$\det(M \otimes A) = [\det(M)]^p \times [\det(A)]^q. \tag{5.9}$$

We know that

$$|\det(M_i)| = 1, \ \forall M_i \in G_w. \tag{5.10}$$

Thus, for all the matrices in the Weyl group, we have:

$$|\det(M_i \otimes (A-B))| = |\det(M_i)|^p \times |\det(A-B)|^q = |\det(A-B)|^2. \tag{5.11}$$

We select a set which has a maximized diversity product from G_{w4} by hand. It is:

$$\begin{aligned} S_{div} =& M_0 \otimes \{M_0, M_4, M_3, M_7, M_9, M_{13}, M_{10}, M_{14}\} \\ & \cup M_1 \otimes \{M_{33}, M_{37}, M_{34}, M_{38}, M_{40}, M_{44}, M_{43}, M_{47}\}. \end{aligned} \tag{5.12}$$

The diversity product of this new set is $\zeta = \frac{1}{2}\min_{0\le k<k'\le 16}|\det(V_k - V_{k'})|^{\frac{1}{M}} = 0.5946$, $V_k \in S_{div}$. The minimum distance of this new set is also $2\sqrt{2}$. The simulation result is shown in Fig. 5.2. We can see that the DSTM scheme with set S_{div} performs about 1 dB better than the DUSTM scheme at the BER level 10^{-3} and slightly better than DSTBC scheme when SNR is greater than 10 dB.

5.1.2 DSTM for 4 transmit antennas with new mapping rule

Like the mapping rule used for 2 two transmit antennas, we can use the similar mapping rule for this scheme. For the first 16 matrices, there are also the relations:

$$\begin{aligned} \{N_4, N_5, N_6, N_7\} &= -\{N_0, N_1, N_2, N_3\} \\ \{N_8, N_9, N_{10}, N_{11}\} &= i\ \{N_0, N_1, N_2, N_3\} \\ \{N_{12}, N_{13}, N_{14}, N_{15}\} &= -i\ \{N_0, N_1, N_2, N_3\}. \end{aligned} \tag{5.13}$$

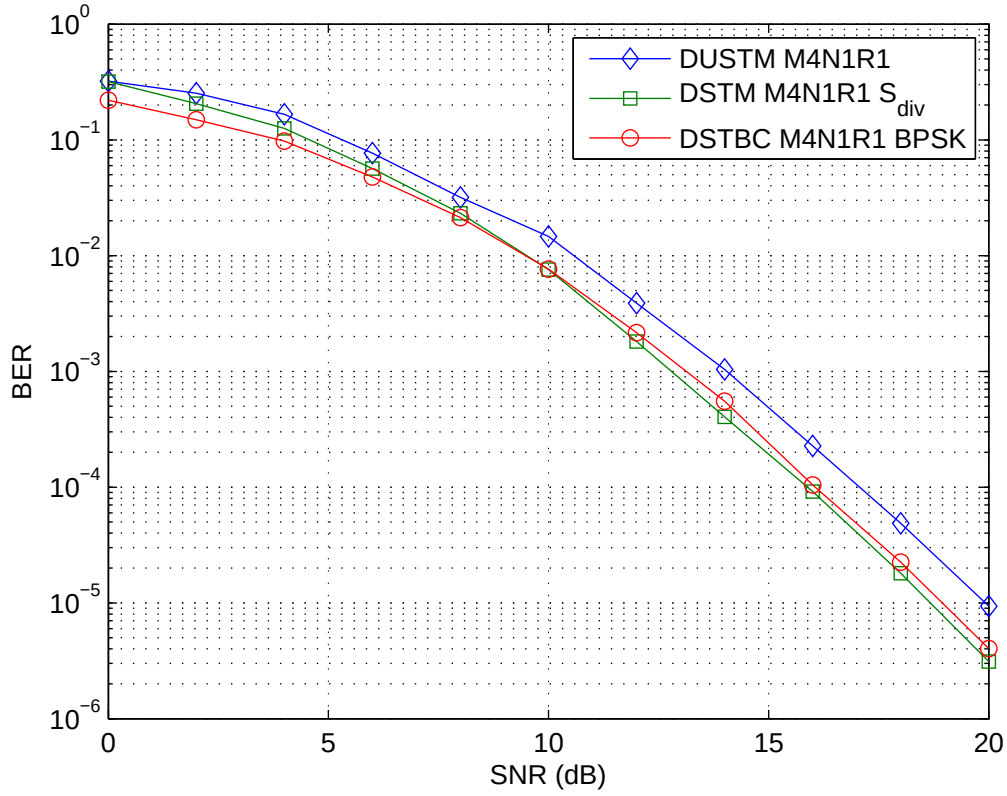

Figure 5.2: Comparison of DSTBC [29], DUSTM [27] and new DSTM scheme with set S_{div} (M=4, N=1, R=1).

We can see that the pairs of matrices in the first and the third rows have the maximun distances. Gray mapping rule can be used for this scheme. Like the mapping rule used in Table 4.2 and Table 4.4, we show Gray mapping rules Table 5.3. We use this mapping rule considering that, the binary vectors with the greatest Hamming distance, i.e., 4, corresponding to the matrices that have the greatest Euclidean distance, i.e., 4. The bit blocks with Hamming distance less than 4, corresponding to the matrices that have the smallest Euclidean distance, i.e., $2\sqrt{2}$.

We get the BER performance for 4 transmit antennas with Gray mapping. The simulation result is shown in Fig. 5.3. We can see that with this new mapping rule, the BER performance can be slightly improved. However, the improvement is limit. This is because there are only 2 different distances in the distance spectrum.

Information bits	Matrix in coset C_{00}
0000	N_0
0001	N_1
0011	N_2
0010	N_3
1111	N_4
1110	N_5
1100	N_6
1101	N_7
0110	N_8
0100	N_9
0101	N_{10}
0111	N_{11}
1001	N_{12}
1011	N_{13}
1010	N_{14}
1000	N_{15}

Table 5.3: The Gray mapping rule from the information bits to set C_{00}.

5.1.3 DSTM for 4 transmit antennas with higher spectral efficiencies (R=2 and R=3)

Furthermore, there are $K = 4608$ distinct matrices in the group G_{w4}. The maximum spectral efficiency we can get is $R = \frac{1}{M}\lfloor \log_2 K \rfloor = \frac{1}{4}\lfloor \log_2 4608 \rfloor = 3$ bps/Hz.

For the spectral efficiency $R = 2$ bps/Hz, $RM = 8$ bits should be transmitted in 4 symbol duration times. The information bits are mapped onto one of the $2^8 = 256$ matrices. We select the first 256 matrices from G_{w4} as the candidate transmission set S_1.

For $R = 3$ bps/Hz, we should transmit 12 bits in 4 symbol duration times. Similarly, we select the first $2^{12} = 4096$ matrices from G_{w4} as the candidate transmission set. The selection of the matrices is arbitrary. The simulation results with different spectral efficiencies are shown in Fig.5.4. As for $R = 3$ bps/Hz, the DUSTM scheme [27] didn't give us a scheme for it and we didn't make a comparison here.

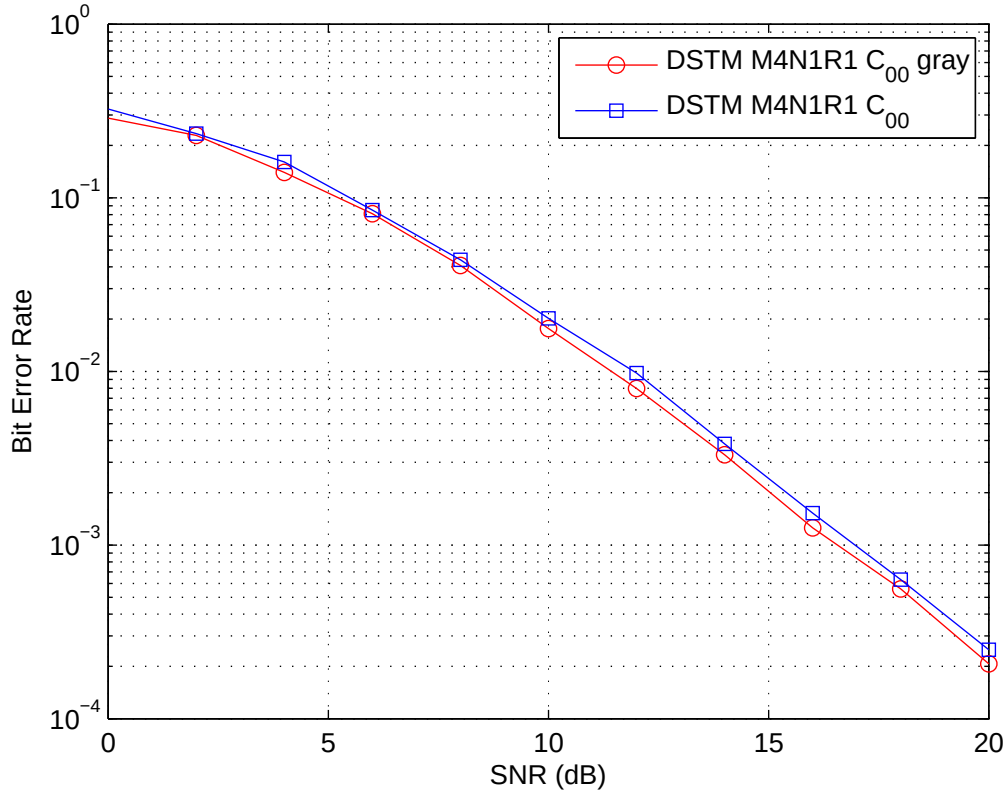

Figure 5.3: Comparison of different mapping rule for DSTM (M=4, N=1, R=1) with set C_{00}.

We then try to improve the BER performance for $R = 2$ bps/Hz with the two design criteria. First, we resort to the distance spectrum design criterion to improve the BER performance. The minimum distance of the first 256 matrices of group G_{w4} is 1.5307. We then try to maximize the minimun distance. We select a set which has minimun distance 2. It is $S_2 = \{N_0, ..., N_{31}, N_{128}, ..., N_{223}, N_{320}, ..., N_{447}\}$. We compare this scheme with the first set S_1 and DUSTM.

The simulation results are shown in Fig. 5.5. We can see that, consider the distance spectrum, the new set performs better than the original one. Our scheme is also better than the DUSTM scheme [27]. We also try to improve the BER performance by selecting the set with the maximum diversity product. We find that, the diversity product of all possible sets with 256 matrices is 0. There is no space to design a best set based on the second design criterion.

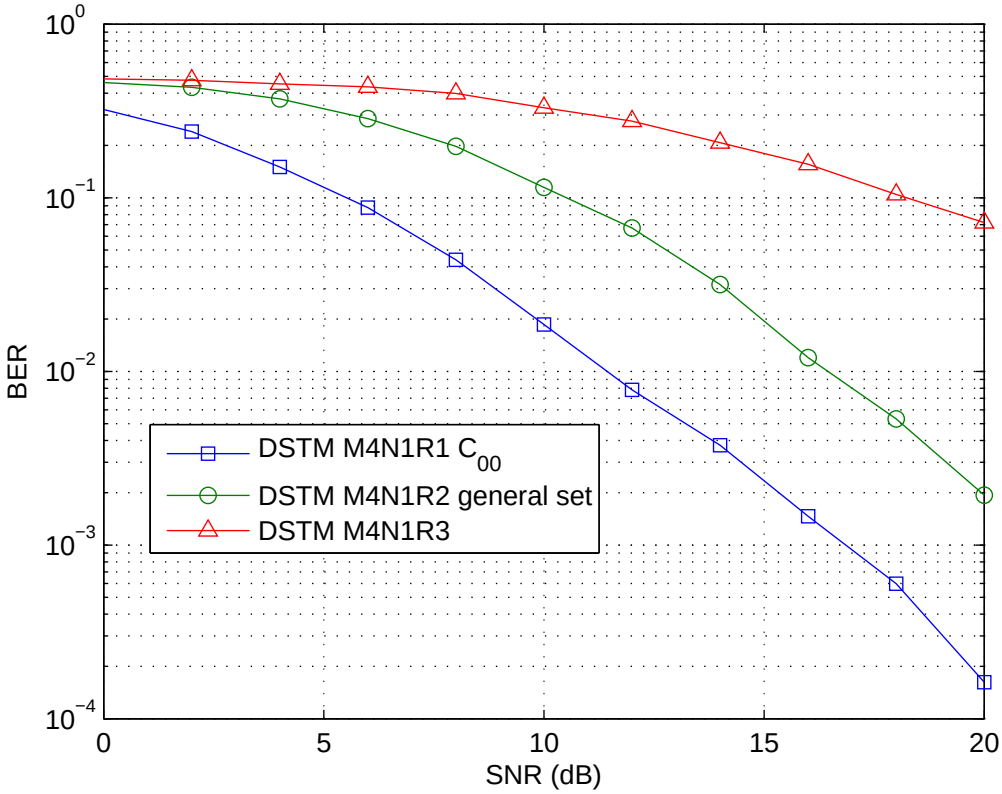

Figure 5.4: Simulation results of the new differential space-time scheme for 4 transmit antennas and 1 receive antenna with spectral efficiency 1, 2 and 3 bps/Hz respectively.

5.2 Differential MIMO systems with 8 transmit antennas

As the scheme used for 4 transmit antennas MIMO systems, we can expand the new scheme to 8 transmit antennas with Kronecker product.

The generated matrices should be with dimension 8×8. Obviously, the set is from $G_w \otimes G_w \otimes G_w = G_w \otimes G_{w4}$. There are $192 \times 4608 = 884736$ matrices in the set $G_w \otimes G_{w4}$. However, only 110592 matrices are distinct, we denote this set of distinct 8×8 matrices G_{w8}. The maximum spectral efficiency we can get is $R = \frac{1}{M}\lfloor \log_2 K \rfloor = \frac{1}{8}\lfloor \log_2 110592 \rfloor = 2$ bps/Hz.

For $R = 0.5$ bps/Hz, we use the 16 matrices of the set $S_{000} = M_0 \otimes (M_0 \otimes C_0)$. As stated by theorem 5.1.2, the set S_{000} has the highest value of $d_{min} = 4$. Then, to improve the BER performance, we use $S_{div2} = M_0 \otimes S_{div}$ as a new information set

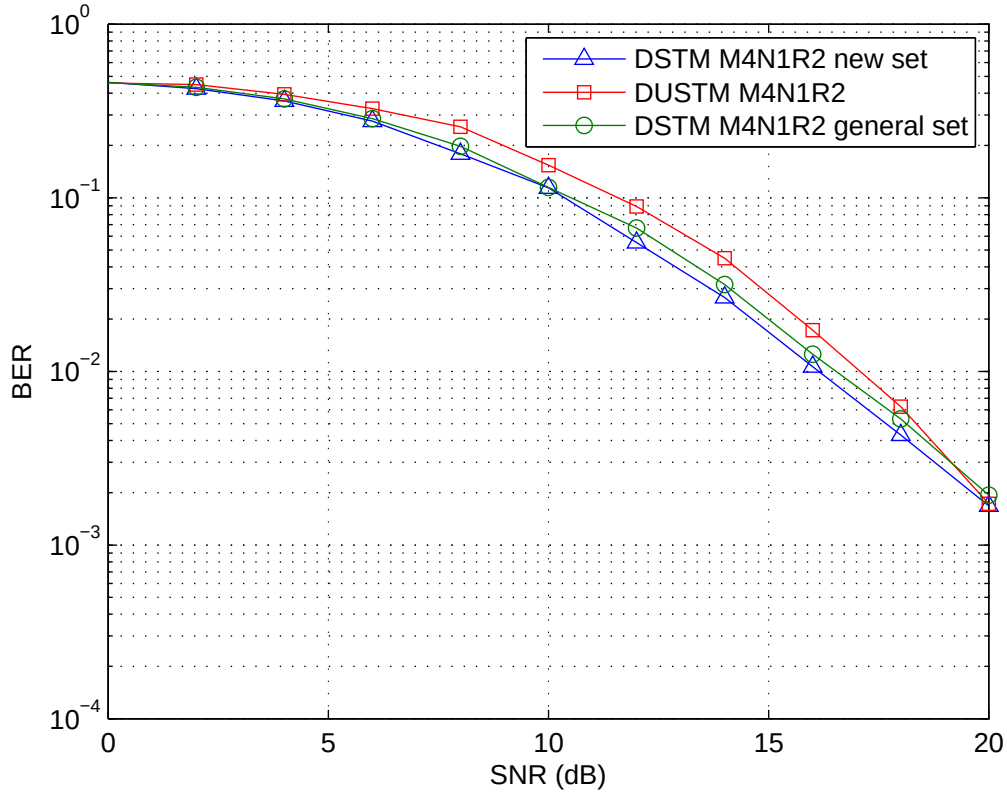

Figure 5.5: Comparison of different differential space-time scheme for 4 transmit antennas and 1 receive antennas $R = 2$ bps/Hz with different set.

which has the best diversity product 0.5946. The diversity product of S_{000} is 0. The simulation results are shown in Fig. 5.6. We can see that the MIMO scheme with S_{div2} is better than the scheme with S_{000}.

For $R = 1$ bps/Hz, first, we use the 256 matrices of the set $S_{m8r1a} = M_0 \otimes S_1$. As for MIMO systems with 4 transmit antennas, $S_{m8r1b} = M_0 \otimes S_2$ is used to improve the BER performance. The minimum distances of the set S_{m8r1a} and S_{m8r1b} are 2.1648 and 2.8284 respectively. The simulation results are shown in Fig. 5.7. We can see that the scheme with set S_{m8r1b} is better than the scheme with set S_{m8r1a}.

Then we construct a new set S_{m8r1c} with the best distance spectrum: first, we get a 4×4 set C_{44} with 16 matrices use Kronecker product between the first 4 matrices of G_w (M_0, M_1, M_2, and M_3). Second, the Kronecker product between C_0 and C_{44} produces a 8×8 set S_{m8r1c} with 256 matrices. The minimum distance of this new set is 4. However, simulation result in Fig. 5.7 shows that the BER performance

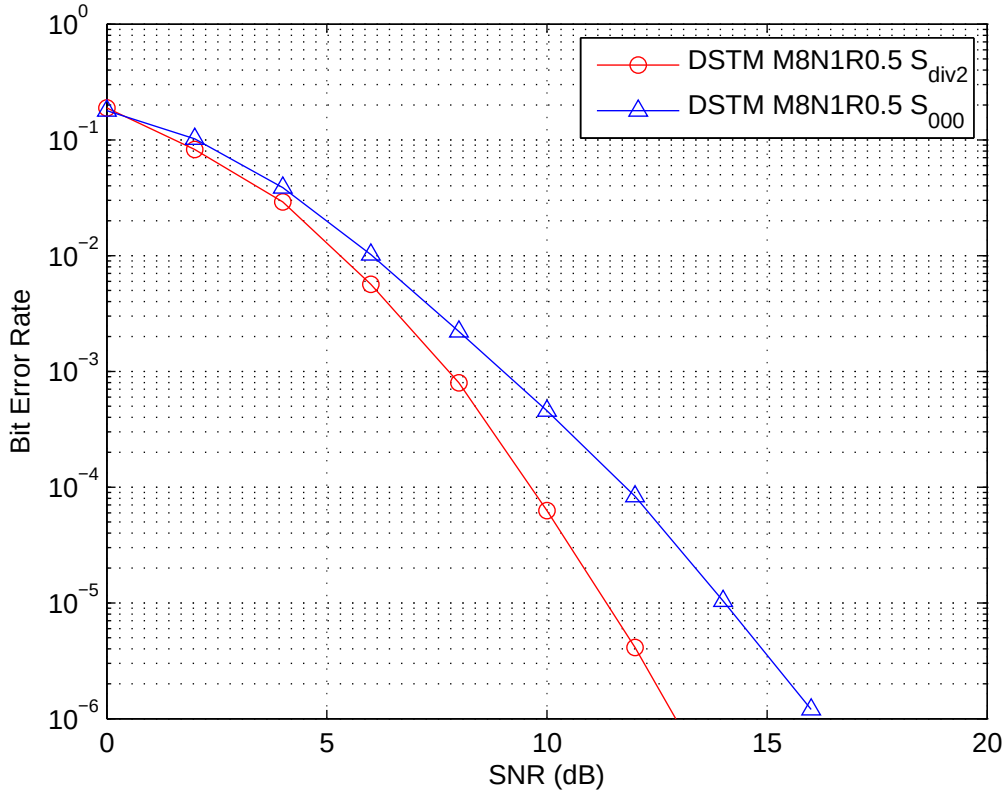

Figure 5.6: DSTM schemes for set S_{000} and S_{div2}. 8 transmit antennas, 1 receive antenna and spectral efficiency $R = 0.5$ bps/Hz.

with the set S_{m8r1c} is similar to the BER performance with the set S_{m8r1b} and a little worse when SNR is greater than 12 dB.

For $R = 1.5$ bps/Hz, we use the first 4096 matrices of the set $C_{0a} = M_0 \otimes G_{w4}$.

For $R = 2$, we select the first 65536 matrices in G_{w8} as the candidate transmission set. The simulation results are shown in Fig. 5.8.

The maximum spectral efficiency of the new differential scheme for 8×8 MIMO systems is 2, which is quite low. Thus new schemes that can be expanded to large spectral efficiencies are supposed to be designed in the future.

5.3 Conclusion

In this chapter, we designed DSTM schemes used for MIMO systems with 4 and 8 transmit antennas. Kronecker product is used to expand the information group

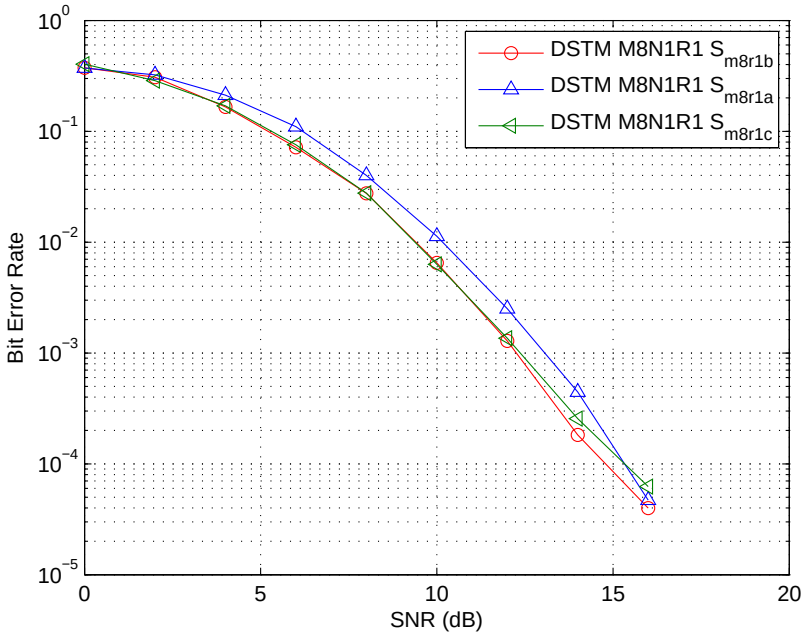

Figure 5.7: DSTM schemes for set S_{m8r1a}, S_{m8r1b} and S_{m8r1c}. (8 transmit antennas, 1 receive antenna and spectral efficiency $R = 1$ bps/Hz).

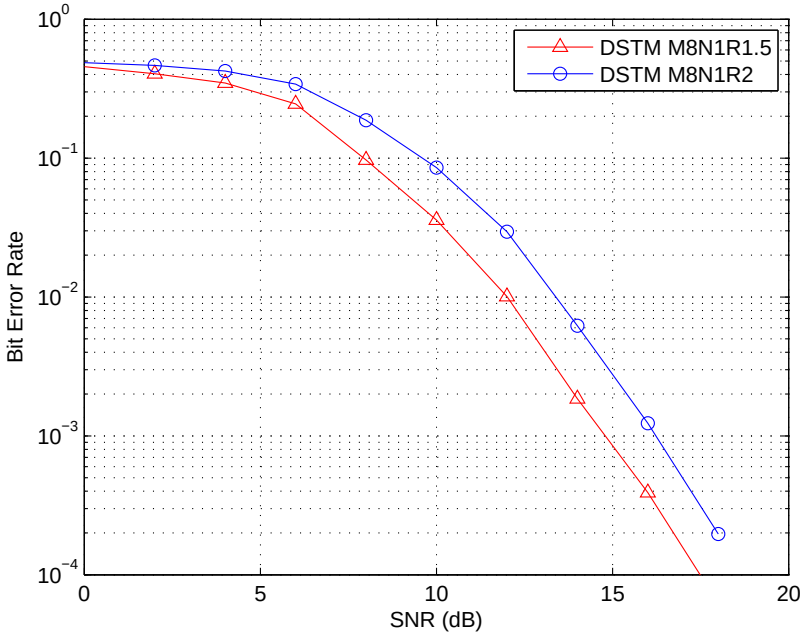

Figure 5.8: Simulation results of the new differential space-time scheme for 8 transmit antennas and 1 receive antennas with spectral efficiency 1.5 and 2 bps/Hz respectively.

(Weyl group).

For MIMO systems with 4 transmit antennas and $R = 1$ bps/Hz, our scheme with the best set S_{div} is better than the corresponding DSTBC and DUSTM schemes. For $R = 2$ bps/Hz, our scheme with general set S_1 and the best set S_2 are both better than the corresponding DUSTM scheme.

For MIMO systems with 8 transmit antennas, we give the best set used for $R = 0.5, 1, 1.5$ and 2 bps/Hz.

6

New time-selective channel model

In this chapter, we propose a new model to simulate the time selective channel due to Doppler effect. Then we evaluate the performance and the robustness of DSTM schemes with two, four and eight transmit antennas over this time selective channel model.

6.1 Usual channel model for differential MIMO systems

As mentioned before, the channel model used in [28, 118, 119] is constant during one frame and changes randomly for the next frame. For example, with the normalized coherence interval $L = 200$, for M transmit antennas and N receive antennas, during the transmission of the first frame of 200 symbols, the same channel matrix H_τ is used for simulation. The next channel matrix $H_{\tau+1}$ is randomly generated to be used for the next 200 symbols. However, this is not the real case. In reality, the channel changes continuously. Furthermore, at the beginning of the new frame, the reference matrix V_0 has to be transmitted again which is not the real situation. This reduces the overall simulation efficiency.

In [26, 27], Jakes' model [63] is used. Each of the channel coefficients $h_{nm,t}$ is assumed to be spatially independent but time correlated with autocorrelation function $J_0(2\pi f_d t)$ where $J_0(\cdot)$ is the zero-order Bessel function of the first kind and f_d is the maximum Doppler frequency. In fact, Jakes' simulator is a kind of sum-

of-sinusoids based fading channel simulator where the received signal is represented as a superposition of a finite number of waves. It is a simplified model of Clarke's Rayleigh fading model. Clarke's model is given by [120]:

$$h(t) = \sum_{n=1}^{N} \alpha_n \exp[j(2\pi f_d t \cos\theta_n + \phi_n)], \tag{6.1}$$

where N is the number of propagation paths, $0 < \alpha_n < 1$ is the attenuation of the nth path, f_d is the maximum Doppler frequency and θ_n and ϕ_n are, respectively, the angle of arrival and random phase of the n^{th} propagation path. Both θ_n and ϕ_n are uniformly distributed over $[-\pi, \pi)$ for all n and they are mutually independent.

Jakes approximates Clarke's model by setting equal strength multipath components, i.e., $\alpha_n = \frac{1}{\sqrt{N}}$ and choosing the N components to be uniformly distributed in angle, i.e.,

$$\theta_n = \frac{2\pi n}{N}, \quad n = 1, 2, ..., N. \tag{6.2}$$

The normalized low-pass fading process of this model is given by [63]

$$\begin{aligned} h(t) = \frac{1}{\sqrt{N}} \Bigg\{ \sqrt{2} \sum_{n=1}^{N_0} \left[e^{j(2\pi f_d t \cos\theta_n + \phi_n)} + e^{-j(2\pi f_d t \cos\theta_n + \phi_{-n})} \right] \\ + e^{j(2\pi f_d t + \phi_N)} + e^{-j(2\pi f_d t + \phi_{-N})} \Bigg\}, \quad N_0 = \frac{1}{2}\left(\frac{N}{2} - 1\right), \end{aligned} \tag{6.3}$$

where ϕ_n is given by

$$\phi_N = \phi_{-N} = 0, \quad \phi_n = \frac{n\pi}{N_0 + 1}, \quad n = 0, 1, ..., N_0. \tag{6.4}$$

6.2 New and improved channel model

Instead of assuming that the channel is constant during a fixed long time, we assume that the channel changes continuously. The narrow-band channel impulse response $h(t)$ is a random process. We consider the flat fading channel. In this case, for a SISO system, the received signal is $y(t) = h(t)x(t) + w(t)$. From the analysis in Chapter 2, we know that $h(t) = h_I(t) + jh_Q(t)$, where $h_I(t)$ and $h_Q(t)$

are jointly Gaussian random processes. The envelope of $h(t)$ is Rayleigh distributed. If we try to obtain intermediate $h(t)$ values between two succesive Rayleigh samples, we should sample $h(t)$ with certain high frequency. From the Nyquist's sampling theorem, we know that if we sample the channel with sufficient large frequency, the impulse response of a SISO channel could by reconstructed by the sampled points. Our new channel model is based on this idea.

Using the well-known Nyquist's sampling theorem, a band-limited signal $x(t)$ can be reconstructed from its samples $x(kT_0)$ as follows:

$$\begin{aligned} x(t) &= \sum_{k=-\infty}^{+\infty} x(kT_0) \frac{\sin f_0\pi(t-kT_0)}{f_0\pi(t-kT_0)} \\ &= \sum_{k=-\infty}^{+\infty} x(kT_0) \frac{\sin \pi(f_0 t-k)}{\pi(f_0 t-k)}, \end{aligned} \tag{6.5}$$

if the sampling frequency $f_0 = 1/T_0 > 2f_M$, where f_M is the maximum frequency of the signal.

With Clarke's model, the channel impulse response $h(t)$ has autocorrelation:

$$R_h(\tau) = 2\sigma^2 J_0(2\pi f_d \tau), \tag{6.6}$$

where $J_0(\cdot)$ is the zero-order Bessel function of the first kind and $\sigma^2 = 0.5\sum_n E[\alpha_n^2]$. Conventionally, people assume that $\sum_n E[\alpha_n^2] = 1$ to ensure that the received signal power equal to the transmitted signal power which results $R_h(\tau) = J_0(2\pi f_d \tau)$. As shown in Fig. 6.1, we know that the function $J_0(x)$ has its first zero-point at $x \approx 2.4048$. It is reasonable to suppose that the channel coefficients separated by $\tau = 2.4048/(2\pi f_d) \approx 0.3827/f_d$ are independent. It clear that the function of $h(t)$ in (6.1) has the maximum frequency f_d. If we try to reconstruct $h(t)$, the sampling frequency should be $f_0 > 2f_d$ and the sample period $T_0 < 0.5/f_d$. Therefore it is possible to reconstruct channel response with independently generated Rayleigh distributed random variables.

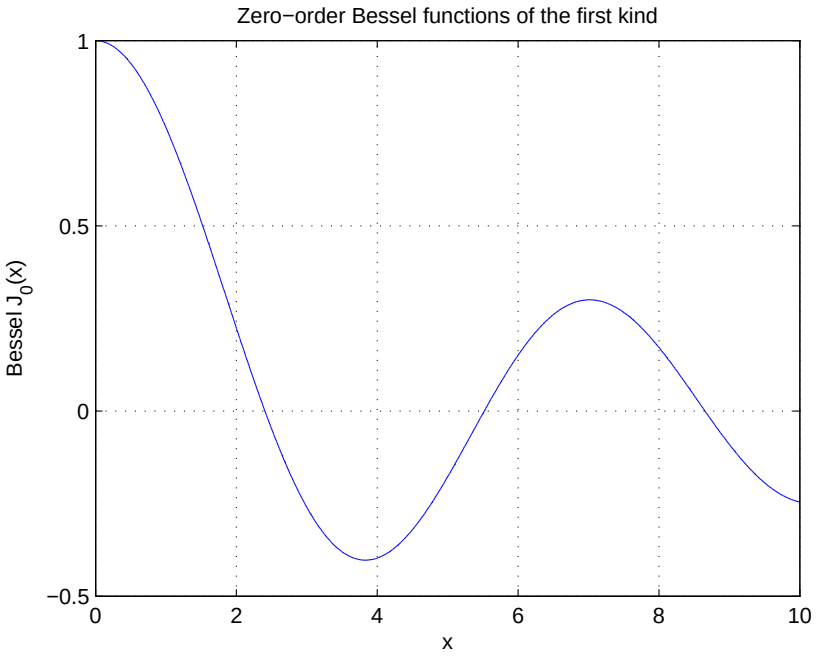

Figure 6.1: The zero-order Bessel function of the first kind $J_0(x) = \frac{1}{\pi}\int_0^{\pi}\cos(x\cos\theta)d\theta$.

6.2.1 Time selective channel model

In this section, we present the generation of time selective channel model with random variables $r_k = g_{kr} + jg_{ki}$ where g_{kr} and g_{ki} are Gaussian distributed random variables with mean zero and variance 0.5. In this case the module of r_k is Rayleigh distributed. As discussed before, we assume that the samples r_k $(k = 1, 2, ..., K)$ are separated by $\tau_0 = 2.4048/(2\pi f_d) \approx 0.3827/f_d$. According to (6.5), with these K randomly generated points, $h(t)$ is constructed by

$$\begin{aligned} h(t) &= \sum_{k=0}^{K-1} r(kT_0)\frac{\sin f_0\pi(t-kT_0)}{f_0\pi(t-kT_0)} \\ &= \sum_{k=0}^{K-1} r(kT_0)\frac{\sin \pi(f_0t-k)}{\pi(f_0t-k)}, \end{aligned} \tag{6.7}$$

where $T_0 = \tau_0 = 2.4048/(2\pi f_d) \approx 0.3827/f_d$ and $f_0 = 1/T_0 \approx f_d/0.3827$. In fact, with K points, the total time that the channel can cover is $T_{sp} = K\tau_0$ and the channel impulse response can only be reconstructed in this time duration. For example, with $f_d = 10$ Hz, $T_{sp} = K\tau_0 \approx 38.27K$ ms. We illustrate the procedure in Fig. 6.2 and

Fig. 6.3. The maximum Doppler shifts are $f_d = 1$ Hz and 10 Hz respectively. We select $K = 200$ for both of these two figures. In simualtions, K is set according to the real situation. The sample periods are $T_0 \approx 0.3827/f_d = 0.3827$ s and 38.27 ms respectively. We can see that the channel with $f_d = 1$ Hz changes more slowly than the channel with $f_d = 10$ Hz.

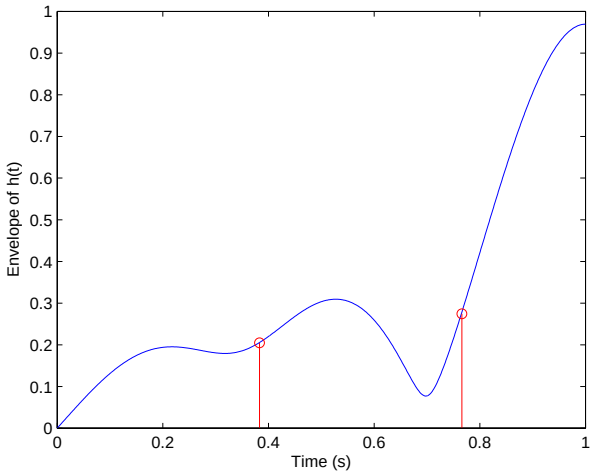

Figure 6.2: Channel reconstruction with $f_d = 1$ Hz, $K = 200$.

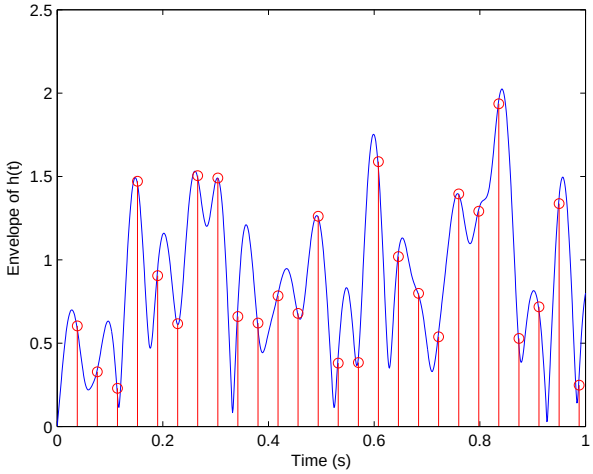

Figure 6.3: Channel reconstruction with $f_d = 10$ Hz, $K = 200$.

6.2.2 Block-constant MIMO channel model

We first examine the BER performance of DSTM schemes over block-constant MIMO channel [121]. The channel is assumed to be constant during the transmission

of one matrix. With M transmit antennas and N receive antennas, during the coherence interval L, $N_m = L/T = L/M$ transmit matrices will be sent. Thus N_m channel matrices are needed to multiply the transmit matrices. We interpolate $N_m - 1$ channel matrices $H(1), \ldots, H(N_m - 1)$ between two successive randomly generated channel matrices R_K and R_{K+1} instead of one constant channel matrix R_K. The $N_m - 1$ interpolated channel matrices are related to the passed channel matrices and also to the future channel matrices.

The interpolated channel sequence $H(1)$, $H(2)$, ..., $H(N_m - 1)$ is generated as follows:

1. A fix number $2K$ of Rayleigh distributed matrices are randomly generated, i.e., R_1, ..., R_K, R_{K+1}, ..., R_{2K}.
2. With the Nyquist's sampling theorem, the channel sequence between R_K and R_{K+1} is generated by sinc interpolation.

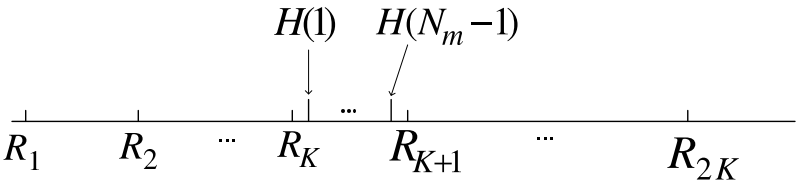

Figure 6.4: Illustration of the interpolation of the channel matrix H.

In our case, the Rayleigh random matrices R_k can be considered as samples of the continuous channel matrix H separated by the coherence interval, so $T_0 = T_c = LT_s$. With $2K$ randomly generated matrices, we get the $N_m - 1$ interpolated channel matrices between the matrices R_K and R_{K+1}:

$$\begin{aligned} H(i) &= \sum_{k=1}^{2K} R_k \frac{\sin \pi \left[f_0(KLT_s + iMT_s) - k \right]}{\pi \left[f_0(KLT_s + iMT_s) - k \right]} \\ &= \sum_{k=1}^{2K} R_k \frac{\sin \pi (K + i/N_m - k)}{\pi (K + i/N_m - k)}, \\ & i = 1, 2, \ldots, N_m - 1. \end{aligned} \tag{6.8}$$

For example, with $2K = 10$ randomly generated Rayleigh channel matrices R_1,

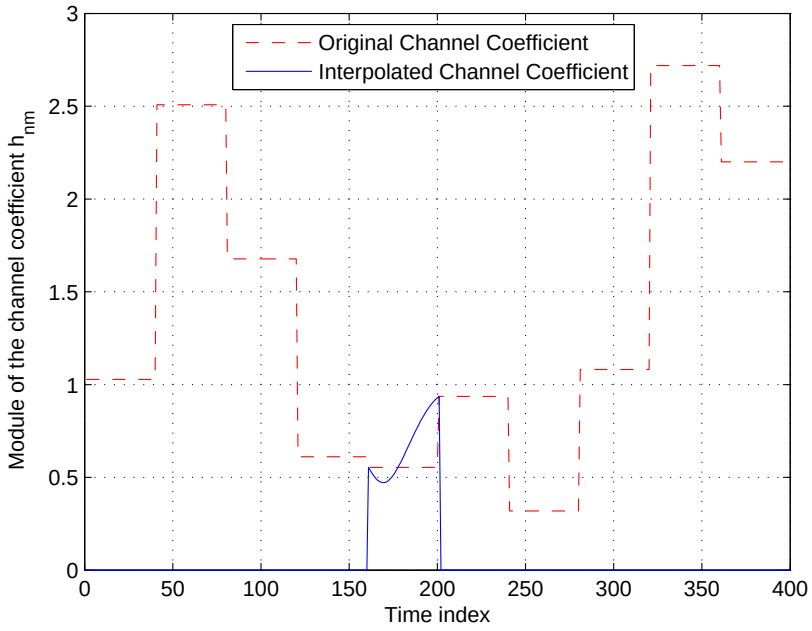

Figure 6.5: Comparison of the two channel models considering one channel coefficient h_{nm}, interpolated with the passed and future random variables.

$\ldots$, R_5, R_6, $\ldots$, R_{10}, the number of transmit antennas $M = 4$, and the normalized coherence interval $L = 160$, we get $N_m - 1 = 39$ interpolated channel matrices $H(i)$ between R_5 and R_6. This procedure is illustrated in Fig 6.4.

The module of one channel coefficient h_{nm} obtained by interpolation between the corresponding elements of R_K and R_{K+1} is shown in Fig. 6.5. A complete figure of the generated channel coefficient h_{nm} compared with the randomly generated Rayleigh values is given in Fig. 6.6.

We can see that the channel generated by this method changes slightly for each two successive transmit matrices as expected.

However, there is still the problem of the selection of the number K. Here, we resort to the relative error to select appropriate K. As discussed before, with $2 \times K$ Rayleigh distributed channel matrices, we get $N_m - 1$ interpolated channel matrices. We select a very large number, for example $K_{max} = 4000$ to get a set of interpolated reference channel matrices. We estimate that $K_{max} = 4000$ is large enough to obtain accurate channel matrices by interpolation. With K decreasing to 1, we get other $K_{max} - 1$ sets of interpolated channel matrices. Compared with the reference set,

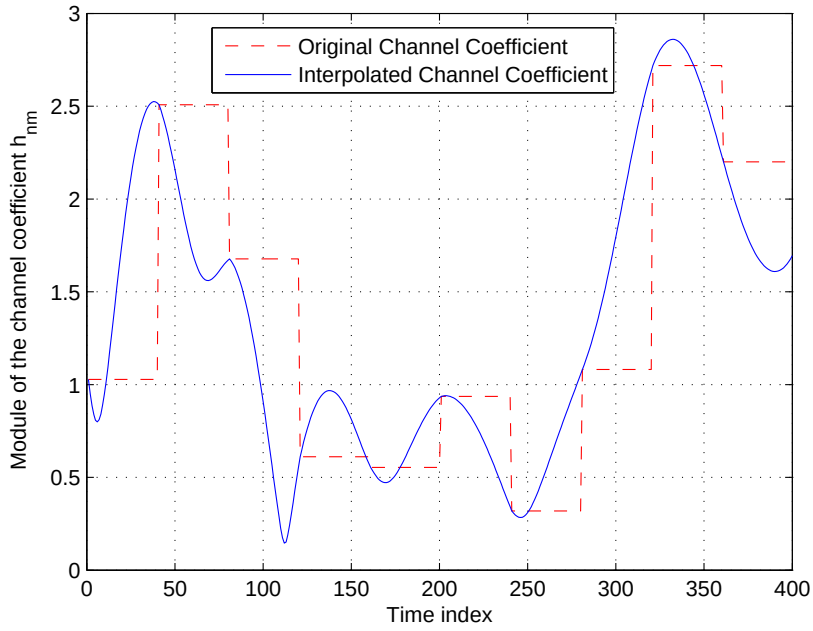

Figure 6.6: Time variation of the module of one channel coefficient h_{nm}.

each set has different variations. The sets of interpolated channel matrices are:

$$\{H^k(1), H^k(2), \cdots, H^k(N_m - 1)\}, k = 1, \cdots, K_{max}. \tag{6.9}$$

We define the mean relative error as:

$$\varepsilon_k = \frac{1}{N_m - 1} \sum_{i=1}^{N_m - 1} \frac{\|H^{K_{max}}(i) - H^k(i)\|}{\|H^{K_{max}}(i)\|}, \quad k = 1, 2, \cdots, K_{max}. \tag{6.10}$$

As the matrices $R_1, \ldots, R_K, R_{K+1}, \ldots, R_{2K}$ are generated randomly, the curve of the relative error is very rough. To smooth the curve, we calculate the relative error 100 times and get the mean as the final relative error. The curve of relative error is shown in Fig. 6.7 with $K_{max} = 4000$ and $N_m = 10, 50$ respectively. We get the table of relative error versus K in Table 6.1 with $N_m = 50$ and $N_m = 10$ respectively. On the basis of these data, we set $K = 30$ in our simulations. In this case, the relative error is below 10%.

The performance of the differential MIMO systems are evaluated over the frame

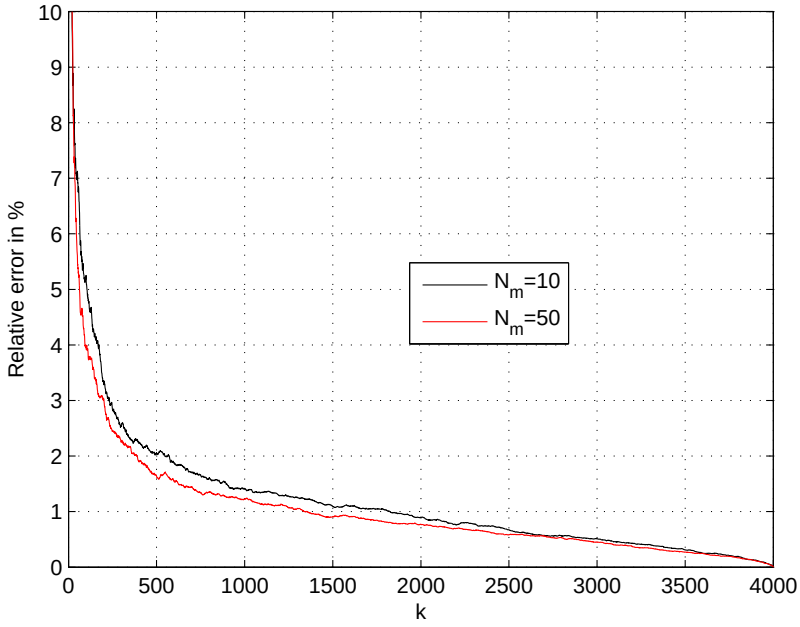

Figure 6.7: The relative error versus different numbers of k with $N_m = 10$ and $N_m = 50$ respectively.

constant channel (step channel) and over the proposed time selective channel (block-constant channel). We set $L = 200$, which means that for 2, 4 and 8 transmit antennas, $N_m = 100, 50$ and 25 respectively.

Fig. 6.8 shows that for $R = 1$ bps/Hz, the M8N8 scheme offers for BER $= 10^{-4}$ a SNR gain of about 5.5 dB compared to the M4N4 scheme and 17 dB compared to the M2N2 scheme on the step channel. Over the new continuous channel, similar gains are obtained with the M8N8 scheme compared to the M4N4 and M2N2 schemes. Furthermore, using the continuous channel leads to a degradation compared to the

$N_m = 50$		$N_m = 10$	
Relative error	K	Relative error	K
2%	389	2%	548
3%	201	3%	229
5%	62	5%	105
9.725%	22	9.678%	21
10.23%	21	10.18%	20

Table 6.1: The values of K for different relative errors with $K_{max} = 4000$.

step channel which is about 1 dB for a BER $= 10^{-4}$ with the M8N8 scheme and 0.6 dB with M2N2 scheme. Similar relative results for $R = 2$ bps/Hz M8N8, M4N4 and M2N2 schemes are obtained in Fig. 6.9. As expected, the M8N8 scheme is more sensitive than the M4N4 and M2N2 schemes to the time selectivity of the channel.

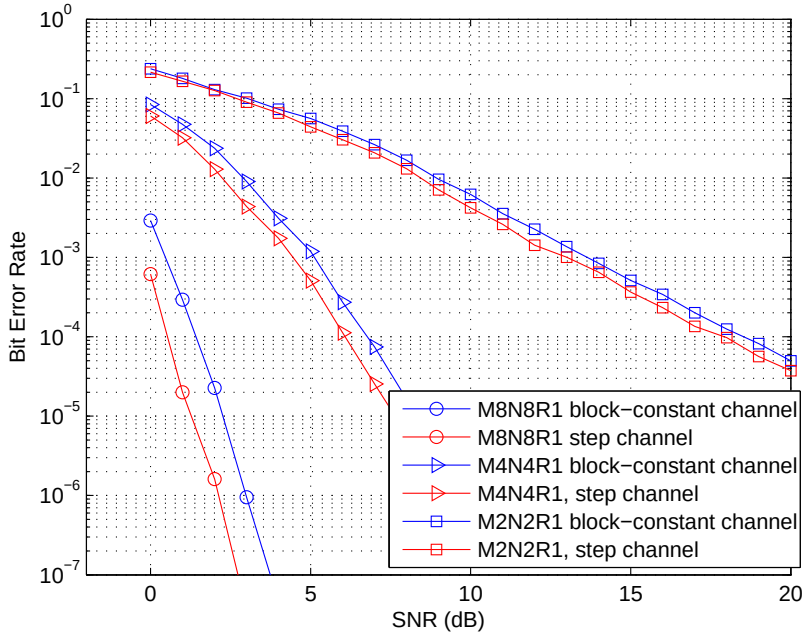

Figure 6.8: Performances of differential space-time schemes with $R = 1$ bps/Hz over different channel models.

Fig. 6.10 presents the performance of M4N4 DSTM scheme with $R = 1$ bps/Hz over the step channel and over the new continuous channel with different normalized coherence time L. As already mentioned, the faster the channel changes, the smaller the value of L. Consistent with our supposition, there is a trend that as L grows the BER performance becomes better. However, for step channel model as used in [28, 29], the BER performances with different Ls are the same.

6.2.3 Continuously changing MIMO channel model

The channel model used in the previous subsection is still constant during the transmission of one matrix. Now we apply continuous channel model to our differential space-time modulation schemes. The relations among the step channel, the block-constant channel and the continuous channel are shown in Fig. 6.11. The

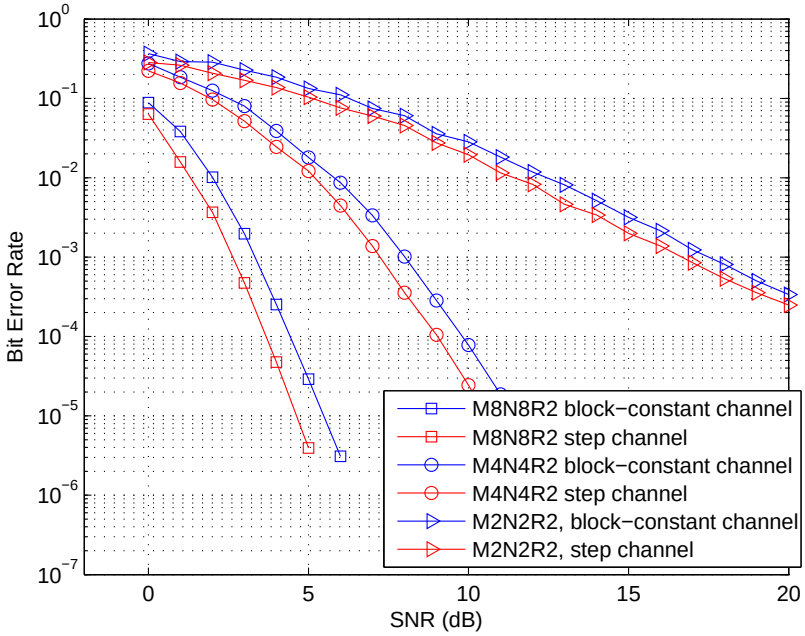

Figure 6.9: Performances of differential space-time schemes with $R = 2$ bps/Hz over different channel models.

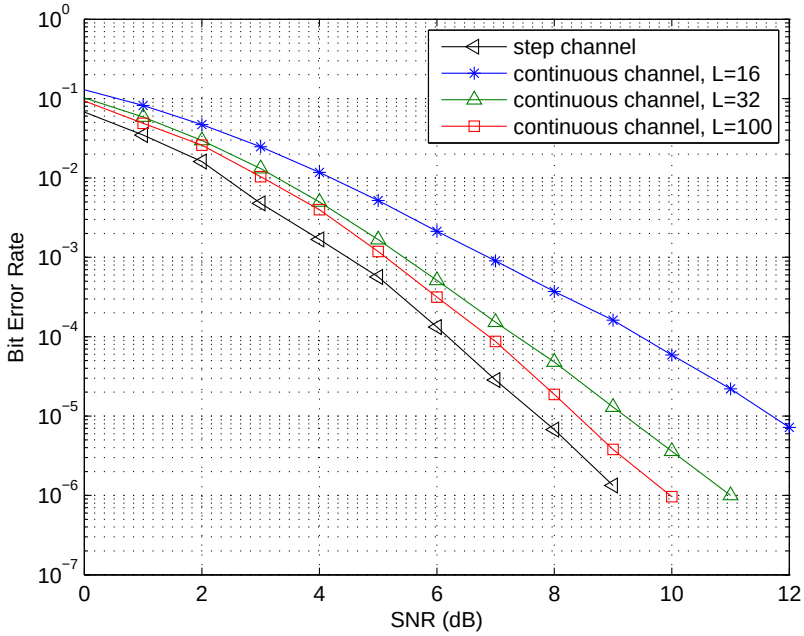

Figure 6.10: Performance of the DSTM M4N4R1 scheme with different L.

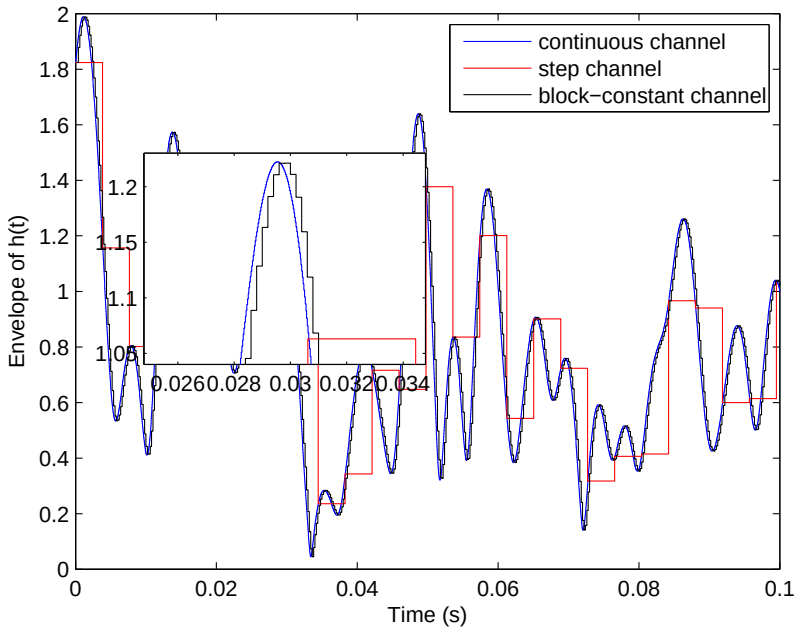

Figure 6.11: Channel interpolation with $f_d = 100$ Hz, $T_s = 25$ μs.

number of transmit antennas is $M = 8$, the maximum Doppler frequency $f_d = 100$ Hz, $T_s = 25\mu$s and $L = T_c/T_s = 200$.

In this new channel model, the channel coefficients used for two successive columns of each transmission matrix are slightly changing. With step channel model, the MIMO system model can be written as:

$$Y_t = HX_t + W_t, \tag{6.11}$$

where the channel matrix H is constant for different transmission matrices. With block-constant channel model, the MIMO system model can be written as:

$$Y_t = H_t X_t + W_t, \tag{6.12}$$

where the channel matrix H_t is changing for different transmission matrices but constant for different columns within the same transmission matrix. With our new continuously changing channel model, the channel matrix H_t is different for each column within the same transmission matrix and the MIMO system model should

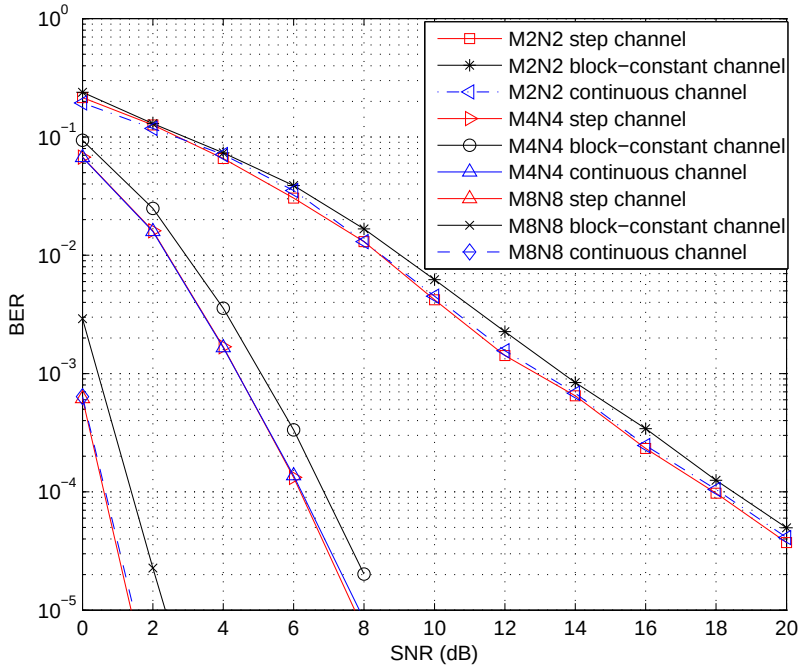

Figure 6.12: Performances of differential space-time schemes with $R = 1$ bps/Hz over different channel models. The normalized coherence time is $L = 200$.

be represent in vector form:

$$\mathbf{y}_t = H_t \mathbf{x}_t + \mathbf{w}_t, \tag{6.13}$$

where $\mathbf{y}_t$, $\mathbf{x}_t$ and $\mathbf{w}_t$ are column vectors from received matrix, transmission matrix and noise matrix respectively.

The performance of the differential MIMO systems are evaluated over these three channel models. We set $L = 200$, i.e., $T_c/T_s = 200$, that means for $f_d = 100$ Hz, $T_s = 25$ μs and symbol rate $f_s = 40$ KHz.

Fig. 6.12 shows that for $R = 1$ bps/Hz, with the normalized coherence time $L = 200$, DSTM scheme over continuous channel performes similar to those over step channel. However, DSTM schemes perform better than those over block-constant channel, which is resulted from the less value of discontinuity of the channel coefficients for two successively transmitted symbols compared to step channel. Similar relative results for $R = 2$ bps/Hz, M8N8, M4N4 and M2N2 schemes are obtained in Fig. 6.13.

Fig. 6.14 presents the performance of M4N1 DSTM scheme with $R = 1$ bps/Hz

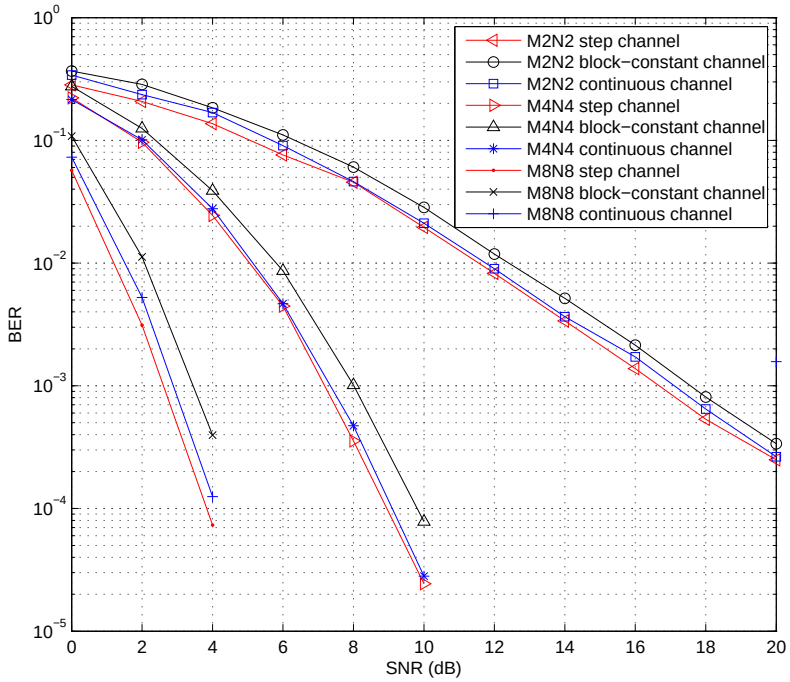

Figure 6.13: Performances of differential space-time schemes with $R = 2$ bps/Hz over different channel models. The normalized coherence time is $L = 200$.

over the step channel and the continuous channel with different normalized coherence time L. The simulation results show that the smaller the coherence time interval is, which means the fading rate is high, the worse the BER performance will be.

6.3 Conclusion

In this chapter we proposed a simple and more realistic time-selective propagation channel in order to obtain more reliable estimations of the performance of DSTM MIMO systems with 2, 4 and 8 transmit antennas. This model is based as usual on random Rayleigh channel matrices but is completed with intermediate channel matrices obtained by sinc-interpolation. During the transmission of two successive matrices, the propagation channel may change, which determines a degradation of the performance of the differential system. This degradation is evaluated by simulation for DSTM MIMO systems using 2, 4 and 8 transmit antennas and for two values of the spectral efficiency. As expected, the degradation is more important for

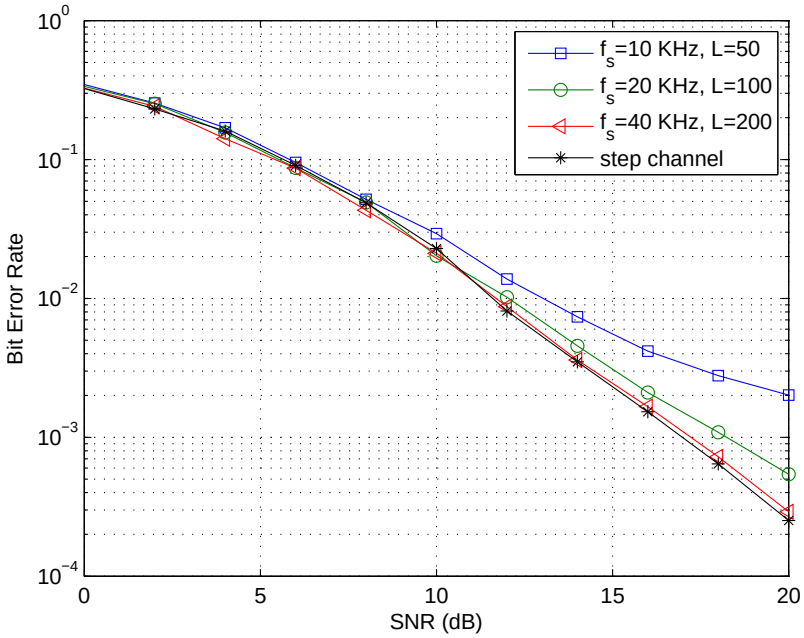

Figure 6.14: Performance of the DSTM M4N4R1 scheme with different L over continuously changing channel model.

MIMO systems using more antennas. Moreover, the degradation is more important if the normalized coherence time is reduced. Thus, the proposed channel model does not make a difference between slow and fast Rayleigh channels, the only parameter making the difference being the normalized coherence time.

Conclusion and prospect

General conclusion

At present, the study of multi-antenna systems MIMO (Multiple Input Multiple Output) is developed in many cases to intensively increase the number of base station antennas ("massive MIMO", "large-scale MIMO"), particularly in order to increase the transmission capacity, reduce energy consumed per bit transmitted, exploit the spatial dimension of the propagation channel, reduce the influence of fading, etc. For MIMO systems with narrowband spectrum or those using OFDM technique (Orthogonal Frequency Division Multiplex), the propagation channel (or the sub-channels corresponding to each sub-carrier of an OFDM system) are substantially flat (frequency non-selective). In this case the frequency response of each SISO channel is invariant with respect to frequency, but variant in time. Furthermore, the MIMO propagation channel can be characterized in baseband by a matrix whose coefficients are complex numbers. Coherent MIMO systems need to have the knowledge of the channel matrix to demodulate the received signal. Therefore, periodic pilot should be transmitted and received to estimate the channel matrix in real time. The increase of the number of antennas and the change of the propagation channel over time, sometimes quite fast, makes the channel estimation quite difficult or impossible. It is therefore interesting to study differential MIMO systems that do not need to know the channel matrix. For appropriate operation of these systems, the only constraint is that the channel matrix varies slightly during the transmission

of two successive information matrices.

The subject of this thesis is the study and analysis of new differential MIMO systems. We consider systems with 2, 4 and 8 transmit antennas, but the method can be extended to MIMO systems with 2^n transmit antennas, the number of receive antennas can be any positive integer.

For MIMO systems with two transmit antennas that were studied in this thesis, information matrices are elements of the Weyl group. For systems with 2^n ($n \geq 2$) transmit antennas, the matrices used are obtained by performing the Kronecker product of the unitary matrices in Weyl group.

For each number of transmit antennas, we first identify the number of available matrices and the maximum value of the spectral efficiency. For each value of the spectral efficiency, we then determine the best subsets of the information matrices to be used (depending on the spectrum of the distances or the diversity product criterion). Then we optimize the correspondence or mapping between binary vectors and information matrices. Finally, the performance of differential MIMO systems are obtained by simulation and compared with those of existing similar systems.

For simulation of the proposed system, we first selected a simple Rayleigh channel model, which is widely used in the literature. In this channel model, the channel matrix is constant for a time interval of a certain length determined by the coherence time of the propagation channel. Each new channel matrix is obtained by a random draw, independent from previous draws. This channel model is impractical and, for the differential systems, need to simulate a periodic reset of the system, whenever using another channel matrix. To evaluate the performance of the new proposed systems in more realistic conditions and escape the periodic reset of the analyzed system, we introduced a variation of the channel matrix between two successive random draws by using the sampling theorem. However, in the first approach, the channel matrix is considered to be constant during the transmission of an information matrix. Simulations with this new channel model made it possible to spotlight some performance degradation due to the channel characteristic, especially when the normalized coherence time with respect to the duration of a transmitted symbol is small and therefore, when the propagation channel varies rapidly.

Finally, we considered the second even closer approach to reality, where the channel matrix remains constant during the transmission of only a symbol. In this case there is a further performance degradation.

Prospects

Our research can be further exploited in four directions. Firstly,we can use error-correcting codes before the DSTM schemes. In order to improve the performance of DUSTM schemes, especially for larger values of the spectral efficiency, an error correcting code can be used, as in the case of SISO systems. Depending on the propagation channel, it is possible to use a simple error-correcting code like Hamming's code or more powerful codes as the Reed-Solomon code RS(255,239).

Secondly, the spectral efficiencies of our proposed systems are limit. For example, the maximum spectral efficiencies for MIMO systems with 2, 4 and 8 transmit antennas are 3.5, 3 and 2 bps/Hz respectively. Therefore, expanded groups should be designed for MIMO systems with large spectral efficiencies.

Thirdly, the proposed schemes are suitable for MIMO systems with 2^n transmit antennas. According to some exiting method [37, 41, 42], our schemes can be expanded to systems with any number of transmit antennas.

Finally, our proposed systems are suitable for point-to-point wireless communications. New methods could be studied to expand our schemes to MIMO systems with multiple users, for example, "large-scale MIMO" or "massive MIMO".

A

Gaussian random variables, vectors and matrices

Gaussian random variables are widely used in the research of wireless communications. In this appendix, we present the definition of Gaussian random variables, vectors and matrices. We also give the entropy for each case.

A.1 Gaussian random variables

If x is real Gaussian random variable with mean μ and variance σ^2, i.e., its pdf is

$$p(x) = \frac{1}{\sqrt{2\pi\sigma^2}} e^{-(x-\mu)^2/(2\sigma^2)}. \tag{A.1}$$

We write $x \sim \mathcal{N}(\mu, \sigma^2)$. The entropy of the random variable x is:

$$\begin{aligned} \mathcal{H}(x) &= -\mathbb{E}[\log p(x)] = \frac{1}{2}\log(2\pi\sigma^2) + (\log e)\mathbb{E}[(x-\mu)^2]/(2\sigma^2) \\ &= \frac{1}{2}\log(2\pi e\sigma^2). \end{aligned} \tag{A.2}$$

If the real and imaginary parts of the complex random variable $z = x + jy$ are independent with the same variance $\frac{\sigma^2}{2}$, and $\mu = \mathbb{E}(z) \in \mathbb{C}$, then we say that z is *circularly symmetric*, and we write $z \sim \mathcal{CN}(\mu, \sigma^2)$. Its pdf is the product of its real and imaginary part:

$$p(z) = \frac{1}{\pi\sigma^2} e^{-|z-\mu|^2/\sigma^2}. \tag{A.3}$$

In fact, by definition, z is circularly symmetric if $e^{i\varphi}z$ has the same probability

distribution as z for all real φ. The entropy of the random variable z is:

$$\begin{aligned}\mathcal{H}(z) &= -\mathbb{E}[\log p(z)] = \log \pi\sigma^2 + (\log e)\mathbb{E}[|z-\mu|^2]/\sigma^2 \\ &= \log(\pi e\sigma^2)\end{aligned} \tag{A.4}$$

A.2 Gaussian random vectors

A real random vector $\mathbf{x} = (x_1, \ldots, x_n)^T$ is called *Gaussian* if its components are jointly Gaussian, that is, if their joint pdf is

$$\begin{aligned}p(\mathbf{x}) &= \frac{1}{(2\pi)^{n/2}\det {R_\mathbf{x}}^{1/2}} \exp\{-\frac{1}{2}(\mathbf{x}-\mu_\mathbf{x})^T R_\mathbf{x}^{-1}(\mathbf{x}-\mu_\mathbf{x})\} \\ &= \frac{1}{(2\pi)^{n/2}\det {R_\mathbf{x}}^{1/2}} \exp\{-\frac{1}{2}\operatorname{Tr}[R_\mathbf{x}^{-1}(\mathbf{x}-\mu_\mathbf{x})(\mathbf{x}-\mu_\mathbf{x})^T]\}.\end{aligned} \tag{A.5}$$

Where $R_\mathbf{x}$ is a nonnegative definite $n \times n$ matrix, the covariance matrix of $\mathbf{x}$:

$$R_\mathbf{x} = E[(\mathbf{x}-\mu_\mathbf{x})(\mathbf{x}-\mu_\mathbf{x})^T] = E[\mathbf{x}\mathbf{x}^T] - \mu_\mathbf{x}\mu_\mathbf{x}^T. \tag{A.6}$$

The probability density function of a circularly symmetric complex Gaussian random vector $\mathbf{z}$ is given by

$$\begin{aligned}p(\mathbf{z}) &= \det(\pi R_\mathbf{z})^{-1} \exp\{-(\mathbf{z}-\mu_\mathbf{z})^H R_\mathbf{z}^{-1}(\mathbf{z}-\mu_\mathbf{z})\} \\ &= \det(\pi R_\mathbf{z})^{-1} \exp\{-\operatorname{Tr}[R_\mathbf{z}^{-1}(\mathbf{z}-\mu_\mathbf{z})(\mathbf{z}-\mu_\mathbf{z})^H]\}.\end{aligned} \tag{A.7}$$

where

$$R_\mathbf{z} = \mathbb{E}[(\mathbf{z}-\mu_\mathbf{z})(\mathbf{z}-\mu_\mathbf{z})^H] = E[\mathbf{z}\mathbf{z}^H] - \mu_\mathbf{z}\mu_\mathbf{z}^H. \tag{A.8}$$

A.3 Gaussian random matrices

List of Figures

2.1 A general point-to-point communication system model. 38

2.2 Spectrum of (a) bandpass and (b) complex baseband representation of the same signal. 41

2.3 QPSK signal constellation. 44

2.4 Power spectral density of AWGN. (a) The original AWGN. (b) Bandpass AWGN. (c) Baseband representation of bandpass AWGN. 50

2.5 A general MIMO system model. 59

2.6 The normalized capacity C/T with independent Rayleigh fading, H is known to the receiver. The SNR is fixed to 0, 10, 20 and 30 dB respectively. 64

2.7 The normalized capacity C/T with independent Rayleigh fading, H is known to the receiver. The numbers of transmit antennas and receive antennas are fixed to 1, 2, 4 and 8 respectively. 65

2.8 The upper bound of Q function. 69

2.9 The Chernoff bound of PEP of coherent space-time codes. Number of transmit antennas $M = 2, 4, 8$ respectively and the number of receive antenna is 1. $\lambda_m = 1$, $m = 1, .., M$. 72

2.10 The Chernoff bound of PEP for coherent space-time codes. Number of transmit antennas $M = 4$ and number of receive antenna is 1. . . 73

2.11 The Chernoff bound of PEP of noncoherent space-time codes. Number of transmit antennas $M = 2, 4, 8$ respectively and the number of receive antenna is 1. $d_m = 0.8$. 75

2.12 The Chernoff bound of PEP for noncoherent space-time codes. Number of transmit antennas $M = 4$ and number of receive antenna is 1 $N = 1$. SNR = 0, 10, 20 dB respectively. 76

3.1 BER performance of DUSTM [27], $R = 1$. 87

3.2 BER performance of DUSTM [27], $R = 2$. 88

3.3 BER performance of STBC and DSTBC. 92

3.4 MIMO-MCM system model. 93

4.1 Distance spectrum of Weyl group. 103

4.2 Distance spectrum of coset C_0 104

4.3 Comparison of performances of MIMO systems with 2 transmit antennas and 2 receive antennas. These three scheme are DSTBC [28] with 4PSK, our new DSTM with coset C_0 (general mapping rule) and DUSTM [27]. 108

4.4 Position of the matrices M_0 and M_4 on the surface of a sphere. 109

4.5 Simulation results of DSTM with coset C_0 (new mapping rule). . . . 109

4.6 Comparison of differential space-time scheme for 2 transmit antennas and 2 receive antennas R = 2 with different set. 111

4.7 Comparison of DSTM for different sets from different design criteria. 2 transmit antennas, 2 receive antenna and $R = 2$ bps/Hz. 113

4.8 Comparison of DSTM for general mapping and Gray mapping. 2 transmit antennas, 1 receive antenna and $R = 1$ bps/Hz. 115

4.9 DSTM with 2 transmit antennas, 2 receive antenna and $R = 3$ bps/Hz. 116

5.1 Comparison of DSTBC [29], DUSTM [27] and our new DSTM scheme (M=4, N=1, R=1). 123

5.2 Comparison of DSTBC [29], DUSTM [27] and new DSTM scheme with set S_{div} (M=4, N=1, R=1). 125

5.3 Comparison of different mapping rule for DSTM (M=4, N=1, R=1) with set C_{00}. 127

5.4 Simulation results of the new differential space-time scheme for 4 transmit antennas and 1 receive antenna with spectral efficiency 1, 2 and 3 bps/Hz respectively. 128

5.5 Comparison of different differential space-time scheme for 4 transmit antennas and 1 receive antennas $R = 2$ bps/Hz with different set. . . 129

5.6 DSTM schemes for set S_{000} and S_{div2}. 8 transmit antennas, 1 receive antenna and spectral efficiency $R = 0.5$ bps/Hz. 130

5.7 DSTM schemes for set S_{m8r1a}, S_{m8r1b} and S_{m8r1c}. (8 transmit antennas, 1 receive antenna and spectral efficiency $R = 1$ bps/Hz). 131

5.8 Simulation results of the new differential space-time scheme for 8 transmit antennas and 1 receive antennas with spectral efficiency 1.5 and 2 bps/Hz respectively. 131

6.1 The zero-order Bessel function of the first kind $J_0(x) = \frac{1}{\pi}\int_0^{\pi}\cos(x\cos\theta)d\theta$.136

6.2 Channel reconstruction with $f_d = 1$ Hz, $K = 200$. 137

6.3 Channel reconstruction with $f_d = 10$ Hz, $K = 200$. 137

6.4 Illustration of the interpolation of the channel matrix H. 138

6.5 Comparison of the two channel models considering one channel coefficient h_{nm}, interpolated with the passed and future random variables. 139

6.6 Time variation of the module of one channel coefficient h_{nm}. 140

6.7 The relative error versus different numbers of k with $N_m = 10$ and $N_m = 50$ respectively. 141

6.8 Performances of differential space-time schemes with $R = 1$ bps/Hz over different channel models. 142

6.9 Performances of differential space-time schemes with $R = 2$ bps/Hz over different channel models. 143

6.10 Performance of the DSTM M4N4R1 scheme with different L. 143

6.11 Channel interpolation with $f_d = 100$ Hz, $T_s = 25$ μs. 144

6.12 Performances of differential space-time schemes with $R = 1$ bps/Hz over different channel models. The normalized coherence time is $L = 200$. 145
6.13 Performances of differential space-time schemes with $R = 2$ bps/Hz over different channel models. The normalized coherence time is $L = 200$. 146
6.14 Performance of the DSTM M4N4R1 scheme with different L over continuously changing channel model. 147

Bibliography

[1] J. C. Maxwell, "A dynamical theory of the electromagnetic field.," *Philosophical Transactions of the Royal Society of London*, vol. 155, pp. 459–512, 1865.

[2] T. K. Sarkar, R. Mailloux, A. A. Oliner, M. Salazar-Palma, and D. L. Sengupta, *History of wireless*, vol. 177. John Wiley & Sons, 2006.

[3] ITU-R, "International mobile telecommunications-2000 (IMT-2000)," February 1997.

[4] ITU-R, "Detailed specificaitons of the radio interfaces of international mobile telecommunications-2000 (IMT-2000)," February 2013.

[5] ITU-R, "Requirements related to technical performance for IMT-Advanced radio interface(s)," 2008.

[6] G. Fodor, E. Dahlman, G. Mildh, S. Parkvall, N. Reider, G. Miklós, and Z. Turányi, "Design aspects of network assisted device-to-device communications," *IEEE Communications Magazine*, pp. 2–9, May 2011.

[7] S. K. Yong and C.-C. Chong, "An overview of multigigabit wireless through millimeter wave technology: potentials and technical challenges," *EURASIP J. Wirel. Commun. Netw*, vol. 2007, no. 1, p. 50, 2007.

[8] M. Cudak, A. Ghosh, T. Kovarik, R. Ratasuk, T. A. Thomas, F. W. Vook, and P. Moorut, "Moving towards mmwave-based beyond-4g (b-4g) technology," in *Proc. IEEE Veh. Technol. Soc. Conf.*, pp. 1–17, 2013.

[9] E. G. Larsson, O. Edfors, F. Tufvesson, and T. L. Marzetta, "Massive MIMO for next generation wireless systems," *IEE Communications Magazine*, pp. 186–195, February 2014. Massive MIMO.

[10] L. Lu, G. Y. Li, A. L. Swindlehurst, A. Ashikhmin, and R. Zhang, "An overview of massive MIMO: Benefits and challenges," *IEEE J. Select. Areas Commun.*, vol. 8, pp. 742–758, October 2014.

[11] T. L. Marzetta, "Noncooperative cellular wireless with unlimited numbers of base station antennas," *IEEE Trans. Wireless Commun.*, vol. 9, pp. 3590–3600, November 2010.

[12] A. Maaref and S. Aissa, "Capacity of mimo rician fading channels with transmitter and receiver channel state information," *IEEE Transactions on Wireless Communications*, vol. 7, pp. 1687–1698, May 2008.

[13] E. Telatar, "Capacity of multi-antenna gaussian channels," *European Transactions on Telecommunications*, vol. 10, no. 6, pp. 585–596, 1995.

[14] G. J. Foschini and M. J. Gans, "On limits of wireless communications in a fading environment when using multiple antennas," *Wireless Pers. Commun.*, vol. 6, pp. 311–335, 1998.

[15] D. Gesbert, M. Shafi, D.-s. Shiu, P. J. Smith, and A. Naguib, "From theory to practice: an overview of mimo space-time coded wireless systems," *Selected Areas in Communications, IEEE Journal on*, vol. 21, no. 3, pp. 281–302, 2003.

[16] A. J. Paulraj, D. A. Gore, R. U. Nabar, and H. Bolcskei, "An overview of mimo communications- a key to gigabit wireless," *Proceedings of the IEEE*, vol. 92, no. 2, pp. 198–218, 2004.

[17] J. Mietzner, R. Schober, L. Lampe, W. H. Gerstacker, and P. A. Hoeher, "Multiple-antenna techniques for wireless communications-a comprehensive literature survey," *Communications Surveys & Tutorials, IEEE*, vol. 11, no. 2, pp. 87–105, 2009.

[18] S. M. Alamouti, "A simple transmitter diversity scheme for wireless communications," *IEEE J. Select. Areas Commun.*, vol. 16, no. 8, pp. 1451–1458, 1998.

[19] R. Heath Jr. and A. J. Paulraj, "Switching between multiplexing and diversity based on constellation distance," in *Proc. of Allerton Conf. Communication, Control and Computing*, October 2000.

[20] L. Zheng and D. N. C. Tse, "Diversity and multiplexing: A fundamental tradeoff in multiple-antenna channels," *Information Theory, IEEE Transactions on*, vol. 49, pp. 1073–1096, May 2003.

[21] V. Tarokh, H. Jafarkhani, and A. R. Calderbank, "Space time block codes from orthogonal designs," *IEEE Trans. Inform. Theory*, vol. 45, no. 5, pp. 1456–1467, 1999.

[22] V. Tarokh, N. Seshadri, and A. R. Calderbank, "Space-time coding for high data rate wireless communication: Performance analysis and code construction," *IEEE Trans. Inform. Theory*, vol. 44, no. 2, pp. 744–765, 1998.

[23] G. J. Foschini, "Layered space-time architecture for wireless communication in a fading environment when using multi-element antennas," *Bell Labs Tech. J.*, vol. 1, no. 2, pp. 41–59, 1996.

[24] B. Hassibi and B. M. Hochwald, "How much training is needed in multiple-antenna wireless links," *IEEE Trans. Inform. Theory*, vol. 49, no. 4, pp. 951–963, 2003.

[25] T. L. Marzetta and B. M. Hochwald, "Capacity of a mobile multiple-antenna communication link in Rayleigh flat fading," *IEEE Trans. Inform. Theory*, vol. 45, no. 1, pp. 139–157, 1999.

[26] B. M. Hochwald and T. L. Marzetta, "Unitary space-time modulation for multiple-antenna communications in Rayleigh flat fading," *IEEE Trans. Inform. Theory*, vol. 46, no. 2, pp. 543–564, 2000.

[27] B. M. Hochwald and W. Sweldens, "Differential unitary space time modulation," *IEEE Trans. Commun.*, vol. 48, no. 12, pp. 2041–2052, 2000.

[28] V. Tarokh and H. Jafarkhani, "A differential detection scheme for transmit diversity," *IEEE J. Select. Areas Commun.*, vol. 18, no. 7, pp. 1169–1174, 2000.

[29] H. Jafarkhani and V. Tarokh, "Multiple transmit antenna differential detection from generalized orthogonal designs," *IEEE Trans. Inform. Theory*, vol. 47, no. 6, pp. 2626–2631, 2001.

[30] A. El Arab, J.-C. Carlach, and M. Hélard, "A new non-coherent MIMO scheme: Matrix coded modulation 'MCM'," in *International Symposium on Communications and Information Technologies (ISCIT)*, pp. 120–125, 2011.

[31] A. El Arab, J.-C. Carlach, and M. Hélard, "Joint space-time coded modulation and channel coding for iterative non-coherent MIMO schemes," in *Wireless Personal Multimedia Communications (WPMC)*, pp. 1–5, 2011.

[32] G. Zaharia, *Caractérisation de la propagation radioélectrique à l'intérieur des bâtiments à 900 MHz - implications sur la qualité d'une transmission numérique CT2-CAI.* PhD thesis, INSA RENNES, Feb. 1997.

[33] T. M. H. Ngo, P. Viland, G. Zaharia, and J.-F. Hélard, "Balanced QPSK space-time trellis codes," *Elect. Lett*, vol. 44, no. 16, pp. 983–985, 2008.

[34] P. Viland, G. Zaharia, and J.-F. Hélard, "Optimal generation of space-time trellis codes via the coset partitioning," *IEEE Trans. Veh. Technol.*, vol. 5, pp. 1413–1420, March 2011.

[35] P. Viland, G. Zaharia, and J.-F. Hélard, "New efficient method to generate optimal 2^n-PSK STTCs with a large number of transmit antennas," *IET Communications*, vol. 5, pp. 1413–1420, July 2011.

[36] T. M. H. Ngo, G. Zaharia, S. Bougeard, and J.-F. Hélard, "4-PSK balanced STTC with two transmit antennas," in *Vehicular Technology Conference, 2007. VTC2007-Spring. IEEE 65th*, pp. 1693–1697, IEEE, 2007.

[37] T. M. H. Ngo, G. Zaharia, S. Bougeard, and J. F. Hélard, "A new class of balanced 4-PSK STTC for two and three transmit antennas," in *Signal Processing Advances in Wireless Communications, 2007. SPAWC 2007. IEEE 8th Workshop on*, pp. 1–5, IEEE, 2007.

[38] P. Viland, G. Zaharia, and J.-F. Hélard, "Euclidean distance decomposition to generate new 16-QAM and 64-QAM space-time trellis codes," in *Personal*

Indoor and Mobile Radio Communications (PIMRC), 2010 IEEE 21st International Symposium on, pp. 385–390, IEEE, 2010.

[39] P. Viland, G. Zaharia, and J.-F. Hélard, "Coset partitioning for the 4-PSK space-time trellis codes," in *Signals, Circuits and Systems, 2009. ISSCS 2009. International Symposium on*, pp. 1–4, IEEE, 2009.

[40] P. Viland, G. Zaharia, and J.-F. Hélard, "Design of the best space-time trellis codes based on coset partitioning," in *Signal Processing Advances in Wireless Communications, 2009. SPAWC'09. IEEE 10th Workshop on*, pp. 324–328, IEEE, 2009.

[41] P. Viland, G. Zaharia, and J.-F. Hélard, "Improved balanced 2^n-PSK STTCs for any number of transmit antennas from a new and general design method," in *Vehicular Technology Conference, 2009. VTC Spring 2009. IEEE 69th*, pp. 1–5, IEEE, 2009.

[42] P. Viland, G. Zaharia, and J.-F. Hélard, "A new method to design balanced space-time trellis codes for several transmit antennas," in *Global Telecommunications Conference, 2008. IEEE GLOBECOM 2008. IEEE*, pp. 1–5, IEEE, 2008.

[43] P. Viland, G. Zaharia, and J.-F. Hélard, "An improved method to design QPSK balanced space-time trellis codes," in *Wireless Conference, 2008. EW 2008. 14th European*, pp. 1–6, IEEE, 2008.

[44] M. L. Honig and M. Barton, *Baseband Signalling and Pulse Shaping, The mobile communications handbook, second edition.* CRC Press, 1999.

[45] E. Bedrosian, "A product theorem for hilbert transforms," *Proceedings of the IEEE*, vol. 51, pp. 868–869, 1963.

[46] A. Goldsmith, *Wireless Communications.* Cambridge University Press, 2005.

[47] D. Tse, *Fundamentals of wireless communication.* Cambridge university press, 2005.

[48] B. Sklar, *Rayleigh Fading Channels, The mobile communications handbook.* CRC Press, 1999.

[49] J. Proakis, *Digital Communications, 4th edition.* McGraw-Hill, 2000.

[50] G. L. Stüber, *Principles of Mobile Communication.* Kluwer Academic Publlishers, 2nd ed., 2001.

[51] M. F. Mesiya, *Contemporary Communication Systems.* McGraw-Hill Education, 2013.

[52] C. E. Shannon, "A mathematical theory of communication," *The Bell System Technical Journal*, vol. 27, pp. 379–423, 623–656, July, October 1948.

[53] W. Vanderkulk, "Optimum processing for acoustic arrays," *Journal Brit. IRE*, vol. 26, pp. 286–292, Octrober 1963.

[54] Y. T. Lo, S. W. Lee, and Q. H. Lee, "Optimization of directivity and signal-to-noise ratio of an arbitrary antenna array," *Proc. IEEE*, vol. 54, pp. 1033–1045, August 1966.

[55] J. Capon, R. J. Greenfield, and R. J. Kolker, "Multidimensional maximum-likelihood processing of a large aperture seismic array," *Proc. IEEE*, vol. 55, pp. 192–211, February 1967.

[56] A. R. Kaye and D. A. George, "Transmission of multiplexed PAM signals over multiple channel and diversity systems," *IEEE Transactions on Communication Technology*, vol. 18, pp. 520–526, 1970.

[57] L. H. Brandenburg and A. D. Wyner, "Capacity of the Gaussian channel with memory: the mulivariate case," *The Bell System Technical Journal*, vol. 53, pp. 745–778, 1974.

[58] W. Van Etten, "An optimum linear receiver for multiple channel digital transmission systems," *IEEE Transactions on Communications*, vol. 23, pp. 828–834, 1975.

[59] W. Van Etten, "Maximum likelihood receiver for multiple channel transmission systems," *IEEE Transactions on Communications*, vol. 24, pp. 276–283, 1976.

[60] J. Saltz, "Digital transmission over cross-coupled linear channels," *AT&T Technical Journal*, vol. 64, pp. 1147–1159, July-August 1985.

[61] S. Anderson, M. Millnert, M. Viberg, and B. Wahlberg, "An adaptive array for mobile communication systems," *IEEE Trans. Veh. Technol.*, vol. 40, pp. 230–236, February 1991.

[62] P. S. Henry and B. S. Glance, "A new approach to high-capacity digital mobile radio," *The Bell System Technical Journal*, vol. 60, pp. 1891–1904, October 1981.

[63] W. C. Jakes and D. C. Cox, *Microwave mobile communications*. Wiley-IEEE Press, 1994.

[64] J. H. Winters, "Optimum combining in digital mobile radio with cochannel interference," *IEEE Journal on Selected Areas in Communications*, vol. 2, pp. 528 – 539, 1984.

[65] A. Wittneben, "Base station modulation diversity for digital simulcast," *Proc. IEEE VTC*, pp. 848–853, 1991.

[66] A. Wittneben, "A new bandwidth-efficient transmit antenna modulation diversity scheme for linear digital modulation," *Proc. IEEE ICC*, pp. 1630–1634, 1993.

[67] S. C. Swales, M. A. Beach, and D. J. Edwards, "Multi-beam adaptive base station antennas for cellular land mobile radio systems," *ProcProc. IEEE. Technol. Conf*, pp. 341–348, 1989.

[68] L. C. Godara, "Application of antenna arrays to mobile communications, part ii: Beam-forming and direction-of-arrival considerations," *Proceedings of the IEEE*, 1997.

[69] J. H. Winters, "On the capacity of radio communication systems with diversity in a rayleigh fading environment," *IEEE J. Select. Areas Commun.*, vol. SAC-5, pp. 871–878, June 1987.

[70] D. S. Shiu, G. Foschini, M. Gans, and J. Kahn, "Fading correlations and effect on the capacity of multielement antenna systems," *IEEE Trans. on Communications*, vol. 48, pp. 502–512, March 2000.

[71] C.-N. Chuah, D. N. C. Tse, J. M. Kahn, and R. A. Valenzuela, "Capacity scaling in mimo wireless systems under correlated fading," *IEEE Trans. on Information Theory*, vol. 48, pp. 637–650, March 2002.

[72] D. Chizhik, G. J. Foschini, M. J. Gans, and R. A. Valenzuela, "Keyholes, correlations, and capacities of multielement transmit and receive antennas," *IEEE Trans. on Wireless Communications*, vol. 1, pp. 361–368, April 2002.

[73] A. Lozano and A. M. Tulino, "Capacity of multiple-transmit multiple-receive antenna architectures," *IEEE Trans. Inform. Theory*, vol. 48, pp. 3117–3128, December 2002.

[74] M. Kang and M.-S. Alouini, "Capacity of MIMO rician channels," *IEEE Transactions on Wireless Communications*, vol. 5, pp. 112–122, Janurary 2006.

[75] A. Goldsmith, S. A. Jafar, N. Jindal, and S. Vishwanath, "Capacity limits of mimo channels," *IEEE J. Select. Areas Commun.*, vol. 21, pp. 684–702, June 2003.

[76] P. Viswanath and D. N. C. Tse, "Sum capacity of the vector gaussian broadcast channel and uplink-downlink duality," *IEEE Trans. Inf. Theory*, vol. 49, pp. 1912–1921, August 2003.

[77] H. Weingarten, Y. Steinberg, and S. Shamai (Shitz), "The capacity region of the gaussian multiple-input multiple-output broadcast channel," *IEEE Trans. Inf. Theory*, vol. 52, pp. 3936–3964, September 2006.

[78] S. Borade and L. Zheng, "Wideband fading channels with feedback," *IEEE Trans. Inform. Theory*, vol. 56, pp. 6058–6065, December 2010.

[79] Z. Rezki and M. S. Alouini, "On the capacity of Rician fading channels with full channel state information at low SNR," in *Proc. IEEE International Workshop on Energy Efficiency in Wireless Networks and Wireless Networks for Energy Efficiency (E2Nets) in conjunction with IEEE International Conference on Communications (ICC 2012)*, June 2012.

[80] F. Benkhelifa, A. Tall, Z. Rezki, and M.-S. Alouini, "On the low snr capacity of mimo fading channels with imperfect channel state information," *IEEE Trans. Commun.*, pp. 303–310, 2014.

[81] P. W. Wolniansky, G. J. Foschini, G. D. Golden, and R. A. Valenzuela, "V-BLAST: An architecture for realizing very high data rates over the rich scattering wireless channel," in *Proc. International Symp. Signals, Systems, and Electronics*, pp. 295–300, 1998.

[82] G. J. Foschini, G. D. Golden, R. A. Valenzuela, and P. W. Wolniansky, "Simplified processing for high spectral efficiency wireless communication employing multi-element arrays," *IEEE J. Select. Areas Commun.*, vol. 17, pp. 1841–1852, November 1999.

[83] M. Sellathurai and S. Haykin, "TURBO-BLAST for wireless communications: Theory and experiments," *IEEE Trans. Signal Processing*, vol. 50, pp. 2538–2546, October 2002.

[84] K. Vishnu Vardhan, S. K. Mohammed, A. Chockalingam, and B. Sundar Rajan, "A low-complexity detector for large MIMO systems and multicarrier cdma systems," *IEEE J. Select. Areas Commun.*, vol. 26, pp. 473–485, April 2008.

[85] Y. Jiang, M. K. Varanasi, and J. Li, "Performance analysis of ZF and MMSE equalizers for MIMO systems: An in-depth study of the high SNR regime," *IEEE Trans. Inform. Theory*, vol. 57, pp. 2008–2026, April 2011.

[86] A. U. Toboso, S. Loyka, and F. Gagnon, "Optimal detection ordering for coded V-BLAST," *IEEE Trans. Commun.*, vol. 62, pp. 100–111, January 2014.

[87] H. Jafarkhani, "A quasi-orthogonal space-time block code," *IEEE Transactions on Communications*, vol. 49, no. 1, pp. 1–4, 2001.

[88] B. Hassibi and B. M. Hochwald, "High-rate codes that are linear in space and time," *IEEE Trans. Inf. Theory*, vol. 48, pp. 1804–1824, July 2002.

[89] B. A. Sethuraman, B. S. Rajan, and V. Shashidhar, "Full-diversity, high-rate space-time block codes from division algebras," *IEEE Trans. Inf. Theory*, vol. 49, pp. 2596–2616, October 2003.

[90] F. Oggier, G. Rekaya, J.-C. Belfiore, and E. Viterbo, "Perfect space time block codes," *IEEE Trans. Inf. Theory*, vol. 52, pp. 3885–3902, September 2006.

[91] A. Sendonaris, E. Erkip, and B. Aazhang, "User cooperation diversity-part i: System description," *IEEE Transactions on Communications*, vol. 51, pp. 1927–1938, November 2003.

[92] A. Sendonaris, E. Erkip, and B. Aazhang, "User cooperation diversity-part ii: Implementation aspects and performance analysis," *IEEE Transactions on Communications*, vol. 51, pp. 1939–1948, November 2003.

[93] J. N. Laneman, D. N. C. Tse, and G. W. Wornell, "Cooperative diversity in wireless networks: efficient protocols and outage behavior," *IEEE Trans. Inf. Theory*, vol. 50, pp. 3062–3080, December 2004.

[94] A. Høst-Madsen, "Capacity bounds for cooperative diversity," *IEEE Trans. Inf. Theory*, vol. 52, pp. 1552–1544, April 2006.

[95] S. Yang and J.-C. Belfiore, "Optimal space-time codes for the MIMO amplify-and-forward cooperative channel," *IEEE Trans. Inf. Theory*, vol. 53, pp. 647–663, February 2007.

[96] T. Wang, A. Cano, G. B. Giannakis, and J. N. Laneman, "High-performance cooperative demodulation with decode-and-forward relays," *IEEE Trans. Commun.*, vol. 55, pp. 1427–1438, July 2007.

[97] D. Gesbert, S. Hanly, H. Huang, S. S. Shitz, O. Simeone, and W. Yu, "Multi-cell MIMO cooperative networks: A new look at interference," *IEEE J. Select. Areas Commun.*, vol. 28, pp. 1380–1408, December 2010.

[98] L. Zheng and D. N. C. Tse, "Communication on the grassmann manifold: A geometric approach to the noncoherent multiple-antenna channel," *Information Theory, IEEE Transactions on*, vol. 48, no. 2, pp. 359–383, 2002.

[99] A. Lapidoth and S. M. Moser, "Capacity bounds via duality with applications to multiple-antenna systems on flat-fading channels," *IEEE Trans. Inf. Theory*, vol. 49, pp. 2426–2467, October 2003.

[100] S. A. Jafar and A. Goldsmith, "Multiple-antenna capacity in correlated rayleigh fading with channel covariance information," *IEEE Trans. Wireless Commun.*, vol. 4, pp. 990–997, May 2005.

[101] B. M. Hochwald, T. L. Marzetta, T. J. Richardson, W. Sweldens, and R. Urbanke, "Systematic design of unitary space-time constellations," *Information Theory, IEEE Transactions on*, vol. 46, no. 6, pp. 1962–1973, 2000.

[102] V. Tarokh and I.-M. Kim, "Existence and construction of noncoherent unitary space-time codes," *Information Theory, IEEE Transactions on*, vol. 48, no. 12, pp. 3112–3117, 2002.

[103] G. Leus, W. Zhao, G. B. Giannakis, and H. Deliç, "Space-time frequency-shift keying," *Communications, IEEE Transactions on*, vol. 52, pp. 346–349, March 2004.

[104] J. Kim, K. Cheun, and S. Choi, "Unitary space-time constellations based on quasi-orthogonal sequences," *IEEE Trans. Commun.*, vol. 58, pp. 35–39, January 2010.

[105] K. Yang, Y.-K. Kim, and P. V. Kumar, "Quasi-orthogonal sequences for code-division multiple-access systems," *IEEE Trans. Inf. Theory*, vol. 46, pp. 982–993, May 2000.

[106] B. L. Hughes, "Differential space-time modulation," *IEEE Trans. Inform. Theory*, vol. 16, no. 7, pp. 2567–2578, 2000.

[107] H. Kdouh, G. Zaharia, C. Brousseau, G. El Zein, and G. Grunfelder, "Zigbee-based sensor network for shipboard environments," in *Proc. of the 20th International Symposium on Signals, Circuits and Systems (ISSCS)*, 2011.

[108] R. Youssef, M. Hélard, M. Crussière, and J.-F. Hélard, "Distributed coding for OFDM-based transmission in cooperative broadcast networks," in *Proc. of the 3rd International Workshop on Cross Layer Design (IWCLD)*, 2011.

[109] T. M. Cover and J. A. Thomas, *Elements of information theory 2nd edition.* Wiley-Interscience, 2006.

[110] H. Jafarkhani, *Space-time coding: theory and practice.* Cambridge university press, 2005.

[111] G. Taricco and E. Biglieri, "Exact pairwise error probability of space-time codes," *Information Theory, IEEE Transactions on*, vol. 48, no. 2, pp. 510–513, 2002.

[112] M. K. Simon, "Evaluation of average bit error probability for space-time coding based on a simpler exact evaluation of pairwise error probability," *Communications and Networks, Journal of*, vol. 3, no. 3, pp. 1–8, 2001.

[113] M. K. Simon and M.-S. Alouini, *Digital communication over fading channels.* John Wiley & Sons, 2005.

[114] D. Zhang, J. Liu, H. Xu, and H. Ji, "Pair-wise error probability and its chernoff upper bound for unitary space-time code," *Science China Information Sciences*, vol. 53, pp. 1613–1621, August 2010.

[115] G. H. Golub and C. F. Van Loan, *Matrix Computations.* Baltimore Maryland: The Johns Hopkins University Press, 3rd ed., 1996.

[116] Y. Jing and B. Hassibi, "Unitary space-time modulation via Cayley transform," *IEEE Trans. Signal Processing*, vol. 51, pp. 2891–2904, November 2003.

[117] F. J. MacWilliams and N. J. A. Sloane, *The Theory of Error-Correcting Codes.* North-Holland Publishing Company, 1977.

[118] H. Ji, G. Zaharia, and J.-F. Hélard, "A new differential space-time modulation scheme for MIMO systems with four transmit antennas," in *20th International Conference on Telecommunications (ICT)*, 2013.

[119] H. Ji, G. Zaharia, and J.-F. Hélard, "A new differential space-time modulation scheme based on weyl group," in *the 11-th International Symposium on Signals, Circuits and Systems (ISSCS)*, 2013.

[120] R. H. Clarke, "A statistical theory of mobile-radio reception," *Bell Labs Tech. J.*, pp. 957–1000, Jul.-Aug. 1968.

[121] H. Ji, G. Zaharia, and J.-F. Hélard, "Performance of dstm mimo systems based on Weyl group in time selective channel," in *European Wireless 2014*, 2014.

INSA de RENNES
Service des Formations

AVIS DU JURY SUR LA REPRODUCTION DE LA THESE SOUTENUE

Titre de la thèse:
Study and optimization of new differential space-time modulation schemes based on Weyl group for the second generation of MIMO systems

Nom Prénom de l'auteur : JI HUI

Membres du jury :
- Monsieur CANCES Jean-Pierre
- Monsieur HELARD Jean-François
- Monsieur ZAHARIA Gheorghe
- Madame BOUCHERET Marie-Laure

Président du jury : ML Boucheret

Date de la soutenance : 09 Novembre 2015

Reproduction de la these soutenue

Thèse pouvant être reproduite en l'état
~~Thèse pouvant être reproduite après corrections suggérées~~

Fait à Rennes, le 09 Novembre 2015

Signature du président de jury

Le Directeur,

M'hamed DRISSI

Résumé

Actuellement, l'étude des systèmes multi-antennaires MIMO (*Multiple Input Multiple Output*) est orientée dans beaucoup de cas vers l'augmentation considérable du nombre d'antennes de la station de base (« massive MIMO », « large-scale MIMO »), afin notamment d'augmenter la capacité de transmission, réduire l'énergie consommée par bit transmis, exploiter la dimension spatiale du canal de propagation, diminuer l'influence des évanouissements, etc. Pour les systèmes MIMO à bande étroite ou ceux utilisant la technique OFDM (*Orthogonal Frequency Division Multiplex*), le canal de propagation (ou les sous-canaux correspondants à chaque sous-porteuse d'un système OFDM) sont pratiquement plats (non-sélectifs en fréquence), ce qui revient à considérer la réponse fréquentielle de chaque canal SISO invariante par rapport à la fréquence mais variante dans le temps. Ainsi, le canal de propagation MIMO peut être caractérisé en bande de base par une matrice dont les coefficients sont des nombres complexes. Les systèmes MIMO cohérents nécessitent pour pouvoir démoduler le signal en réception de disposer de la connaissance de cette matrice de canal, donc le sondage périodique, en temps réel, du canal de propagation. L'augmentation du nombre d'antennes et la variation dans le temps, parfois assez rapide, du canal de propagation, rend ce sondage de canal difficile, voire impossible. Il est donc intéressant d'étudier des systèmes MIMO différentiels qui n'ont pas besoin de connaître la matrice de canal. Pour un bon fonctionnement de ces systèmes, la seule contrainte est que la matrice de canal varie peu pendant la transmission de deux matrices d'information successives.

Le sujet de cette thèse concerne l'étude et l'analyse de nouveaux systèmes MIMO différentiels. On considère des systèmes à 2, 4 et 8 antennes d'émission, mais la méthode utilisée peut être étendue à des systèmes MIMO avec 2^n antennes d'émission, le nombre d'antennes de réception étant quelconque.

Pour les systèmes MIMO avec 2 antennes d'émission qui ont été étudiés dans le cadre de cette thèse, les matrices d'information sont des éléments du groupe de Weyl. Pour les systèmes avec 2^n antennes d'émission, ($n \geq 2$), les matrices utilisées sont obtenues en effectuant des produits de Kronecker des matrices unitaires du groupe de Weyl.

Pour chaque nombre d'antennes d'émission on identifie d'abord le nombre de matrices disponibles et on détermine la valeur maximale de l'efficacité spectrale. Pour chaque valeur de l'efficacité spectrale on détermine les meilleurs sous-ensembles de matrices d'information à utiliser (selon le spectre des distances ou le critère du produit de diversité). On optimise ensuite la correspondance ou *mapping* entre les vecteurs binaires et les matrices d'information. Enfin, on détermine par simulation les performances des systèmes MIMO différentiels ainsi obtenus et on les compare avec celles des systèmes similaires existants.

Pour la simulation des systèmes proposés, on a d'abord sélectionné un modèle simple de canal de Rayleigh, largement utilisé dans la littérature, en considérant la matrice de canal constante pendant un intervalle de temps d'une certaine durée déterminée par le temps de cohérence du canal de propagation. Chaque nouvelle matrice de canal s'obtient par un tirage aléatoire, indépendant des tirages précédents. Ce modèle de canal est peu réaliste et, pour les systèmes différentiels, impose pour la simulation une réinitialisation périodique du système, chaque fois qu'on utilise une autre matrice de canal. Afin de déterminer les performances des nouveaux systèmes proposés dans des conditions plus réalistes et échapper à la réinitialisation périodique du système analysé, nous avons intégré une variation de la matrice de canal entre deux tirages aléatoires successifs en utilisant le théorème de l'échantillonnage. Cependant, dans cette première approche, la matrice de canal est considérée comme constante durant l'émission d'une matrice. Les simulations effectuées avec ce nouveau modèle de canal ont permis de mettre en évidence une certaine dégradation des performances, surtout quand le temps de cohérence normalisé par rapport à la durée d'un symbole émis est réduit et donc, quand le canal de propagation varie rapidement.

Dans un second temps, nous avons considéré une seconde approche encore plus proche de la réalité, pour laquelle la matrice de canal reste constante durant uniquement l'émission d'un symbole. On observe dans ce cas une dégradation supplémentaire des performances.

Abstract

At present, the study of multi-antenna systems MIMO (Multiple Input Multiple Output) is developed in many cases to intensively increase the number of base station antennas ("massive MIMO", "large-scale MIMO"), particularly in order to increase the transmission capacity, reduce energy consumed per bit transmitted, exploit the spatial dimension of the propagation channel, reduce the influence of fading, etc. For MIMO systems with narrowband or those using OFDM technique (Orthogonal Frequency Division Multiplex), the propagation channel (or the sub-channels corresponding to each sub-carrier of an OFDM system) are substantially flat (frequency non-selective). In this case the frequency response of each SISO channel is invariant with respect to frequency, but variant in time. Furthermore, the MIMO propagation channel can be characterized in baseband by a matrix whose coefficients are complex numbers. Coherent MIMO systems need to have the knowledge of the channel matrix to be able to demodulate the received signal. Therefore, periodic pilot should be transmitted and received to estimate the channel matrix in real time. The increase of the number of antennas and the change of the propagation channel over time, sometimes quite fast, makes the channel estimation quite difficult or impossible. It is therefore interesting to study differential MIMO systems that do not need to know the channel matrix. For proper operation of these systems, the only constraint is that the channel matrix varies slightly during the transmission of two successive information matrices.

The subject of this thesis is the study and analysis of new differential MIMO systems. We consider systems with 2, 4 and 8 transmit antennas, but the method can be extended to MIMO systems with 2^n transmit antennas, the number of receive antennas can be any positive integer.

For MIMO systems with two transmit antennas that were studied in this thesis, information matrices are elements of the Weyl group. For systems with 2^n ($n \geqslant 2$) transmit antennas, the matrices used are obtained by performing the Kronecker product of the unitary matrices in Weyl group.

For each number of transmit antennas, we first identify the number of available matrices and the maximum value of the spectral efficiency. For each value of the spectral efficiency, we then determine the best subsets of information matrix to use (depending on the spectrum of the distances or the diversity product criterion). Then we optimize the correspondence or mapping between binary vectors and matrices of information. Finally, the performance of differential MIMO systems are obtained by simulation and compared with those of existing similar systems.

For simulation of the proposed system, we first selected a simple Rayleigh channel model, which is widely used in the literature. In this channel model, the channel matrix is constant for a time interval of a certain length determined by the coherence time of the propagation channel. Each new channel matrix is obtained by a random draw, independent from previous draws. This channel model is impractical and, for the differential systems, need to simulate a periodic reset of the system, whenever using another channel matrix. To evaluate the performance of the new proposed systems in more realistic conditions and escape the periodic reset of the analyzed system, we integrated a variation of the channel matrix between two successive random draws by using the sampling theorem. However, in the first approach, the channel matrix is considered to be constant during the transmission of a matrix. Simulations with this new channel model made it possible to spotlight some performance degradation due to the channel characteristic, especially when the normalized coherence time with respect to the duration of a transmitted symbol is reduced and therefore, when the propagation channel varies rapidly .

Finally, we considered the second even closer approach to reality, where the channel matrix remains constant during the transmission of only a symbol. In this case there is a further performance degradation.

N° d'ordre : 15ISAR 24 / D15 - 24

Institut National des Sciences Appliquées de Rennes
20, Avenue des Buttes de Coëmes • CS 70839 • F-35708 Rennes Cedex
Tel : 02 23 23 82 00 - Fax : 02 23 23 83 96